In situ gelling nanoparticulate systems as scaffolds for tissue engineering using stem cells

Submitted in partial fulfillment of the requirements

Of the degree of

Doctor of Philosophy

Of the
Indian Institute of Technology, Bombay, India
and
Monash University, Australia

By

Edmund Carvalho

Supervisors:

Prof Rinti Banerjee (IIT Bombay)

Prof Kerry Hourigan (Monash University)

Prof Paul Verma (Monash University)

The course of study for this award was developed jointly by
Monash University, Australia and the Indian Institute of Technology, Bombay
and was given academic recognition by each of them.
The programme was administrated by The IITB-Monash Research Academy

(2015)

DECLARATION

I declare that this written submission represents my ideas in my own words and where others' ideas or words have been included, I have adequately cited and referenced the original sources. I also declare that I have adhered to all principles of academic honesty and integrity and have not misrepresented or fabricated or falsified any idea/data/fact/source in my submission. I understand that any violation of the above will be cause for disciplinary action by the Institute and can also evoke penal action from the sources which have thus not been properly cited or from whom proper permission has not been taken when needed.

Notice 1

Notice 2

I certify that I have made all reasonable efforts to secure copyright permissions for third-party content included in this thesis and have not knowingly added copyright content to my work without the owner's permission.

Student Name: Edmund Carvalho
IITB ID: 09430402

ACKNOWLEDGEMENTS

I would like to offer my years of work as a PhD student to God and to my two pillars, my parents, who have supported me all through with their prayers and support whether financially or emotionally. They have been by my side following each and every up and down within my tenure as a student.

I thank my supervisors especially Prof Rinti Banerjee, who has been a source of constant support and guidance all through. Her guidance has allowed me to achieve this work and will constantly spur me to do my best at research. I thank Prof. Paul Verma who has supported my work as my PhD supervisor. I remember the games of football which were a welcome relief at MIMR. He managed to turn me into an Australian by the end of my stint there and captured it while having a lunch of beef pies. Prof Kerry Hourigan came on board late and I am extremely grateful to him for opting to supervise me at that juncture. His constant support and prompt feedback, is what kept me going.

I thank IITB Monash research academy for giving me the opportunity to pursue a joint collaborative project and experience the research cultures of two continents.

I thank Monash institute for medical research(MIMR) for the facilities to pursue research at Monash, Monash center for electron microscopy(MCEM) for electron microscopy facilities, Monash micro imaging(MMI) for Confocal facilities and Melbourne center for nanofabrication(MCN) .

I thank Prof Sarika Mehra for allowing me to use some of the instruments in her lab especially the Nanodrop and the Q-PCR for my work. I thank Kamal Prasad and Yesha Patel for their help in setting up my work at chemical engineering. I thank Prof Mahesh Tirumkudulu for allowing me to independently work with the Anton Paar Physica 310 for all my rheology experimentation, and especially thank

Meena Menghrajani for her help in standardizing rheology and troubleshooting with the instrument. I thank Prof N.S. Punekar, and Khyati Mehta for facilitating key experiments without which my work would not be complete. I thank Prof. Bahadur and Saumya Nigam for help with experimental work at material sciences.

I thank my friends and colleagues at IITB and Monash, whether in good times or in bad they have helped me grow as an individual. They have taught me that the greatest strength is in picking oneself up to see the light of a new day, a new experiment. I especially thank Kanika Jain for the support in the lab from orienting me to the workings of facilities at Monash to acquainting me to the Clayton campus to teaching me molecular techniques. I thank Amrita Sarkar for the constant support as a friend and as a colleague in the lab, from teaching me western blotting to being a constant support during the days of the thesis submission. I thank my colleagues at IITB, Dharmendra Jain, Apurva Shah, Shruti Guhasarkar, and Rekha Sehgal for accompanying me on this journey of PhD. I thank lab members including junior PhD students, Mtech students and interns who have helped shape my ever changing understanding of academics.

I thank Jun Liu, Luis Malaver, Corey Heffernan, and Raj Verma for their constant support and timely help at MIMR.

I would like to thank the CEO Mohan Krishnamoorthy, for being there to aid grievances during the tenure of the PhD and for his encouragement all though the PhD. I thank the staff at the IITB Monash academy, Mrs. Anasuya Banerjee for being the go to person during my initial days at the academy, Mrs. Kuheli Banerjee for the constant support with financial issues and due diligence during my thesis submission, Mrs. Jayasree Narayanan for being the go-to person for any and all candidature issues, and Mrs. Laya Vijayan and Mrs. Nancy Sowho. I thank Adrian Gertler for being the go-to person at Monash and David Lau for prompt help with any administrative issues at Monash.

Abstract

The aim of the current study was to ascertain whether three dimensional scaffold delivery systems could be developed along with nanoparticles to mediate differentiation in situ using the properties of the hydrogel scaffold and nanoparticles. The work was divided into three sections, 1. The development of in situ gelling scaffold systems, 2. Encapsulation and differentiation of ES cells within the scaffold systems, 3. Nanoparticulate approaches to facilitate ES cell differentiation towards the cardiac lineage.

Gellan which can be crosslinked with calcium to form scaffolds while HPMC which was thermoresponsive were chosen to form scaffolds. Gellan and gellan HPMC blends were prepared to further employ the thermoresponsiveness of HPMC to improve the properties of the *in situ* gelling scaffolds prepared. It was found that the average gelation time of the gellan HPMC crosslinked with 3mM calcium blends 9:1 and 8:2 was 12 min and 16 min respectively and that for 0.5% gellan blended with 3mM calcium, was 26 min which was within the range of ASTM standards for in situ gelation. The volume of pores present in all of the blends were in the range of 80 to 90 % suggesting that the porous volume of the scaffolds was occupied completely with water once hydrated The calcium crosslinked gels were porous and non-toxic indicating that the gels suitably network and ensure a viable environment. The 0.5GH8:2-3 blend showed promise and indicated that an increase in the concentration coupled with the addition of calcium improves the overall properties of the hydrogel so formed. Temperature dependent rheology suggested that 0.5GH8:2-3 shared properties similar to 0.5G-3. The extended viability of the cells as well as tan δ in *vitro*, makes 0.5%GH 8:2 with 3mM calcium more similar to 0.5% G-3mM calcium. We finally considered gellan crosslinked with calcium for encapsulation of embryoid bodies. Scanning electron microscopy indicated EB presence within scaffold matrix. EB, beating efficiency on day 19 from 1.5 mM to 3 mM and 6 mM. showed that there was a significant difference in the beating rate of EBs encapsulated in 0.5G 1.5mM compared to 0.5G 3mM and 0.5G 6mM at $p<0.05$ and significant difference in beating rates between 0.5G 3mM and plated controls at $p<0.005$. Gene expression of early

marker Flk 1 was present in all samples. Late cardiac marker Mlc2v was absent in 1.5mM crosslinked gel on day 19 its expression was faintly present in 3mM calcium encapsulated EBs on both day3 and day 5. Its expression was prominent in 6mM calcium encapsulated gellan and absent in day 3 and day 5 plated EBs. Atrial marker MLC 2a was expressed uniformly in all of the treatment sets while cardiac TnT too was expressed from day 5 onwards in treated and untreated samples. Tenfold expression of Mlc 2v, four fold Flk 1 and three fold cardiac TnT expression was observed compared to plated controls on day 5 of encapsulation and plating. The gelling time and gene expression studies indicated that a stiffer matrix induced greater expression of cardiac specific genes. Since 3mM calcium crosslinked gellan had a gelling time within ASTM standards for *in situ* gelling agents; nanoparticle nanoparticle encapsulated molecular mediators could be used to facilitate differentiation along with 3mM crosslinked gellan.

Cardiac tissue specific lipids were chosen to prepare liposomes. It was found that the average hydrodynamic diameter for SPC liposomes were found to be of 178 nm $\pm$13nm before loading and 153nm $\pm$ 15nm after loading with retinoic acid. While average size for SPC: POPE liposomes were found to be of 210nm $\pm$ 7nm and 255nm - $\pm$20nm after retinoic acid loading. The surface charge for SPC and SPC-RA was - 32 $\pm$3 mV and - 30 $\pm$ 4 mV respectively, while that of SPC: POPE and SPC: POPE-RA were - 26 $\pm$ 2.5 mV and - 27$\pm$ 2.6 mV respectively. The encapsulation efficiency for the SPC-RA liposomes was 57.2% $\pm$ 0.9 and while that for PCPE-RA liposomes was 54.8% $\pm$ 0.5. SPC: POPE liposomes resulted in a lower retinoic acid release over 24 hours as compared to SPC loaded retinoic acid. SPC-POPE liposomes showed an initial burst release for 2 hours with a sustained release at an average of 30% thereon until 24 hours as compared to 100% release for SPC liposomes. Proliferation studies revealed that there was a significant difference between PC-RA at 10^{-9} M treated embryoid bodies and those treated with free retinoic acid at a concentration of 10^{-9} and 10^{-11} Moles at $p<0.05$ and $p<0.01$ respectively. The number of beating bodies were low in the free 10^{-9} M retinoic acid and the PCPE 0.3 loaded liposomes, this did not change from day 9 to day 13. There was a greater change in the percentage beating bodies

with the untreated EBS , DMSO treated, free 10^{-11} M, SPC:POPE 10^{-11} M and SPC:POPE 10^{-11} M from day 9 to day 13. There was a greater change in the percentage beating bodies with the untreated EBS , DMSO treated, free 10^{-11} M, SPC 10^{-11} M and SPC POPE 10^{-11} M from day 9 to day 13. Early gene Flk 1 expression diminished after day 7. Mlc2a i.e. atrial myocin expression was only observed on day 7 embryoid bodies. Mlc2v was expressed on day 7 EB and at very low levels in samples treated with retinoic acid. Low expression was observed in the presence of RA concentration at 10^{-11}M in the presence of PC nanoparticles. Cardiac TnT expression was observed at levels slightly lower than levels observed on day7 in all samples.

The tunable rheological properties of the gellan can further be used for the differentiation of stem cells *in vitro*. Liposome entrapped molecular mediators can be used in conjunction with tunable scaffolds to drive in situ differentiation in ES cells

Keywords: biomaterials, pluripotent stem cells, embryonic stem cells, nanoparticles, liposomes, differentiation, stem cell delivery, stem cell differentiation, gellan, retinoic acid, *in situ* gelling scaffolds,

Table of contents

List of figures and tables

Figures

Tables

List of abbreviations

1- ethyl-3-(3-dimethylaminopropyl)-carbodiimide	(EDC)
All trans retinoic acid	(ATRA)
Brain-derived neurotrophic factor	(BDNF)
Bone morphogenetic protein	(BMP)
Beta Fibroblast growth factor	(bFGF)
Cardiac stem cells	(CSC)
Cardiac progenitor cells	(CPC)
Cardiosphere	(CS)
Cardiosphere-derived cardiac progenitor cells	(CDC)
Central nervous system	(CNS)
Chondroitin sulfate proteoglycans	(CSPGs)
Ciliary neurotrophic factor	(CNTF)
Cluster of differentiation	(CD)
Complimentary-Dioxyribonucleic acid	(cDNA)
Coronary artery bypass grafting	(CABG)
Cycle thresholds	(cT)
Dimethyl Sulphoxide	(DMSO)
Dorsal root ganglion	(DRG)
Dulbecco's minimal essential medium	(DMEM)
Dynamic light scattering	(DLS)
Extra cellular matrix	(ECM)
Embryonic stem cells	(ESC)
Engineered heart tissue	(EHT)
Ethylene diamine tetra acetate	(EDTA)
Fetal Bovine serum	(FBS)
Field Emission gun transmission electron microscopy	(FEG-TEM)
Fibroblast growth factor	(bFGF-2)
Food and drug administration	(FDA)

Glycosaminoglycan	(GAG)
Green fluorescent protein	(GFP)
High pressure liquid chromatography	(HPLC)
High resolution transmission electron microscopy	(HR-TEM)
Hydroxyl propyl methyl cellulose	(HPMC)
Hyaluronan and Methyl cellulose	(HAMC)
Hyaluronic acid	(HA)
Induced pluripotent stem cells	(iPSC)
Left ventricular ejection fraction	(LVEF)
Left ventricular assist devices	(LAVD)
Lower critical solution temperature	(LCST)
Magnetic resonance imaging	(MRI)
Matrix metalloproteases	(MMPs)
Mesenchymal stem cells	(MSC)
Methylprednosolone	(MP)
Mouse embryonic fibroblast	(MEF)
Mouse Leukemia Inhibitory factor	(mLIF)
Minor histocompatibility complex	(MHC)
Mono amine-terminated poloxamer	(MATP)
Myelin associated glycoproteins	(MAG)
N-hydroxylsuccinimide	(NHS)
Nerve growth factor	(NGF)
Neurotrophin-3	(NT-3)
Non-essential amino acids	(NEAA)
1-palmitoyl-2-oleoyl-*sn*-glycero-3-phosphoethanolamine	(POPE)
Phosphate buffered saline	(PBS)
Platelet derived growth factor	(PGDF)
Placental growth factor	(PGF)
Poly-D lysine	(PDL)
Poly ethylene glycol	(PEG)

Poly (ethylene oxide)	(PEO)
Poly ethylene imine	(PEI)
Poly (propylene oxide)	(PPO)
Poly-Lactic-Co-Glycolic Acid	(PLGA)
Peripheral nervous system	(PNS)
Poly (ester-urethane)	(PEU)
Poly (glycerol-sebacate)	(PGS)
Poly vinyl chloride	(PVC)
Polyurethane	(PU)
Polyester urethane urea	(PEUU)
Poly (2-hydroxyethyl methacrylate)	(pHEMA)
Poly (2hydroxypropyl methylacrylate	(pHPMA)
Propidium Iodide	(PI)
Quantitative-Polymerase chain reaction	(Q-PCR)
Ribonucleic acid	(RNA)
Reverse transcriptase polymerase chain reaction	(RT PCR)
Rhodamine 6G	(R6G)
Scanning electron microscopy	(SEM)
Simulated tear fluid	(STF)
Simulated aqueous humor	(SAH)
Somatic cell nuclear transfer	(SCNT)
Sodium dodecyl sulfate	(SDS)
Solid lipid nanoparticles	(SLNs)
Soya phosphatidylcholine	(SPC)
Spinal cord injury	(SCI)
Tumor necrosis factor α	(TNFα)
Transmission electron microscopy	(TEM)
Upper critical solution temperature	(UCST)

Chapter 1

1.1 Introduction: Anatomy of heart

The heart is a muscular organ placed in the upper thoracic cavity, medial to the lungs and posterior to the sternum. The muscular walls of the heart consist of the epicardium, myocardium and the endocardium. Epicardium is another name given to the visceral layer of the pericardium, while the myocardium is the middle muscular layers of the heart involved in the pumping of blood from the heart, the epicardium is a thin internal layer made up to prevent adherence of blood to the heart and the formation of clots therein. The heart is musculature is supplied by coronary arteries. The left coronary artery distributes blood to the left side of the heart, the left atrium and ventricle, and the interventricular septum. The left coronary artery gives rise to the circumflex artery which traces the coronary sulcus to the left and further fuses with the small branches of the right coronary artery. The larger left anterior descending artery (LAD) traces the anterior interventricular sulcus and gives rise to smaller branches that interconnect with the branches of the posterior interventricular artery and form anastomoses.

1.2 Physiological conditions

Partial blockages in any part of tissue result in normal flow of blood to that area through redirection by anastomosis. The small size of anastomoses in the heart restricts their ability to fulfill the role of redirection of blood. Therefore, coronary artery blockage often results in myocardial infarction causing death of the cells supplied by the particular vessel. The resultant ischemia that is caused post blockage, leads to muscular death and necrosis. Ischemic injury of the heart causes loss of blood flow along the coronary arteries supplying the heart mainly affecting the flow to the ventricular portion of the heart. This leads to tissue death and subsequent scar formation due to fibroblast infiltration. The

relatively low regenerative potential of the resident cardiac stem cells (CSC) is insufficient to repair this type of damage. The primary event at the site of infarct is cellular necrosis, with edema localized at the site of ischemia. Studies suggest apoptosis of cardiomyocytes is the major cause for remodeling of the heart after a myocardial infarct. Although seemingly insignificant, a persistent 0.2% cell apoptosis can, over a lengthy period of time, cause substantial damage to the heart [1]. The apoptosis at the site of infarct also induces expression of fetal genes such as brain natriuretic peptide and atrial natriuretic peptide. Oxidative stress at the site of the infarct causes expression of tumor necrosis factor resulting in free radical production causing fetal gene expression [2-6]. Cardiac myocyte contractions are inhibited when cytokines released during inflammation activate nitric oxide synthetase-2 [7, 8].There is infiltration of fibroblasts with the deposition of collagen and fibrin, resulting in scar tissue formation [9]. The resultant damage leads to an increase in the tensile strength, elongation and wall thinning of the heart, commonly known as "infarct expansion" [10]. Details of the mechanisms involved in the process can be found in the thorough a review by Pfeffer and Braunwald [9]. Tumor growth factor-β (TGFβ), angiotensin and endothelin expression are a direct result of myocardial stretching [11-13]. Furthermore stretching of the myocardium can induce cardiac myocyte death [14].

1.3 Strategies for treatment

The strategy required to mitigate the extent of infarct involves control and treatment at various levels of infarct progression. The primary goal should be to target the infarct as early in its progression as possible, ideally before scar tissue is formed. This can involve administration of anti-apoptotic agents in order to reduce cellular necrosis and resultant apoptosis that occur due to lack of oxygen [15]. The second goal should be the replacement of the scar tissue with cellular/molecular mediators that promote cardiac tissue regeneration and replacement of the scar. While figure 1 gives the broader nature of the application of cells after an infarct, figure 2 indicates the various cell sources that can be used for the treatment of Myocardial infarction (MI). Cardiac tissue primarily consists of cardiac myocytes comprising the musculature and vasculature. The vasculature consists of vascular endothelial cells and smooth muscle cells. The cellular populations to be delivered must incorporate these two types. The modes of delivery of cellular payload may be

systemic or localized. Various strategies for the transplantation of cells have been elucidated for the treatment of a myocardial infarct. An elegant review by Lin *et al*. discusses in detail the current landscape of clinical trial and the cells examined [16].

1.4 Properties of an ideal cellular delivery system

The properties of an ideal cellular delivery system are as follows

- It must share matrix similarities with the tissue of interest; for the heart, the tissue in question is given in table 1. It must be as similar to the native normal heart as possible.
- The material must be porous enough to allow the proliferation of cells as well as allow differentiation at the same time
- The material must be hydrophilic to allow transfer of nutrient media
- Neither the material nor its degradation products should be toxic
- Tunable stiffness can and should be incorporated into the system so that the material can be administered through the trans-catheter system will be minimally invasive.

Table 1 Material properties of scaffolds used for cardiac tissue engineering

Fibrin	50Pa [194]
Matrigel1	30–120 Pa[195]
Type I collagen gels	20–80 Pa for 1–3 mg/ml[196]
N-isopropyl acryl amide	100–400 Pa-[197, 198]
Alginate	100 Pa to 6 kPa-[199]
Polyethylene glycol	1–3 kPa -[200]
Heart	50 kPa normal hearts , 200–300 kPa CHF hearts [201-205]

1.5 Aim of the study

The broad aim of the present study is to develop *in situ* gels based on gellan and to analyse whether they may be used for the delivery and differentiation of pluripotent stem cells towards the cardiac lineage.

This goal was divided in to three parts

1. The first aim of the study was the development and characterization of various hydrogel with varying concentration and crosslink with various concentrations of calcium chloride

2. The second aim of the study was to analyse whether Gellan when blended with HPMC improves the properties of the overall scaffold matrix enough to make a difference in the delivery of and differentiation of cells

3. The final aim was to immobilize signaling moieties within the gellan matrices for differentiation

1.6 Thesis outline

The thesis is divided into 6 chapters. The first describes the introduction with the inspiration to carry out the work. The second chapter describes current literature in the space of scaffold material and nanoparticulate systems that have been used to deliver small molecules for differentiation of stem cells for cardiac regeneration. Further this chapter also elucidates the gaps in the literature that need to be addressed. The third chapter describes the methodology and plan of work that was undertaken to tackle the problem at hand. Chapter 4 describes the characterization of gellan and gellan blended with other materials to evaluate their properties when crosslinked with different concentrations of calcium chloride as a crosslinker. This is important when used as an *in situ* gelling agent for, when administering the crosslinking and the polymer separately to gel at the site of infarct. Chapter 5 discusses how different crosslinking densities of gellan affect the

differentiation properties of embryonic stem cells towards a cardiac lineage. Chapter 6 describes the characterization and differentiation of cells with nanoparticulate systems delivering retinoic acid which is a well-known agent for the differentiation towards a cardiac lineage.

Chapter 2

Literature survey

2.1 Introduction

Ischemic heart disease related deaths account for 11.2% of deaths worldwide, and top the list of reasons for death according to the World Health Organization (WHO) statistics (http://www.who.int/mediacentre/factsheets/fs310/en/index.html 2012). Ischemic injury of the heart causes loss of blood flow along the coronary arteries supplying the heart mainly affecting the flow to the ventricular portion of the heart. This leads to tissue death and subsequent scar formation due to fibroblast infiltration. The relatively low regenerative potential of the resident cardiac stem cells (CSC) is insufficient to repair this type of damage. The primary event at the site of infarct is cellular necrosis, with edema localized at the site of ischemia. Studies suggest apoptosis of cardiomyocytes is the major cause for remodeling of the heart after a myocardial infarct. Although seemingly insignificant, a persistent 0.2% cell apoptosis can, over a lengthy period of time, cause substantial damage to the heart [1]. As has been indicated by a comprehensive review, apoptosis is a normal occurrence during fetal development [17]. The apoptosis at the site of infarct also induces expression of fetal genes such as brain natriuretic peptide and atrial natriuretic peptide. Oxidative stress at the site of the infarct causes expression of tumor necrosis factor resulting in free radical production causing fetal gene expression [2-6]. Cardiac myocyte contractions are inhibited when cytokines released during inflammation activate nitric oxide synthetase-2 [7, 8].There is infiltration of fibroblasts with the deposition of collagen and fibrin, resulting in scar tissue formation [9]. The resultant damage leads to an increase in tensile strength and elongation and wall thinning of the heart, commonly known as “infarct expansion” [10]. Details of the mechanisms involved in the process can be found in the thorough a review by Pfeffer and Braunwald [9]. Tumor

growth factor-β (TGFβ), angiotensin and endothelin expression are a direct result of myocardial stretching [11-13]. Furthermore stretching of the myocardium may induce cardiac myocyte death [14].

Stem cells, being the most ubiquitously available proliferative cells that can differentiate into cardiomyocytes and smooth muscle cells, are most sought after to replace scar tissue. There is also a need to arrest the progression of the infarct with various means immediately after the infarct. Methods such as cardiac restraints, hydrogels, and patches have been proposed for the infarct condition, and while some of the methods are still nascent needing more research, others have reached clinical trials. Furthermore, scaffold materials are used to deliver cells temporarily or permanently to support the infarcted section of the heart.

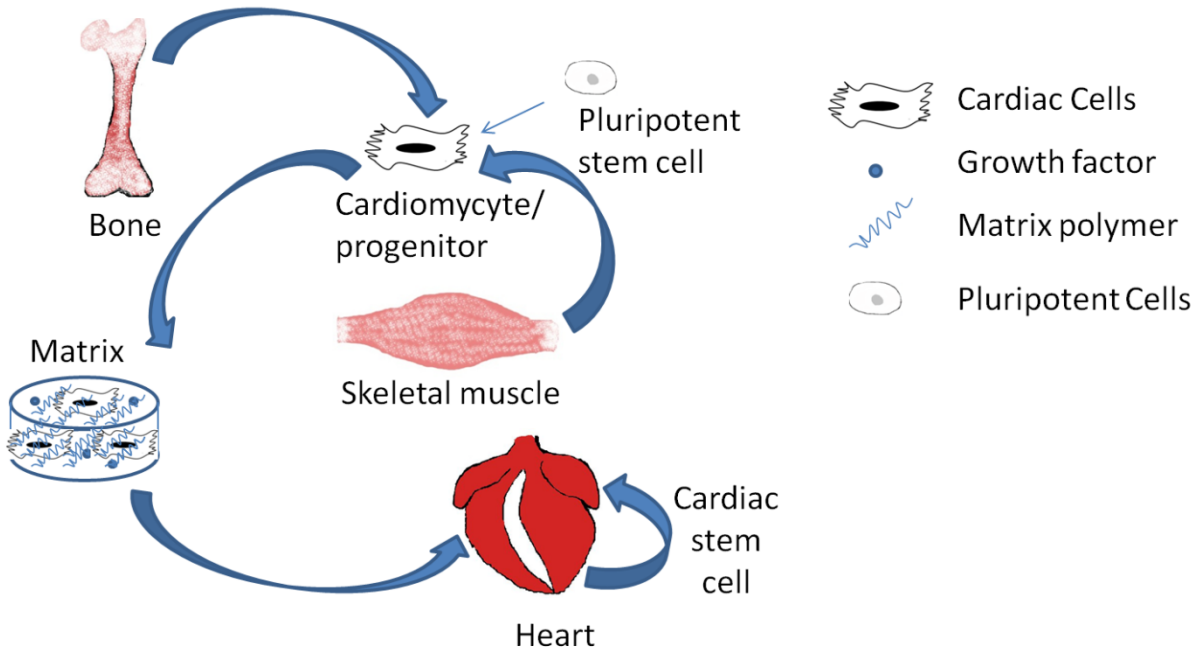

Figure 1: Cell sources for incorporation within scaffolds for delivery into cardiac tissue

2.2 Cell sources

The strategy required to mitigate the extent of infarct involves control and treatment at various levels of infarct progression. The primary goal should be to target the infarct as early in its progression as possible, ideally before scar tissue is formed. This may involve administration of anti-apoptotic agents in order to reduce cellular necrosis and resultant apoptosis that occur due to lack of oxygen [15]. The second goal should be the replacement of the scar tissue with cellular/molecular mediators that promote cardiac tissue regeneration and replacement of the scar. While figure 1 gives the broader nature of the application of cells after an infarct, figure 2 indicates the various cell sources that may be used for the treatment of Myocardial infarction (MI). Cardiac tissue primarily consists of cardiac myocytes comprising the musculature and vasculature. The vasculature consists of vascular endothelial cells and smooth muscle cells. The cellular populations to be delivered must incorporate these two tissue types. The modes of delivery of cellular payload can be systemic or localized. Various strategies for the transplantation of cells have been elucidated for the treatment of a myocardial infarct. An elegant review by Lin *et al*. discusses in detail the current landscape of clinical trial and the cells examined [16].

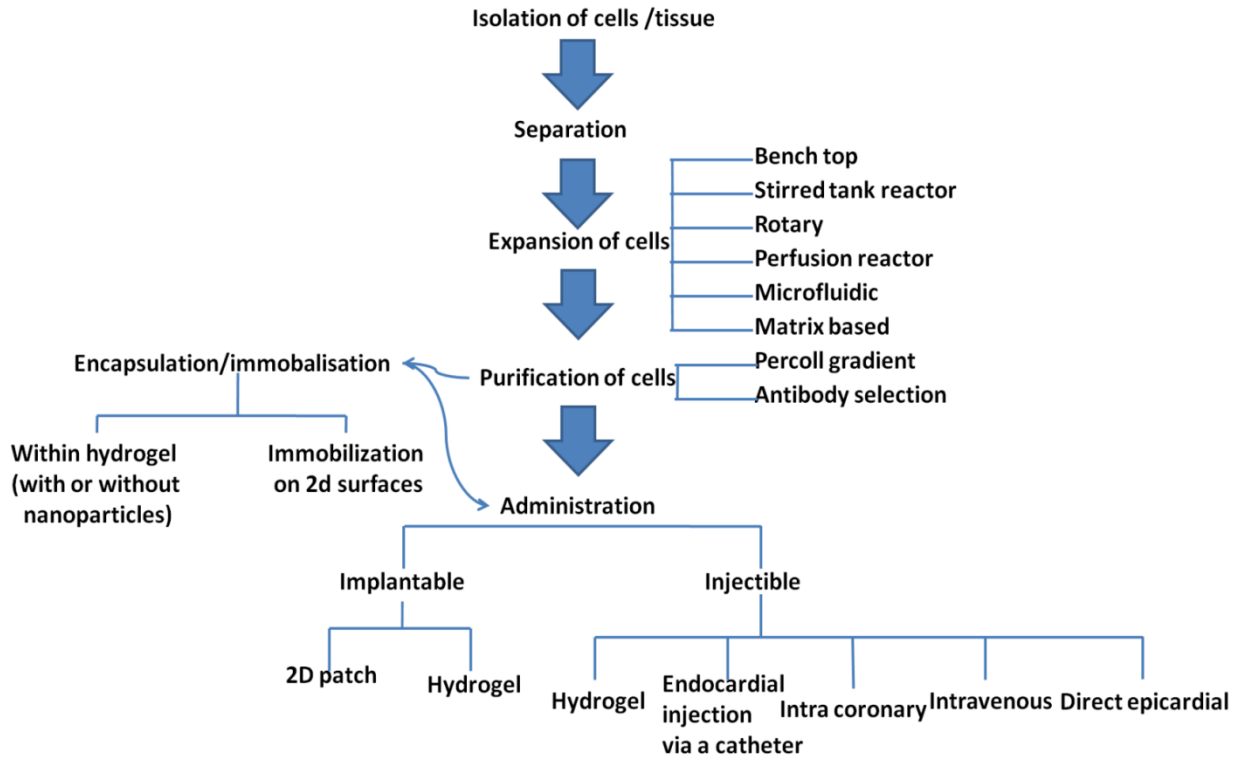

Figure 2 Schematic for differentiation through the embryoid body technique

2.2.1 Skeletal muscle myoblast

Skeletal myoblasts (satellite cells)have been classically identified as a stem cell population resident within non cardiac musculature, which can differentiate into various lineages, such as bone, cartilage and fat and identified by the markers Pax7 [18]. Recently, non-satellite $CD34^-$ and $CD45^-$ and Sca 1^- stem cell populations isolated from skeletal muscle cells have demonstrated rhythmic beating similar to cardiomyocytes in *in vitro* culture[19].These cells, once identified and isolated from muscle biopsies of patients, can then be expanded to the required number of around 0.6-0.8 billion cells *in vitro* [20]. These cells can further be modified to express markers like VEGF before transplantation into the heart.

Non satellite skeletal myoblast cells, when transplanted in adult mice, have shown trans-differentiation into cardiac tissue [19]. The resistance of satellite cells to ischemia *in vivo* has resulted in better retention times as well as higher survival rates [21]. Furthermore, new muscle formation which was found to beat when electrically stimulated [22].

Clinical application of these satellite cells needs to take into account the homing and retention of the cells, and the benefits accrued due to the cells. It was found that the catheter-mediated delivery of cells resulted in increased wall thickening at the target site and improved ejection fractions [23, 24]. Further improvements in the catheter mediated delivery resulted in 3-8% improvements in the ejection fractions, even to the extent of ventricular remodeling [25].

The autologous nature of the satellite cells, along with the structural benefits that these cells endow, does create a case for the suitability of this stem cell population for transplantation. Nevertheless, there is doubt as to whether the cells provide only structural benefits rather than form new cardiac tissue, due to lack of trans-differentiation to cardiac tissue[26, 27]. Furthermore, there are issues with engraftment; studies have reported low engraftment with over 90% injected cells dying within the first few days. This could, however, be prevented by entrapping the cells within scaffolds, providing continuous blood supply through angiogenesis, and activating survival pathways. Arrhythmia has been reported in ventricles of patients injected with injected with skeletal myoblasts [20]. Also, in view of limited clinical data to prove the efficacy of these cells, there is further scope for research [22, 28, 29]. Ongoing trials in this area are also trying to assess catheter mediated delivery of cells to the heart [30].

2.2.2 Adult bone marrow and blood derived stem cells

Bone marrow stem cells have been known to supply the entire repertoire of cells in the hematopoietic lineages, cardiomyocytes and various other lineages [31-38]. Among the various populations found, Lin^- c-kit^+, $CD133^+$, $CD133^-CD34^+$and c-kit^+ and $Sca1^+$ cells have been found to be suitable for cardiac regeneration [38, 39]. Although trans-differentiation of these cells has been reported [40], other studies refute these claims [41]. However, scaffolds prepared from type I collagen in the form of three dimensional (3D) conduit encapsulating bone marrow cells, having pores ranging from 1-10μm, have been developed [42].Cells within the scaffold expressed cardiac structural genes like α-MHC and β-MHC to sustained high levels for 28 days of culture, suggesting that the collagen scaffold environment was conducive to the growth and differentiation of the cells.

Adult bone marrow derived stem cells have shown positive effects in their regenerative potential. c-kit$^+$ and Sca-1$^+$ cells, when transplanted in mice, improved survival, cardiac function, regional strain, attenuated remodeling and decreased infarct size [43]. Lin$^-$ c-kit$^+$ cells, when transplanted, resulted in a significant occupation of the infarct areas with the transplanted cells [38]. Furthermore, the improvement accrued through c-kit$^+$ BMC cells transplantation was not due to cell fusion [44].Canine models have been studied for a comparison of catheter-based endocardial with direct epicardial injections of blood derived endothelial progenitors, as an alternative to intravenous administration of cells as shown in Table 1 [45]. No difference was found between endocardial and epicardial administration.CD 34$^+$ and CD 133$^+$ populations isolated from the umbilical cord blood have shown marked improvements in the heart when tested on infarct models [46-48]. This cell population was transplanted after transfection with AAV-Ang1 and/or AAVVEGF 165, resulting in improvements *Vis a Vis* improved diastolic pressures, increased contraction and improved ejection fractions.

Clinical trials like the TOPCARE-AMI trial and others suggest improvements within the heart are made with the administration of progenitors derived from blood and bone marrow [49, 50]. Although none have reported improvements in cardiac function, there is evidence to suggest that bone marrow stem cells, when administered at the site of ischemia, may reverse the effects of remodeling of the heart through paracrine signaling [51].

Furthermore, various reviews have reported a range of improvements in ejection fractions, varying from a minimum of 2 to a maximum of 7% improvement [52-54], but these improvements do not include LV remodeling [55]. In studies using the CD34$^+$ cell population, retrieval of clinically relevant numbers are not generated if *in vitro* expansion is performed before administration [48]. CD133$^+$ purified hematopoietic stem cells (HSCs) have also been tested but have shown only limited improvement in cardiac function [39, 56, 57]. Other studies have demonstrated that these stem cells do not transdifferentiate into cardiomyocytes in an infarcted heart [58]. Furthermore, Breitbach *et al.* have reported calcification and ossification at the infarct site, with the use of bone marrow stem cells [59]. To promote further work in this area, ongoing clinical trials are trying to assess the efficacy further [60-63].

2.2.3 Mesenchymal stem cells

Mesenchymal stem cells (MSCs) are defined by their property of adherence to plastic cell culture, expression of antigenic receptors for ($CD105^+$/$CD90^+$/$CD73^+$, $CD34^-$/$CD45^-$/$CD11b^-$ or $CD14^-$/$CD19^-$ or $CD79alpha^-$/$HLA\text{-}DR1^-$) specific antibodies. They also have the property of *in vitro* differentiation to lineages such as osteogenic, chondrogenic, and adipogenic [64].Koninckx *et al*. have shown that TGF-β enhances the myocardial differentiation of bone marrow–derived MSCs by the expression of TnT in monoculture and MHC in co-culture with rat neonatal cardiomyocytes [57]. They have also suggested that co-cultured hMSCs expressed the transcription factor GATA- 4, but did not express Nkx2.5 [65]. Although rat MSCs are able to differentiate towards cardiomyocytes when induced with 5-azacytidine or dimethylsulfoxide, human MSCs do not [41, 66]. Bone morphogenetic protein 2 (BMP2), or fibroblast growth factor (FGF)-4 have also been used to enhance the differentiation potential of rat MSCs *in vitro* [67]. Novel approaches for entrapment of cells within hyaluronic acid based 3D scaffolds have demonstrated that cell spreading occurs when matrix degradation moieties are present within the scaffold, especially in the presence of the RGD peptide moieties [68]. Furthermore, matrix stiffness has been shown to be a key factor in MSC proliferation within fibrin scaffolds [69].

Some studies suggest that MSCs, when injected intramyocardially, differentiated to vascular smooth muscle cells or endothelial cells *in vivo* and showed improvements via angiogenesis, in a porcine model of ischemia [70]. Furthermore, human umbilical cord blood derived MSCs, when transplanted into mice, resulted in improvements through paracrine effects [71]. Preconditioning of these stem cells with 5-azacytidine (5-Aza) resulted in differentiation of MSCs to cardiomyogenic cells, when transplanted into mouse models of MI; this prevented infarct expansion and eventually improved heart function improvement [67, 72]. Note, however, that 5-Aza is toxic in that it is a known DNA methylation inhibitor. BMP2 and FGF4 may alternatively be used for the differentiation of MSCs towards cardiomyocytes. Studies report that BMP2- and FGF4-treated MSCs, when transplanted into rat models, demonstrated improvements similar to 5-Aza treated cells [67]. Contrary to claims made about the lack of differentiation potential of MSCs, studies have shown that they differentiate to cardiomyocytes or fibroblast scar tissue when transplanted in rats, depending on the local microenvironment [73]. Furthermore,

Adipose-derived mesenchymal stem cells, on the other hand, have been used as cell sheets to repair the infarcted myocardial cells in rats, resulting in reversal of wall thinning of the myocardium [74].Cellular retention studies in porcine animal models transplanted with bone marrow derived MSCs, have shown that infarct border zone injection retained more cells than direct injection into the heart [75]. Cardiac functional improvements in porcine models after transplantation of bone marrow derived MSCs have attributed improvements to paracrine effects, while reporting retention of as low as 0.035% cells at infarct site after peri-infarct injection of cells [76]. A study by Toma *et al.* (2002) has shown that human mesenchymal stem cells, when injected intraventricularly into SCID mice, differentiated into cardiomyocytes with the expression of cardiac-specific troponin T, α-MHC, α-actinin, and phospholamban with visible striated fibers [77]. Furthermore ablation of pro-inflammatory receptors TNF-α on MSC has been linked to increased survival and reduced infarct size [78].

When allergenic hMSCs were transplanted, at various single dosages of (0.5, 1.6, and 5 million cells/kg), intravenously into human subjects in double-blind, placebo-controlled, randomized, dose-ranging phase I clinical trials, the subjects showed marked improvements with reduction of arrhythmias and improved left ventricular function [79]. The actual mechanism of action suggested is through a paracrine effect rather than cell fusion, or differentiation towards the cardiac lineage [80, 81]**.**

Clinical studies have shown that the administration of MSCs to the heart leads to a therapeutic result via a paracrine effect rather than differentiation of MSCs to cardiomyocytes, while others have suggested differentiation towards a lineage based on the environment. To realize the full potential of MSCs as therapeutic agents, their differentiation to cardiomyocytes, in order to replace the cellular losses caused due to an infarct, is vital. Cardiomyocytes as well as angiogenic progenitors, if produced by the MSCs, will replenish the cells from the depleted heart and increase circulation to the affected area. Clinical studies are underway to assess the advantages of autologous hMSC transplantation, transendocardially [82].

2.2.4 Cardiac stem cells

Cells expressing stem cell properties of clonogenicity, self-renewal potential and multipotency, in that they can differentiate to smooth muscle and endothelial cells have been found in the heart. These cells, by definition, fulfill the requirement of a stem cell: namely self-renewal, differentiation potential, repopulation of damaged tissue, and repopulation in the absence of damage. These cells were found to divide through paracrine signaling in the event of Ischemia [83], but the local loss of cells is not compensated by this division [84]. These cells renew at the rate of 1% per year at age 25 and 0.45% at age 75[85, 86].The different cell populations isolated and characterized are c-kit$^+$ cells, stem cell antigen 1 Sca1$^+$ (CD31$^-$) cells; isl-1$^+$ (c-kit1$^-$ and Sca1$^-$) cells and cardiosphere derived cells [87]. Sca1$^+$ when induced by 5-azacytidine (5-Aza-C) [84] or oxytocin [88] resulted in expression of cardiac transcription factors such as cardiac troponin1, sarcomeric a-actin, myosin heavy chain and Nkx2.5. Oxytocin induces differentiation of the Sca1$^+$ /c-kit$^+$ population to cardiomyocytes. Sca-1$^+$/CD31$^-$ cells differentiate to cardiac myocytes and endothelial cells in the presence of fibroblast growth factor (FGF), 5-Aza-C and Wnt antagonist Dkk-1 [88]. The cardiosphere (CS) is a cluster of self-adherent cells formed when human and murine heart biopsy specimens are expanded *in vitro* [89]. The core of the cardiosphere is composed of c-kit+ cells, while cells that exhibit endothelial and stem cell markers (Sca-1, CD34 and CD31) are on the periphery [90].

FGF-2 has been shown to play a critical role in the mobilization and differentiation of resident cardiac precursors in the treatment of cardiac diseases *in vivo* [91].Meanwhile, c-kit$^+$ cells have been found to solely mitigate regeneration of a damaged heart [92]. They also induce neovascularisation on transplantation via a paracrine effect [88, 93, 94]. Oxytocin activated c-kit-positive cardiac progenitor cells (CPCs), when injected at the site of coronary occlusion, differentiate to smooth muscle cells and endothelial cells [95]. Sca1$^+$ cells, on the other hand, show Connexin 43, cardiac troponin-I (cTnI) and sarcomeric a-actin expression after intravenous infusion into mouse hearts following ischemia/reperfusion [84]. Cardiosphere-derived cardiac progenitor cells contribute to improving ventricular function in mouse and swine models [90, 96, 97].

Autologous c-kit$^+$ cardiac stem cells isolated from the right atrial appendage have been clinically administered through coronary infusion into patients after expansion [98].

Left ventricular ejection fraction increased from 30 to 38% and the infarct volume decreased from 32.6 to 7.2 gm within 4 months of infusion [98]. Stamm *et al.* noted that the study although significant, used 13 non randomized subjects and changed the ratio of treated to control from (24:32) to (7:3) by the analysis stage, apart from publishing results mid way into the study, highlighting a few limitations with the study[99]. A separate study has harvested CDCs after generating cardiospheres from end myocardial autografts and demonstrated reduction in scar mass and increase in viable tissue in phase 1 clinical trials [100].

Clinically, relevance of this CDC transplantation is possible only after autologous cardiac tissue is harvested from patients during procedures like coronary artery bypass grafting (CABG). Although phase 1 clinical trials suggest improvements of left ventricular ejection fraction (LVEF) over bone marrow cell transplantation, there is further need for clinical data to ascertain the efficacy of these cells [100]. Additional work is required to ascertain the therapeutic role of these cells and their application.

2.2.5 Pluripotent stem cells

Embryonic stem cells (ESC) are cells isolated from the inner cell mass of blastocysts and which can give rise to the three germ layers, as well as giving rise to all the cardiac subtypes. With the advent of induced pluripotent stem cells in 2006 [101], a new opportunity presented itself towards the generation of pluripotent ES-like cells from somatic cells. It was shown that normal somatic cells could be converted to what are known as “induced pluripotent stem cells” (iPSC) by the forced expression of 4 crucial factors transcription factors: Oct4, Sox2, c-Myc and Klf4 [101]. This technology has proved itself by its application across various species and tissues [102]. ESCs have been studied to demonstrate the differentiation towards a cardiac lineage and expression of cardiac functions [103-109] and further to prove their proliferative capacity, since a large number of cells are required at the site of infarct [110, 111]. IPSCs too have shown properties of differentiation similar to ESCs [112-116]. Figure 3 indicates the various directed differentiation approaches used to differentiate ESCs towards the cardiac lineage. *In vitro* differentiation of ESCs has been optimized in mouse and human cell lines [117]. Protocols

have incorporated microparticles made from gelatin, agarose and Poly Lactic-co-Glycolic Acid (PLGA), into cellular aggregates to form differentiated spheroids, and to improve gene expression [118]. END-2 cells have been used to direct differentiation to the cardiac lineage and to improve the yield of cardiomyocytes population generated [105, 119, 120]. Extra cellular matrix [ECM] material stiffness is another aspect that is being studied to direct differentiation. A study showed that a dynamic module of ~8.6 Pa is suitable, and that differentiation was better in the presence of ECM as against collagen hydrogels supplemented with cardiac growth factors alone [121]. Conflicting results suggest that a matrix modulus of 31–35 kPa can support cardiospheres and show high expression of cardiac markers (cTnT and MYH6)[122], while hyaluronic acid/PEG hydrogel scaffolds with a dynamic modulus from 1–8 kPa influenced differentiation of chicken embryonic cells [123].

Although differentiation protocols have succeeded in increasing the efficiency of differentiation, a cause for concern with respect to the final administration of iPSC is the undesirable transfer of pathogens and ethical approval for transfer of cells co-cultured with other cells lines [124]; and thirdly isolation of cardiomyocytes from the undifferentiated population [125]. Immunological safety of iPSC were raised by Zhao *et al*. [126], but the obtaining of implanted tissue grafts from iPSC derived cells implies that these cells are safe to take to the next level in tissue engineering of patient specific cells[127]. Xeno transplants of mouse ESC into ovine models have proved that ESCs are immune privileged, as shown in table 1[128]. Cardiomyocytes derived from human ESCs have been able to repopulate rat hearts, suggesting an encouraging scenario for their use with humans [129].

Various aspects of cardiac regeneration - such as effective differentiation of stem cells, electrical and mechanical integration and especially long term effects without adverse side effects - are yet to be dealt with in addressing the issue of regeneration of the heart at the site of myocardial infarction [130]. In view of these shortcomings, there is a requirement for a concerted effort to enable the delivery of cells towards the site of infarct. IPSC and ESC are efficient autologous candidates towards that goal, more so since they develop into spontaneously beating cells *in vitro*. The Japanese government has given permission to conduct clinical trials for the treatment of macular degeneration using iPSCs,

suggesting a paradigm shift towards the use of pluripotent stem cells for therapy [131]. However, there is a risk of teratoma formation after the administration of pluripotent stem cells. Somatic cell nuclear transfer (SCNT) or somatic cell reprogramming offers a solution for the isolation of patient specific cells for treatment.

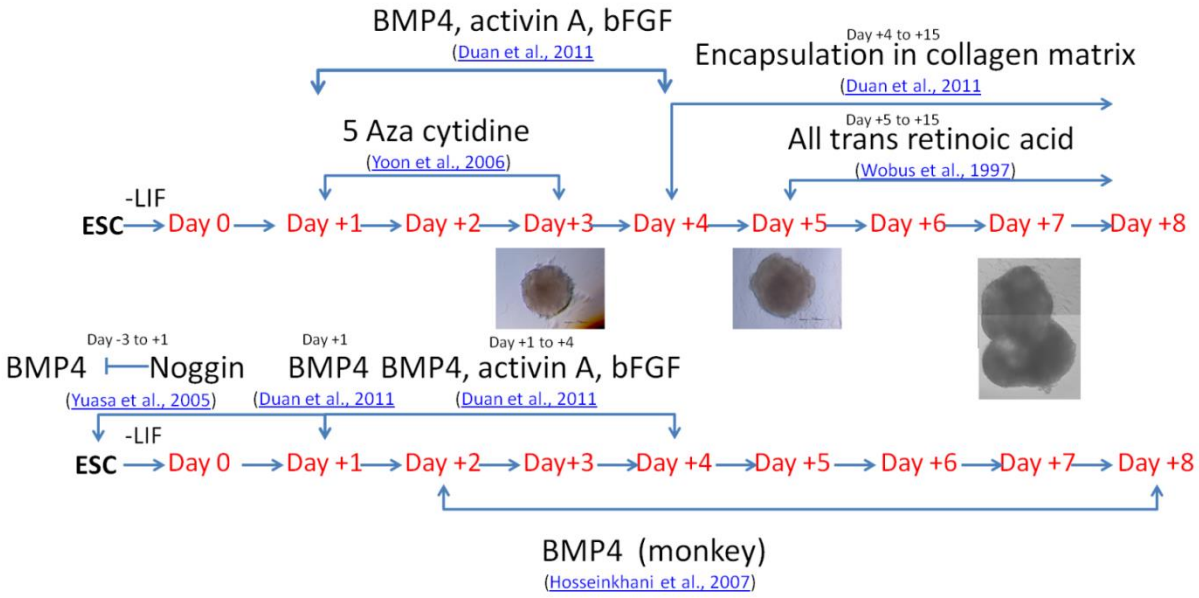

Figure 3 Schematic for differentiation through the embryoid body technique

2.3 Nanoparticulate systems

Classically nanoparticulate approaches were designed to deliver small molecules and drugs to patients, reducing the need for high dosages, and furthermore targeted approaches gave a tissue specific localization of the nanoparticulate matter resulting in amelioration only at the diseased site. Nanoparticles can be used here to deliver small molecules, i.e. anti-inflammatory drugs, to prevent inflammation caused by injury and ischemia; anti-oxidants, to reduce the free radicals produced as a result of inflammation; signaling molecules for differentiation, to aid directed differentiation of administered stem cells approaches. The approaches would restrict the area of inflammation and hence resultantly the area of scarring, thus reducing the impact of ischemia on the death of cells and neighboring tissue. Signaling molecules released under sustained conditions will

provide long term availability, in order to facilitate differentiation until the scar is healed completely.

2.3.1 Metallic nanoparticles

Super paramagnetic iron oxide nanoparticles have been used for labeling stem cells for MIR tracking [132]. Their suitability as agents for MRI tracking have been evaluated and it has additionally been proved, that the particles do not affect the differentiation potential of the stem cells nor affect their normal behavior in any manner. Superparamagnetic nanoparticles have been tagged to mesenchymal stem cells in order to facilitate targeting to the infarcted heart, which has resulted in reduced cardiac remodeling and improved cardiac function [133]. Silver nanoparticles used in many applications for implants have been shown to negatively impact the differentiation potential of mesenchymal stem cells [134]. Gold nanoparticles, on the other hand enhance the adipogenic differentiation in Mesenchymal stem cells [135]. Cerium oxide nanoparticles have controlled the progression of cardiac remodeling via inhibiting oxidative stress related proteins, the same mechanism has proved also to protect cardiac progenitors from oxidative stress related damage [136, 137]. Gold nanoparticles coated on to electrospun fibers have resulted in conductive surfaces, enhancing contractile motion of cardiomyocytes grown on the surface [138]. ECM scaffolds, employing a coating of gold nanoparticles, reduced fibroblast proliferation, reduced the excitation threshold for cardiac cells grown on the scaffolds and allowed faster electrical connectivity between neighboring cells within the scaffold [139]. Titanium oxide nanoparticle usage in cardiac imaging and treatment has been envisaged but not without its concerns about toxicity and reduced cardiac potential [140, 141]. Silica nanoparticles have been used as a carrier for adenosine, a cardioprotective agent, resulting in reduced remodeling in the heart further reducing the infarct size [142]. Magnetic nanobeads, have been used for the delivery of the VEGF gene, the transfection of which resulted in increased capillary density at the infarct site [143].

2.3.2 Natural lipid and polymeric nanoparticles

Lipid, oil in water emulsion systems for the delivery of bioactive agents has been in the offing, and the relatively reduced side effects have proved their usefulness. They are biodegradable, and nontoxic. In the cardiac space they have proved useful. Melatonin, a potent antioxidant, delivery and activity was enhanced when delivered through SLNs eliciting cardio protection [144]. SLNs have been employed to encapsulate and solubalise water insoluble agents, like all trans retinoic acid (ATRA), additionally act as a protectant for this light sensitive molecule [145-147]. Furthermore SLNs form effective carriers for the distribution and clearance of ATRA from the system [148]. Lipid nanoparticles, namely liposomes have been employed to encapsulate ascorbic acid [149]. Chitosan has been used to deliver EGF and FGF as growth factors in tissue constructs [150]. Furthermore chitosan has been successfully used for delivery of rhEGF in wound healing and tissue repair within fibrin gels [151]. Liposomes tagged with IgG antibodies, loaded with VEGF have provided a targeted mechanism towards the delivery of VEGF to the heart after an infarct. There was a 74% increase in perfused vessels and 21 % increase in anatomical vessels [152].

2.3.3 Synthetic polymer nanoparticles

Differentiation was induced in the HL-60 (Human promyelocytic leukemia cell line), by the delivery of retinoic acid via poly (ethylene glycol) (PEG)-poly (l-lactide) and PEG-poly (epsilon-caprolactone) polymer nanoparticles [153]. Retinoic acid was also successfully delivered through PEI nanoparticles, and elicited neuronal differentiation in mouse ES cells [154]. PEI has also been used for the delivery of VEGF gene for cardio protection. The delivery led to a significant increase in blood vessel density, subsequently improving heart function measured via improved ejection fraction and contractile function of the heart. Ascorbic acid is a potential signaling molecule for cardiac differentiation, and has been successfully encapsulated and delivered [155]. Nanoparticle delivery has also been used to deliver VEGF for the treatment of hypoxia for myocardial repair [156]. Delivery of placental growth factor (PGF), carried out through PLA PGA co block polymer nanoparticles, showed a higher expression of TIMP-2 and MMP proteins, suggesting a mechanism that may promote the expression recovery of TIMP-2 subsequently activating MMPs [157]. This would further inhibit the formation of scar tissues and improve

ventricular remodeling. Polyketal nanoparticles were successful in delivering the mitogen-activated protein kinase p38 inhibitor to apoptotic cardiomyocytes after infarction to prevent remodeling due to apoptosis and subsequently improving cardiac function [158].

2.4 Modes of application of stem cells in myocardial infarction

Table 2: Stem cell population used for clinical trials

Cells	Number of cells	Location and mode of delivery
Skeletal muscle cells	296 +/- 199 $\times 10^6$	NOGA-guided catheter system for transendocardial Injections[23]
Bone marrow stem cells	$7.35 \pm 7.31 \times 10^6$	Intracoronary infusion[50]
Mesenchymal stem cells	0.5 x 10^6, 1.6 x 10^6, and 5 x 10^6 cells/kg of the patients	Intravenous infusion[79]
Cardiac stem cells	500 000 12 x 10^6-25 x 10^6	Intracoronary infusion[98] Intracoronary infusion[98]

Various modes of delivery of cells to the site of infarct have been discussed extensively by Wozniak *et al*. plus the resulting inefficiencies of the methods involved [130]. There have been issues with retention of cells as well as homing of cells, with methods like intravenous infusion [159], intracoronary injection [160] and direct epicardial [161] or endocardial injection via a catheter [162, 163]. Although catheter based clinical trials for transplantation of skeletal myoblast showed improvements in the infarcted heart [23, 28], there are other studies to suggest a completely contrary scenario to the transplantation of

these cells [27].A method that will allow a small population of progenitor cells - either unipotent, multipotent or pluripotent - to be encapsulated and delivered to the site of infarct is desirable. This will facilitate retention until differentiation, and create a barrier between the undifferentiated population and the adult cells, preventing any adverse effects due to the undifferentiated population. This should facilitate paracrine effects, if any, without the harmful effects of the delivered cells, such as ossification and calcification. Furthermore, there is a need for direct contact of the tissue with the delivered material and cells.

2.4.1 Implantable systems

Cardiac patches

2D approaches have been pioneered in order to have strict control on the constructive elements that go into the scaffold, namely, growth factors, cells, and small molecules. Cardiac patches were developed to place elastic support with/without cells along the external ventricular wall of the myocardium for regeneration. ECM collagen has been used to prepare patches for treatment of MI by the transplantation of CD 133+ cells. Although there was visible angiogenesis at the site, the cells failed to differentiate to cardiomyocytes [164].Polyurethane (PU) and poly (ester-urethane) (PEU) rubbers are suitable candidates for the heart [165, 166]. When cardiomyocytes were grown on biodegradable polyester urethane urea (PEUU), the membrane could contract the patch [167]. Other studies have shown that phytic acid cross linked peptides, prepared by electro spinning; mimic the extracellular matrix in the heart [168]. Mouse iPSC derived cardiomyocyte cells have been used to prepare tissue sheets on thermo responsive polymers [169]. Poly(glycerol-sebacate) (PGS), another material whose mechanical characteristics can be tailored to match the heart, promoted the growth and beating of ES cell derived cardiomyocytes *in vitro* [170].Constructs with a combination of polytetrafluoroethylene, polylactide mesh, and type I and IV collagen hydrogel have been used to encapsulate MSCs [171].

PU is elastic and degradable *in vivo*. Animal trials of biodegradable PU patches promoted contractile phenotype smooth muscle tissue formation and improved cardiac

remodeling and contractile function at the chronic stage [167]. IPSCs derived tissue sheets, when implanted in mice, reduced left ventricular remodeling [169].

Poly (tetrafluoroethylene) reinforced porous poly (L-lactic acid) mesh seeded with bone marrow-derived mesenchymal cells and soaked in type I and IV collagen were sutured onto the rat infarct wall after a ventriculotomy. This resulted in a reduction in aneurysm elongation [171].

A combined approach using cells and nanoparticles within fibrin loaded patches was used after an infarct was induced in rats, resulting in significantly improved local and global heart function. Ventricular dilation was improved in hearts with patches containing cells and nanoparticles as compared to patches with only iron nanoparticles [172]. This provides evidence for a combined cell nanoparticle and scaffold approach for treatment

Ex situ gelled: Hydrogel scaffolds

Hydrogels have been widely used as their mechanical properties can be fine-tuned to match those of cardiac tissue. Table 3 compares the stiffness of various gels and the cardiac matrix.

Hydrogels with stiffness lower than heart tissue can be used as temporary space filling moieties, and further can be used to deliver stem cells and/or molecules for growth. In this regard, collagen injections into the ventricular wall have been shown to prevent progressive wall thinning, a sequel to permanent heart dysfunction, in rats [173]. Proof of concept for further application for collagen was envisaged by the encapsulation of chick cardiomyocytes and rat neonatal cardiomyocytes [174, 175]. Furthermore, hydrogels made up of ECM and collagen were able to differentiate human ESCs *in vitro* to cardiomyocytes [121]. Growth factor bFGF, along with mesenchymal stem cells, whereas delivered via encapsulating within thermoresponsive N-isopropylacrylamide (NIPAAm), N-acryloxysuccinimide, acrylic acid, and hydroxyethyl methacrylate-poly (trimethylene carbonate). These hydrogels were able to sustain the growth of the cells through bFGF release [176]. bFGF has also been used for improvement in vasculature by Iwakura *et al*. [177].

Leor *et al.* implanted, ESCs encapsulated in collagen type I, into intramural pouches at the infarct wall, resulting in reduction of fractional shortening. Carbohydrate polymers, like alginate, have been used for seeding cells and further implantation into mice to prove their efficacy as carriers for cells. These implants reduced left ventricular remodeling, and have been proposed as carrier scaffolds for iPSCs [178]. A novel approach was developed by Zimmerman *et al*., who developed tissue by casting a mixture of collagen type I along with neonatal rat cardiomyocytes into molds to form engineered heart tissue (EHT). These constructs were developed into ring-shaped flexible structures and sutured onto peri-cardiectomised rat hearts [179]. The ETH transplant became vascularised and electrically integrated *in vivo* and, furthermore, since these were prepared in serum free media conditions, immunosupression was not required during transplantation [179, 180].

Of all the constructs developed, the ones that were successful were those derived from native heart tissue. Further collagen type I and IV have also been successful in supporting cellular growth, cellular vascularisation and allowing electrical integration within the heart. In case of transplantation of pluripotent stem cells, it will be essential to differentiate these at the site with molecular mediators entrapped within the hydrogel; alternatively, one may use the stiffness characteristics of the hydrogel to differentiate the cells. Although robust, these approaches can be employed only by surgical intervention.

2.4.2 Injectable systems

In-situ gelling systems

Implantable systems can only be administered through invasive surgical approaches. Thus, implantation of these constructs will have to accompany procedures like CABG. *In situ* gelling systems, on the other hand, are defined by a sol to gel transition from *in vitro* to *in vivo* setups, respectively. This method of gelation may facilitate the administration of the gelling polymer through a catheter or as an injectable, facilitating a minimally invasive approach to cardiac treatment. In regard to this, the materials that have been studied extensively are fibrin glue [181, 182], collagen [173], matrigel [183], hyaluronic acid [184], keratin [185], extra cellular matrix [186, 187], alginate [178, 188, 189]. There are many potentially useful materials that can fulfill this role and are yet to be

tested in this application [190-193]. Endothelial cells home to a self-assembling injectable RAD16-II peptide scaffold and cause more angiogenesis as compared to matrigel. Potential myocyte progenitors also populate the peptide microenvironment created *in vivo*, and the retention of myocytes is higher as compared to matrigel [194]. Furthermore, this study demonstrated that ESC spontaneously differentiated to αMHC positive cells *in vivo* within the peptide scaffold. Cell survival was better within fibrin glue when delivered through injectable fibrin glue scaffolds compared with the cellular cardiomyoplasty technique, additionally inducing neovascularization and reducing infarct expansion [182].This was followed up with a study that suggested short term improvements of the alginate fibrin blends at the site of infarct [195]. *In vivo* studies via injection through a catheter to a rat heart demonstrated the injectability of a porcine heart derived matrix as well as endothelial cell infiltration within the matrix [186, 187].The method of delivery has been known to induce improvements within the cardiac environment with and without bone marrow mononuclear cells when injected with fibrin, collagen and matrigel, albeit separately [196, 197]. Other methods have been studied, such as collagen through catheter encapsulated with bone marrow cells [198] and without cells [173]. Both these studies showed improvement in LV function without vascularisation, but in the study by Huang *et al*, there was also an improvement in vascular density [197]. Another widely available tissue culture matrix called Matrigel™, has been used as an *in situ* gel. Studies have demonstrated improvement in LV function with the gel, and embryonic stem cells delivered along with it caused increased vascularization at the site of infarct [199, 200].Simulation of injection of material to the heart injected at various sites post infarct suggests that administration of a non-contractile material at the site of infarct helps reduce stresses on the myocardium [201]. Self-assembling peptides have been useful in the delivery of insulin-like growth factor IGF to the heart and permit the sustained release of the growth factor along with aiding the positive effects accrued to the cells delivered together with the peptide matrix [202]. Ungerleider &Christman have dealt with injectables and large animal models in detail, and according to their opinion, shorter gelling times are the main culprits for the failure of delivery of injectable gels through catheters [203]. Furthermore, expansion and encapsulation through cGMP processes, if not performed with adequate robustness, result in inefficient scaffolds. Alginate without cells is being currently

clinically tested for its efficacy to prevent ventricular remodeling [204-206]. Radhakrishnan *et al* have emphasized the importance of appropriate mechanical properties and electrical conductivity of the polymers used as injectables to be important in their overall regenerative potential [207].

2.5 Translational to the clinic (regulation and application, and mode of application)

With the innovations in cardiac support devices to provide care immediately after an infarct and to prevent cardiac remodeling, it was envisaged that the devices and innovations market in the cardiac space would get a boost [208-212]. But after a 10 year battle with the US FDA, the cardiac mesh support device has not seen the light of day, even after positive clinical results. Regulations are established for implantable devices, like cardiac stents, valves, pace makers and left ventricular assist devices (LAVD) like HeartMate® I and II [213], CentriMag, SynCardia Total Artificial Heart [214, 215]. However, there is no regulation for other implant materials, with or without cells, to mitigate therapy. On the other hand, heart injectable regulations are structured towards delivery of small molecules via intra coronary, intracardiac injections or with trans catheter approaches [203].

Properties of toxicity, biodegradability and physical characteristics, like stiffness of implant materials, are established in the literature. Implantation of patches, supports like cardiac assist support, and injectable non contractile supports are studied. Cardiac support patches can be administered in the event of superficial scarring of the heart, leading to loss of contractile tissue. In this approach, injectable hydrogels accompanied with cells can also be administered at the border zone to prevent remodeling due to scarring. Furthermore, reperfusion procedures, such as CABG, can be accompanied with such implantation of hydrogel grafts at multiple sites along the epicardium. This, along with reperfusion, will facilitate the in growth of stem cells and their final differentiation to cardiomyocytes. Additionally, with degradable materials, it is possible after a limited time period that the cells will be the only remnant of the procedure. Injectable materials like self-assembling

peptide matrices, e.g., RAD-16, fibrin glue with and without cells, alginate and agarose can be administered via a trans-catheter system, or a normal cardiomyoplastic approach, epicardially or endocardially [181, 182, 187]. Pluripotent stem cells accompanying the implant could address the problem of remodeling. The administration of hydrogel material serves as a two pronged approach; first, acting as a matrix to support the heart and prevent any remodeling due to the infarct; and, second, to allow retention of cells administered within it, further improving LV ejection fractions. Furthermore the hydrogel must be able to degrade over time and allow cells to take over the supporting role after tissue re-growth [216]. Although there are immense regulatory and translational challenges in the administration of just hydrogels materials, their application along with cells and growth factors is a long term goal [203].

2.6 Summary of literature

Cardiovascular diseases have the potential of becoming the leading causes of deaths in a few years. The site of infarct is a complex environment for the delivery of agents and many studies have elaborated on the outcome of therapies [130]. Various treatment methodologies are currently under extensive study for the mitigation of the sequel to the cardiac condition after an infarct [217]. Considering the drawbacks of delivery of bone marrow stem cells, mesenchymal stem cells, and cardiac stem cells to the site of infarct, it is necessary to investigate other suitable approaches for the treatment of the myocardial infarct [218]. Delivery of cells is fraught with issues like homing and retention of cells with the intravenous infusion [159], intracoronary injection [160] and direct epicardial [161]. Embryonic stem cells and induced pluripotent stem cells form a major source of self-renewing cells that can be differentiated into all types of cardiac tissue cells. These cells seem underutilized at the moment due to the ethical concerns in relation to embryonic stem cells, and the unknown potential of iPSC. These cells, especially induced pluripotent stem cells, can be taken forward by differentiation and proliferation. This is especially the case since many alternative approaches to the original integrative approach are available today for the generation of iPSCs [219-221]. Also, there is evidence to suggest that teratomas are not formed in immunocompetent individuals [222].

Therapies for cardiac regeneration require a multipronged approach including cellular, scaffold and growth factor *Vis a Vis* small molecule delivery. The importance of scaffolds and micro carriers is being realized in this regard [223]. Although catheter based systems being used for the delivery of skeletal muscle cells for clinical trials have proven to be better than most, there is still the need to innovate materials in order to deliver cells at a smaller dose with a targeted approach. This could include approaches wherein a small dose of pluripotent stem cells or a larger dose of Flk-1, isl1+, c-kit + or Nkx 2-5 positive cells are introduced within a tunable matrix to facilitate differentiation and intercalation *in-vivo*. Materials like alginate [178, 188], collagen [179] and porous poly (L-lactic acid) [171], have been studied for this effect. Transplantation of cells within matrices with preconditioning moieties like BMP4 and Activin can indeed be performed before administering these at the site of infarct. Furthermore pluripotent stem cells can be encapsulated within these matrices with modulated stiffness to differentiate and form cardiomyocytes [224]. These materials will have to mimic the stiffness of the developing heart and allow the cells to differentiate to the cardiac lineage.

Chapter 3

Plan of work

3.1 Objectives

The primary motive behind the study was to design injectable scaffolds for potential applications after the occurrence of a myocardial infarct. An i*n situ* gelling scaffold was designed in order to deliver the scaffold material minimally invasively through a catheter based approach. The scaffold is intended to be used to provide support as well as space filling in case there is infarct expansion, for the initial period until the stem cells differentiate to musculature and replace the scar tissue. Another aim was to facilitate the growth of myocardial tissue at and around the site of the scarring. Pluripotent embryonic stem cells were chosen which may grow through the scaffold network and also differentiate to cardiac tissue i.e. predominantly muscle. As against approaches which deliver skeletal cells that do not show integration, this approach is intended to deliver native cardiomyocytes. Further stem cells will provide a ready source of self-renewing cells to allow the growth and integration of the newly forming cardiac tissue. The entire approach envisaged with the use of in situ injectable scaffolds in conjunction with pluripotent stem cells is to evaluate whether this approach will provide materials in conjunction with cells at the site. With ES cells there is a need to isolate them from surrounding tissue in order to prevent immunologic reactions as well as teratogenic growth [1]. Encapsulating within degradable scaffolds can fulfill this criterion. The differentiated cells may proliferate towards the infarcted heart and healing can begin, at the same time the cells within the scaffold may provide a source of un-differentiated ES cells.

3.2 Selection of scaffolds material

In situ gelling systems have been used on various occasions for therapeutic usage. The mechanisms involved in *in situ* gelling are pH induction, e.g., cellulose acetate; temperature, e.g. phthalate polycarbophil and poloxamer; ionic. e.g., Alginate [2] and Gelrite[3] ™. Gellan gum is an exocellular microbial heteropolysaccharide that is secreted by the strain Sphingomonas paucimobilis. It is a linear anionic polysaccharide that consists of glucose, glucuronic acid, and rhamnose in the molar ratio of 2:1:116. The chemical structure is 1-3, instead of a 1-4, glycosidic linkage between the βD glucose and the αL rhamnose of the next repeat unit; this induces a twist in the linear chain of this polysaccharide, thus allowing for a helical conformation. Gellan random coils form double helices and subsequently aggregate to form three dimensional networks in an appropriate aqueous environment. Both monovalent and divalent cations stabilize the networks through cross-linking gellan double helices via carboxylate groups of gellan molecules. However, monovalent and divalent cations follow different mechanisms of gellan gelation. Divalent cations (M++) cross-link double helices directly (double helix-M++-double helix), while monovalent cations (M+) cross-link double helices indirectly (double helix-M+-water-M+-double helix) [4]. As a result of different gelation mechanisms, divalent cations are more effective on gel formation than monovalent cations [5]. Gellan has been studied for drug delivery and tissue engineering applications. Blends of Gellan HA [7]. Gellan blended with hyaluronic acid based gels have been designed as substitutes for the vitreous humor [225].

There has been interest in the combination of thermally responsive polymers with other naturally occurring polymers to modulate gelation characteristics as well as improve other properties like biocompatibility and biodegradability [8]. Of the polysaccharides under consideration are pH sensitive polymers like chitosan and ion sensitive polymers like alginate [9-12]. Blended polymer compositions like gellan and HPMC, ion and temperature responsive materials, respectively, have not been assessed to study their characteristics for tissue engineering applications. The study of such combinations that impart dual characteristics, in terms of gelation and variable stiffness, can shed new light towards preparation of tissue mimicking substrates.

3.2 Characterisation of scaffolds

In order to test the suitability of the scaffold material *in vitro* studies were performed to ascertain the suitability of the scaffold for its use as an *in situ* gelling material, its safety and its ability to support the growth of cells within its matrix. The following parameters were employed to study the characteristics of the polymer in solution so as to optimize the conditions under which it will behave as scaffolds for stem cell differentiation at the site of infarct.

1. Hydrogel formation and gelation time

Gellan was prepared and tested by the inverted tube test to ascertain the time for gelation along with varying the calcium concentration and temperature which would be required for it to transition from a sol to gel *in vivo* [13].

2. Rheology

Gellan was prepared with and without calcium ions to assess the differences in its rheological properties. From the storage G'' and loss moduli G" the flow characteristics of a material was characterized. Tan δ which is a ratio of G" to G' indicates whether a material will retain elastic characteristics over viscous characteristics. The higher the value of tan δ, the more liquid-like the sample, with a value of 1 considered to be a threshold between liquid and gel behavior. Further temperature and time sweep measurements can shed more light on the type of gelling characteristics the material will have at different temperatures. Strain sweep was carried out after which frequency sweep from 1-10 hertz was carried out at a constant strain of 0.5%. Temperature sweep was carried out at high frequency of 10 Hz and constant strain of 0.5%.

3. Contact angle

Wettability or hydrophilicity decides whether the materials will allow diffusion of nutrients within its matrix. Hence to evaluate wettability, the contact angle of the gels was measured with MilliQ™ water, phosphate buffered saline and serum in accordance with the procedure of Zhang et al. [14].

4. Imaging

Scanning electron microscopy (SEM) (Hitachi 3400N, USA) was performed on the lyophilized hydrogels. The imaging was performed at 100x and 200x magnification at 5kV.

5. Cellular cytocompatibility

Cellular cytocompatibility was performed to assess the relative toxicity if any that the material would have on the cells encapsulated within the matrix. This was performed with normal cell line e.g. L929 and Mouse Oct4 GFP ES cell line by SRB assay according to the method of Saehan *et al*.[15],

6. Cloud point measurements

This was performed to assess at what temperatures thermoresponsive material HPMC would fall out of solution and render the solution in homogenous. This is undesirable since phase separation would not be suitable to the characteristics of the scaffold.

3.3 Selection and Characterisation of nanoparticles

1. Choice of signaling molecule

The role of molecules like ascorbic acid [16], retinoic acid [17], etc. have been studied. We were interested in molecules that could generate cells with a higher ventricular morphology since the myocardial infarct regions are more focused towards the ventricular regions of the heart. In this regard, the role of retinoic acid is documented [18, 19].

2. Preparation of nanoparticulate systems

Lipid components were chosen from those that are abundantly present in heart tissue [20]. For the preparation of vesicles Soya PC and POPE were chosen and vesicles were prepared by modified thin film hydration method [21]. These vesicles were prepared with and without the retinoic acid.

3. Hydrodynamic size and zeta potential

The lipid nanovesicles thus prepared were analysed for size and net charge

4. Imaging

Further characterization of nanoparticles was carried out with imaging techniques like scanning electron microscopy and transmission electron microscopy.

3.4 Differentiation

Differentiation protocols were to be followed as adaptations from those given in figure 3. In this protocol the ES cells were plated as hanging drops in the absence of LIF for 3 and 5 days after which they were plated in the presence of lipid nanovesicles and suitable controls till day 7. Media was changed to that of a lower concentration of serum on day 7 and further differentiated until day 19.

1. Differentiation within scaffolds

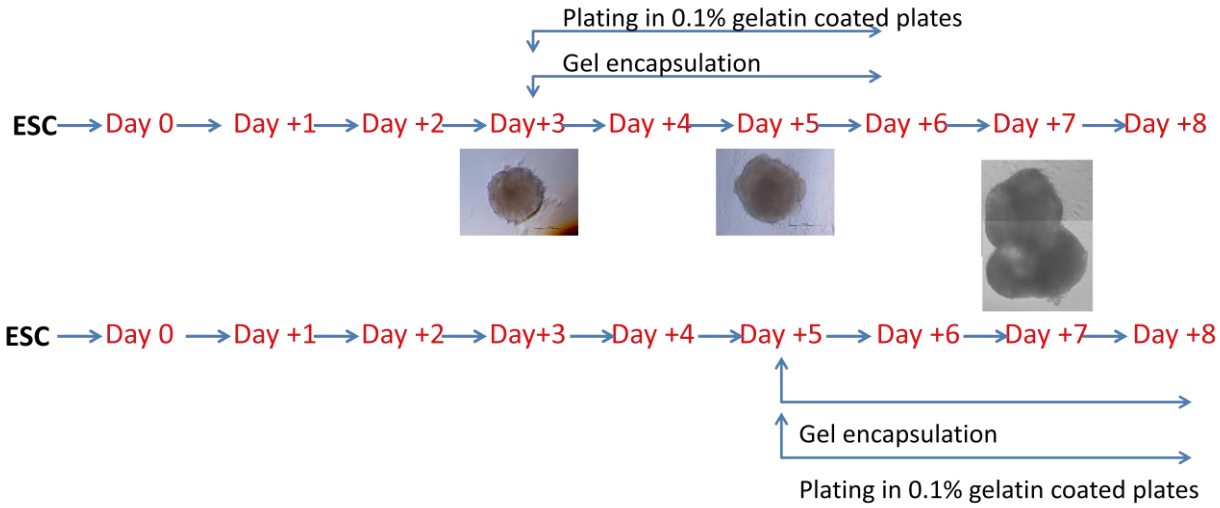

Figure 4 Differentiation protocol for scaffold mediated differentiation

2. Differentiation with nanoparticles

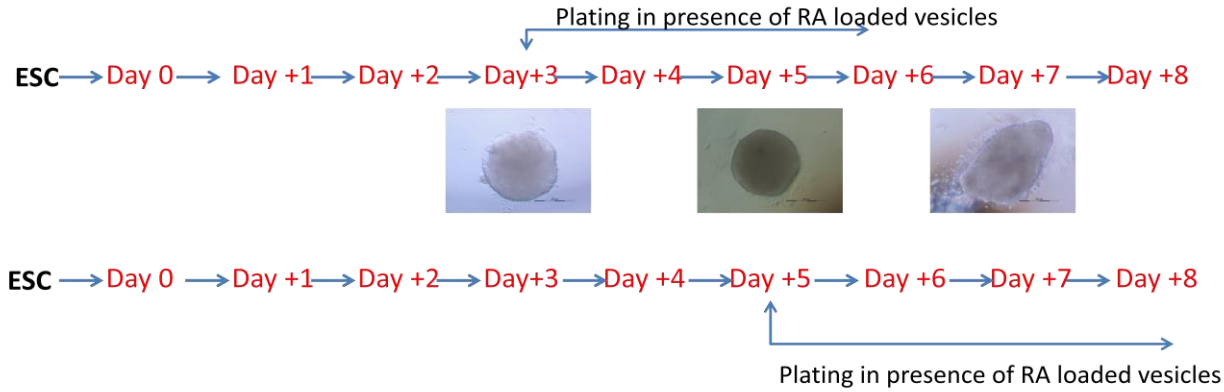

Figure 5 Differentiation protocol for nanoparticle mediated differentiation

Scaffolds were prepared after crosslinking with increasing concentration of calcium ions with an aim to evaluate whether a stiffer matrix is able to effect better differentiation. Hence we prepared varying concentrations of scaffolds to evaluate this approach.

Similarly partially differentiated cells were incubated in the presence of varying concentrations of retinoic acid encapsulated within lipid nanovesicles to analyse the difference of the presence of lipid nanoparticles to effect differentiation. It was expected that the increasing stiffness via the crosslinking with calcium would promote better differentiation of ESCs to cardiac lineage. We hypothesized that the use of lipid nanovesicles to deliver ATRA would in effect improve the delivery of ATRA; induce differentiation at a lower concentration of ATRA or both.

Chapter 4

Characterization of Gellan and Gellan Hydroxy propyl methyl cellulose (HPMC) blends for differentiation

Gelation of biopolymers like gellan and HPMC occurs as a result of triggers that bring about a change in the polymer network sufficient for it to aggregate and form hydrogels. The triggers range from chemical signals, such as pH, metabolites and ionic factors or physical stimuli, such as temperature or electrical potential. The main focus of much of current research has been temperature triggered and pH triggered systems due to their physiological significance [226-231]. Thermally responsive polymers can be defined as those with an upper critical solution temperature (UCST) i.e. shrink by cooling below the UCST; those with lower critical solution temperature (LCST) i.e. contract by heating above the LCST. Hydroxypropyl methylcellulose (HPMC) is an example of such a polymer, chemically presented as C6H7O2 (OH) x (OCH3) y (OC3H7) z with x + y + z = 3, which has the property of reversibility from sol to gel state mediated by temperature [232]. This property of HPMC has been utilized in drug release systems [233-235].This mechanism of gelation has been used to devise delivery systems and also in tissue engineering as non-invasive in *situ* systems [236]. Ion triggered polymers like Gellan gum, an exocellular microbial heteropolysaccharide that is secreted by the strain Sphingomonas *paucimobilis,* are also of interest [237]. It is a linear anionic polysaccharide that consists of glucose, glucuronic acid, and rhamnose in the molar ratio of 2:1:116. Gelation in Gellan as indicated in figure 6 is triggered by mono as well as divalent cations like sodium and calcium. The combination of the two polymers as a blend scaffold was envisioned to utilize the triggers for gelation of both polymers in order to create a faster gelling matrix for tissue engineering applications.

There has been interest in the combination of thermally responsive polymers with other naturally occurring polymers to increase their gelation characteristics as well as improve other properties like biocompatibility and biodegradability [238]. Of the polysaccharides under consideration are pH sensitive polymers like chitosan, ion sensitive polymer like alginate [228, 229, 236, 239]. Blended polymer compositions like gellan and HPMC, which are ion and temperature responsive materials respectively, have not had assessed their characteristics for tissue engineering applications. The study of such combinations that impart dual characteristics, in terms of gelation and variable stiffness, can shed new light towards preparation of tissue mimicking substrates.

The basis of this chapter is to ascertain whether the ion responsive gellan alone or when blended with thermoresponsive HPMC, can form a suitable triggered system for tissue engineering. Different blends of the polymers at varying ratios of the components were prepared. The thermal behavior of the hydrogel systems was evaluated by cloud point measurements on blends without crosslinking and rheology measurements at various temperatures with the crosslinked hydrogels. The hydrogel was also tested for hydrophilicity with contact angle measurements with fluids like water, phosphate buffered saline and fetal bovine serum. Scanning electron microscopy was performed to visualize the internal architecture of the gels. Furthermore cellular compatibility was tested with MouseOct4 GFP ES cell line.

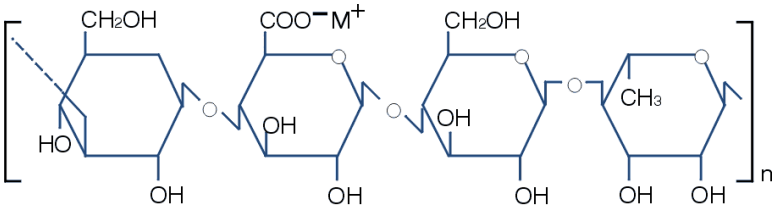

Figure 6 Structure of Gellan*Error! Reference source not found.*

4.1 EXPERIMENTAL METHODS

4.1.1 Material and methods

Gellan, in its deacetylated form, (food grade, KELCOGEL) was kindly provided by CP Kelco U.S. (Chicago, IL), Calcium chloride , D-Glucose, disodium hydrogen phosphate,

potassium chloride, potassium dihydrogen phosphate, glacial acetic acid and hydrochloric acid were purchased from Qualigen Fine Chemicals (Mumbai, India). HPMC, Calcein AM, Propidium Iodide (PI), Penicillin streptomycin, Sulphorhodamine B (SRB) were procured from Sigma Aldrich (St Louis, USA). Dulbecco's minimum essential media (DMEM), minimal essential amino acids (NEAA), Glutamax™ , Fetal Bovine serum (FBS) was procured from Invitrogen private limited (Carlsbad, CA, USA).

4.1.2 Hydrogel formation and gelation time

Gellan (G0.5) and gellan HPMC at ratio of 8:2w/w (0.5GH8:2) and 9:1w/w (0.5GH9:1) was weighed to the final concentration of 0.5% and heated to 90°C until a clear solution was obtained. Then it was heated to a constant temperature of 37°C until temperature is attained, 50mM calcium chloride was also maintained at the same temperature. When both attained 37°C the $CaCl_2$ was added into gellan and gellan HPMC solution, at continuous stirring of 650 rpm. This was then poured into tubes and time for gelation was assessed by inverted tube method [240]. Values reported are an average of three experiments$\pm$ Standard deviation.

4.1.3 Viscoelasticity

The rheological measurements were performed using a modular compact rheometer (Physica MCR 310). Fully hydrated samples were placed onto the plate of the instrument, using parallel plate geometry, to give a gap of ~3 mm [225]. The viscoelastic properties were quantified in terms of G' and G", the real and imaginary components of the complex shear modulus of the material. G', the storage modulus gives the elastic nature of the gel, while G", the loss modulus gives the viscous nature. Both moduli were calculated by using the instrument software Rheoplus/32 software version V3.21 (Anton Paar, Graz, Austria) that tracked the magnitude and phase lag of the torque for a given oscillatory frequency of the plate. G' and G" were plotted against the frequency of oscillatory stress and the resulting spectra termed as mechanical spectra was used to demonstrate the gel character and to discriminate between different classes of gels. G' and G" were measured across various frequencies from 0.01 to 10 Hz at the constant strain of 0.5%. All measurements were performed at physiological temperature of 37°C. The relative

contribution of the elastic and viscous natures can be quantified by the loss tangent, tan a, which is the ratio of the loss to the storage modulus:

$$\tan a = G'/G''.$$

The higher the tan a, the more liquid-like the sample, with a value of 1 considered to be a threshold between liquid and gel behavior.

Temperature sweep was also performed from 25°C to 80°C at a constant strain of 0.5% and at 10Hz.

4.1.4 Cloud point measurements

Thermal responsiveness of HPMC in aqueous solution is connected to its insolubility in aqueous solutions when the temperature is raised, which is referred to as its cloud point [241]. UV–VIS spectrophotometry (Perkin–Elmer Lambda 35) was used to determine the cloud point of the gellan, HPMC and gellan HPMC blends at ratios of 8:2 and 9:1 dispersed in Milli Q water to a final concentration of 0.5% w/v. To obtain the spectra, the temperature was raised at a rate of 2 °C/min and the optical density (O.D.) was measured over a temperature range of 25–90 °C. The LCST values were determined as given by Liu *et al.*, (2008).

4.1.5 Contact angle

To evaluate wettability, the contact angle of the gels was measured with MilliQ™ water, phosphate buffered saline and serum in accordance with the procedure of Zhang *et al*., [242]. Contact angles of gel were measured by the sessile drop technique using a CAM-100 optical contact angle meter (KSV Instruments, Finland), by depositing a 2 µl drop of water from a micro-syringe on the surface of gel dried onto the surface of a glass slide. The image of the drop was analyzed by an automated curve fitting program using the in-built software. All measurements were made immediately following deposition of the drop. All reported data are mean values of three experiments.

4.1.6 Scanning electron microscopy

Scanning electron microscopy (SEM) (Hitachi 3400N, USA) was performed on the lyophylised hydrogels. The imaging was performed at 100x and 200x magnification at 5kV. Pore diameter was calculated in software ImageJ of six images each of the hydrogels.

4.1.7 Pore Volume

Lyophylised scaffolds were immersed in a non wettable solvent n Hexane for a period of 5 min with constant mixing to ensure no bubbles were retained within the lyophilized samples and the porosity was measured (n =3)[243] . The porosity was calculated according to the following formula:

$$\text{Porosity} = ((W2 - W1)/ (W2 - W3)) \times 100$$

Where W1 is the dry weight of the scaffold, W2 is the wet weight of scaffold (including PBS solution), and W3 is the weight of the scaffold in PBS solution

4.1.8 Enzymatic biodegradation

To assess biodegradation, lyophilized gellan and gellan HPMC scaffolds were placed in a solution with 100 units/ml, amylase and 0.02% sodium azide, and shaken in a water bath maintained at 37° C. After the determined time, the scaffolds were removed, and washed three times with deionized water, pipetting was performed to ensure the all the water was removed. The scaffolds were then lyophylised to measure the dry weight of the undegraded matrices. The remaining weight (%) of the gelatin scaffold was calculated using the following equation:

$$\text{Remaining weight} = W_t/W_0 \times 100$$

Where W_0 is the initial weight of scaffold and W_t is the weight of the scaffold after degradation with amylase

4.1.9 Cell cytocompatibility

Cellular cytocompatibility studies of the hydrogel composites were evaluated with Oct4 GFP ES cell line by SRB assay according to the method of Skehan *et al*. [244], with

slight modifications. G0.5%, GH8:2 and GH9:1 at different ratios were made up to a final concentration of 0.5% and the required amount of calcium chloride was added such that final calcium ion concentration was of 1.5, 3mM and 6mM, and autoclaved. Gels were allowed to set and incubated with complete media for 24 h at 37 °C for extraction. Cells were grown in DMEM supplemented with 10 % FBS, NEAA, and Glutamax ™ and incubated in CO_2 incubator IncuSafe (Sanyo, Osaka, Japan) at 37°C under a 5% CO2 and saturated humid atmosphere. Nearly confluent cells in 25 cm2 tissue culture flasks were trypsinized with TrypLE™ Select (Invitrogen, USA) solution and resuspended in fresh medium. Cell counts were determined by haemocytometry. Resuspended cells were diluted accordingly and were plated at a concentration of 1×10^4 cells per well in a 96-well tissue culture plate and incubated in a CO2 incubator for 24 hours. After 24 h the medium was replaced with gel extract in quadruplicate and incubated for a further 24 hours. After 24 h the SRB assay was conducted. In brief, old medium with the insert extract was discarded and 100 µl of fresh medium was added. Cells were fixed by adding 50 µl of ice-cold 50% trichloroacetic acid slowly to the medium and incubating at 4 °C for 1 h. The plates were washed five to ten times with deionized water and dried in air. A 100 µl aliquot of 0.4% SRB dissolved in 1% acetic acid was added to the fixed cells, which was kept at room temperature for 20 min. The plates were washed with 1% acetic acid to remove unbound dye and dried at room temperature. An aliquot of 100 µl of 10 mM Tris base (Sigma, USA) was added to each well and incubated at room temperature for 20 min to solubilize the dye. Plates were read at 560 nm on a plate reader (Thermo Electron Corp., USA). Cell viability was measured as:

Viability= absorbance of sample/absorbance of control x100

4.2 RESULTS AND DISCUSSION

4.2.1 Gelation time

The rationale of keeping gellan separated from the crosslinker at a concentration where in it cannot gel by itself, is to facilitate *in situ* gelation via the crosslinker [245]. The gelation time becomes significant while administering the hydrogel polymers along with the crosslinker *in vivo* to obtain a solid gel *in situ*. Various researchers have mentioned standards for *in situ* gelation time, and a gelation time of ~30 min has been found to be suitable[246, 247]. Furthermore gelation time can be enhanced with the addition of HPMC,

which is thermoresponsive [248]. In this respect the average gelation for Gellan HPMC at a ratio of 8:2 was found to be 12 min at 37°C with 3 mM calcium, while with 9:1 with 3 mM calcium it was found to be 16 min, as shown in Table 3.

Table 3 Gelling time for the various gellan and gellan HPMC blends

Blends	Average Gelling time at 37°C
Gellan 0.5% with 1.5mM calcium	>30 min
Gellan 0.5% with 3mM calcium	26 min
Gellan 0.5% with 6mM calcium	<30 sec
Gellan: HPMC 0.5% 9:1 with 3mM calcium	12 $\pm$ 2.4 min
Gellan: HPMC 0.5% 8:2 with 3mM calcium	16 min

This suggests a difference of 6 minutes with the increase in the amount of HPMC. This difference was significant with a p value of 0.05. Gelation time of just gellan with 3mM calcium was found to be at 26 min, which was much higher than the blend after crosslinking. The difference in the gelation time can be attributed to the thermo responsiveness of HPMC at 37°C.

4.2.2 Viscoelasticity

The properties of the gel formed after crosslinking were assessed with the rheometer from frequency of 0.01 to 10Hz and plotted at frequency 10Hz as shown in Fig 7. It was also observed that in the absence of calcium the loss moduli of 0.5G is higher than the storage moduli, resulting in a loss tan value of >1 suggesting a blend with relatively more viscous nature as compared to the blends of gellan and HPMC.

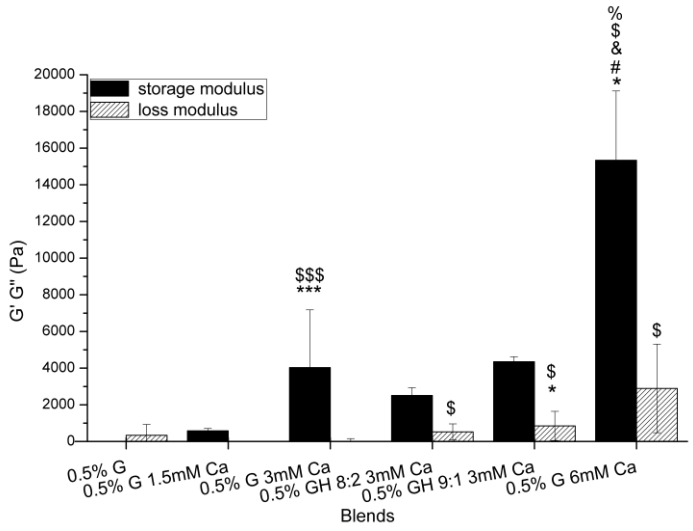

Figure 7Storage G' and loss G" moduli of various ratios of Gellan and gellan: HPMC ratios a. comparative storage and loss moduli plotted at 10Hz; b. storage moduli profile from 0.01 to 10 Hz. * indicates significant difference at p<0.05 at n=3, *** significant difference at p<0.005 at n=3. *Difference between gellan without calcium and others $ 1.5 and others %- 0.5GH82 3mMCa and 0.5G 6mM Ca storage; # indicates 0.5G 3mM Ca storage 0.5G 6mM Ca storage, &- 0.5GH91 3mMCa and 0.5G 6mM Ca storage, $$$ indicates p<0.005

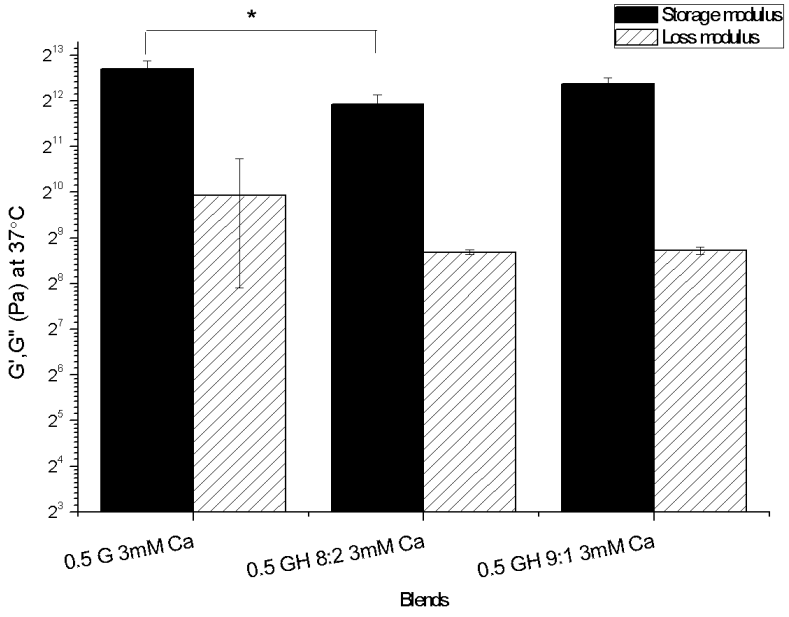

Error! Reference source not found.

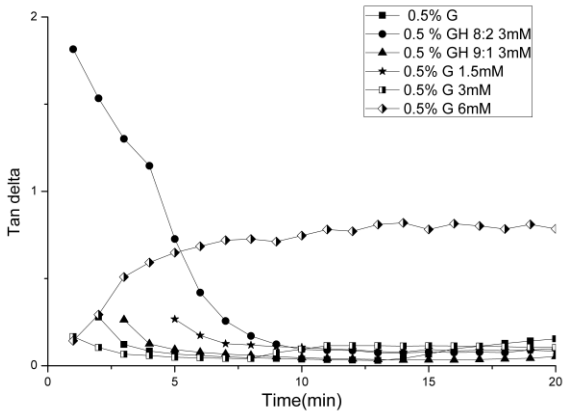

Figure 8*Time sweep of molten gellan and gellan HPMC blends at 37 ºC after the addition of calcium at a final concentration of 3 mM, at a constant frequency of 10 Hz. The plot indicates the ratio of G"/G'.*

An average tan δ for 0.5GH8:2 was 0.3 and for 0.5GH9:1 without calcium was 0.5 suggesting that HPMC increases the storage moduli as compared to 0.5G. A comparison of the gellan, HPMC and gellan HPMC blends crosslinked with calcium to form hydrogels showed that there is a significant difference between the loss moduli of 0.5GH9:1 with and without calcium and 0.5GH8:2 with and without calcium at $p<0.05$. There was a significant difference between storage moduli of 0.5G and 0.5G with calcium at $p <0.005$. There was also a significant difference in the storage moduli as well as loss moduli of 0.5GH8:2 with and without calcium suggesting in both cases that the increase in concentration of HPMC and addition of calcium affected both the storage and loss moduli. While in the 0.5GH9:1 blend only the loss moduli was significantly affected suggesting that the basal HPMC concentration has to be high enough to have a significant difference when calcium is added to the blend. This indicated that the gelation is triggered by calcium and the gelation time can be modulated on addition of HPMC (Table 3). Although there is significant difference between the storage moduli of the 0.5% gellan with calcium and that of gellan HPMC 8:2, the tan δ is not significantly affected at a $p<0.05$. The tan δ value is also not affected in the 9:1 ratio suggesting that the strength is similar to 0.5G crosslinked with calcium [249].

Temperature sweep measurements were performed from 25°C to 80°C at a constant frequency of 10 Hz, and data was plotted for 37°C as shown in figure 8. The results suggest

a significant decrease in storage moduli of 0.5GH8:2 with calcium as compared to G0.5 with calcium, while there is no significant difference with the GH9:1. The reduction in storage of 0.5GH8:2 showed no significant difference in the tan δ suggesting that the gel strength was similar to that of 0.5G. Tunable viscoelastic properties are known to be an asset to hydrogel materials for tissue engineering applications, and gellan HPMC gels can be used in this respect to be delivered as a support matrix and for cellular delivery [250]. Another property of relevance is the *in situ* injectibility of these materials which makes them ideal candidates for delivery of cells as well as small molecules. This is evident in all the matrices prepared that can be induced by calcium mediated gelation. Time sweep measurements of gellan HPMC gels as shown in figure 9 suggest a reduction of the tan δ within the first few minutes of addition of calcium after incubation at 37°C. This suggests that the storage moduli begin to increase over the loss moduli rapidly on the addition of calcium.

4.2.3 Cloud point measurements

One assessment of whether the polymer chains precipitate out of solution when blended is by the measurement of the cloud point of the blend. The change in transmittance by sweeping temperature from 25°C to 80°C is measured for all blends and that of G0.5%.

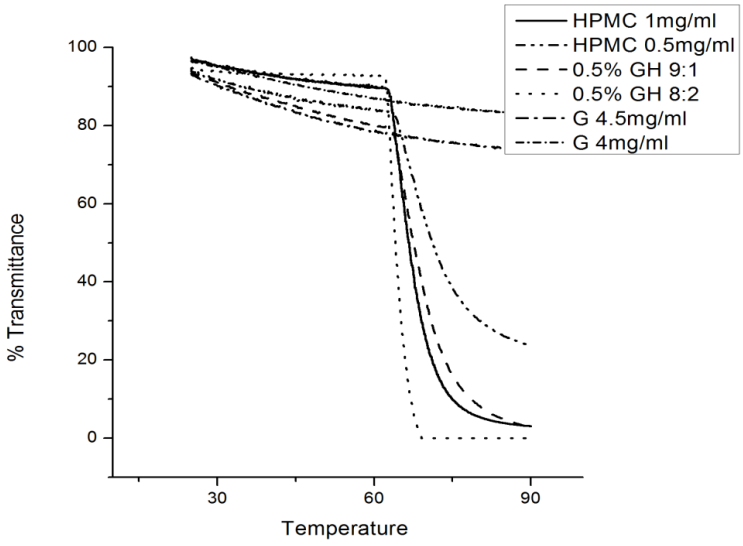

Figure 9 ***Cloud point plot of different ratios of Gellan and HPMC without the addition of calcium, with a temperature sweep from 25°C to 90°C. - HPMC at 1mg/ml; -.. HPMC 0.5mg/ml; --- 0.5% gellan HPMC at 9:1; ...0.5% gellan HPMC at 8:2; -.-. Gellan at 4.5 mg/ml; -. Gellan at 4.0 mg/ml***

It was observed that the transmittance decreased and this can be attributed to increase in opacity of the solutions as the temperature increases, also known as the cloud point as shown in Fig 10.The path of pure gellan dispersed and solubalised in water shows that there was no dramatic loss of transmittance on increase in temperature. As compared to gellan there was a dramatic loss of transmittance as the cloud point was approached in the gellan HPMC blends and HPMC dispersed in water alone. This can be attributed to the contraction of HPMC polymer strands in solution after reaching their LCST. The difference in the cloud point between the gellan HPMC blends and between the HPMC concentration can be explained by a concentration dependent difference in the onset and progression in the pattern on the graph in Fig 10[241]. 0.5GH8:2 showed a sharper decline in the LCST value as compared to the blends with just HPMC and that of 0.5GH9:1 and HPMC 1mg/ml as well as 0.5 mg/ml. This suggests that HPMC in the presence of gellan has a higher LCST value than HPMC alone. This property of the blend can be of use while applying in vivo. This phenomenon of concentration dependence of LCST, can explain the increased gelling time of 12 minutes of the gellan:HPMC 8:2 blend over the 16 minutes compared to the gellan HPMC 9:1 blend. Furthermore this phenomenon can enhance the temperature stability of the final hydrogels after crosslinking with calcium.

4.2.4 Contact angle measurements

The wettability and conversely the hydrophilicity can be determined by the angle of contact made by water and other biological fluids such as serum with the material. The gel matrix when tested for contact angle measurements with water, phosphate buffered saline and serum as seen in Fig 11. The angle of contact was found to be much less than <90°, suggesting that the hydrogels are wettable and hydrophilic in nature after gelation.

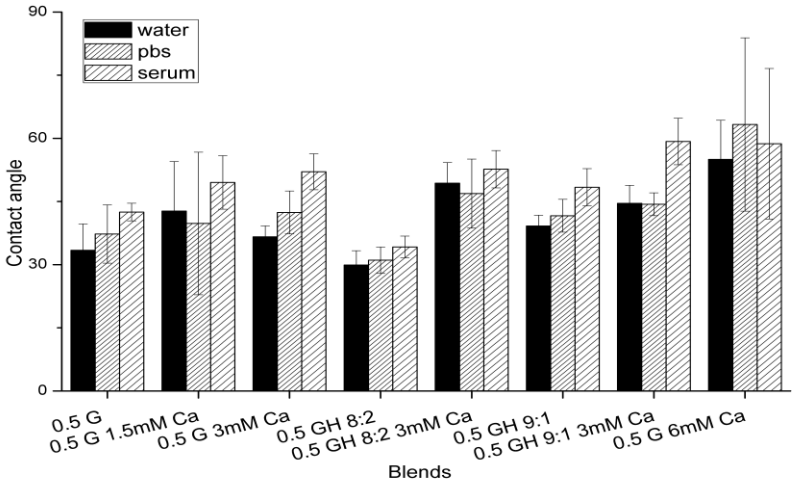

Figure 10*: Contact angle measurements with water, PBS and Serum of gellan and gellan HPMC blends with and without the addition of calcium.*

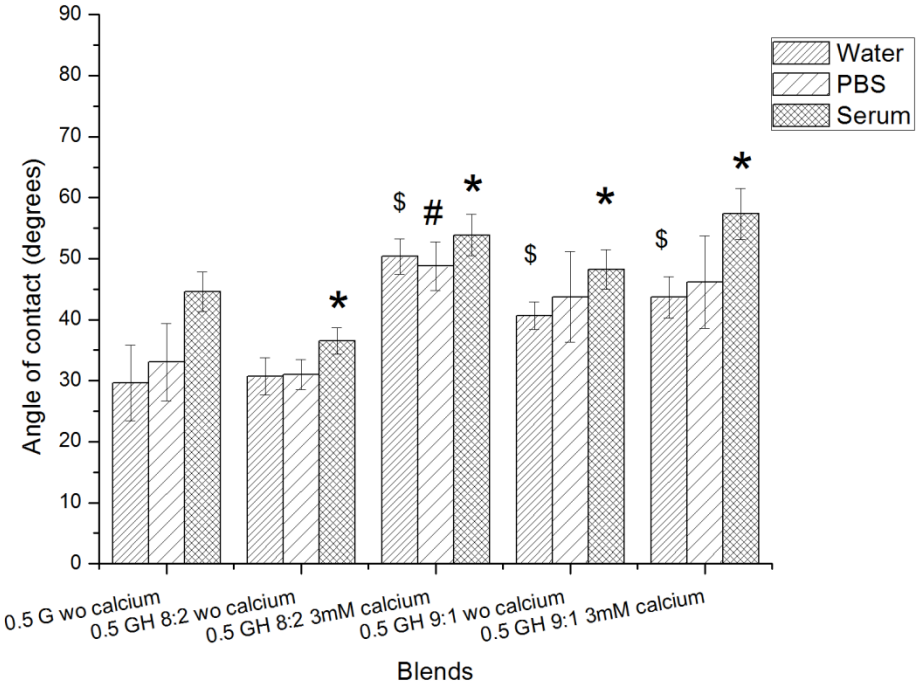

Figure 11 ***Contact angle measurements with water, PBS and Serum of gellan HPMC gels with and without the addition of calcium, * indicates a significant difference of serum contact angle as compared to 0.5% gellan without calcium at p<0.05. # indicates a significant difference of PBS contact angle as compared to 0.5% gellan without calcium at p<0.05. $ indicates a significant difference of Water contact angle as compared to 0.5% gellan without calcium at p<0.05***

As seen in figure 12 the contact angle for water with 0.5GH8:2 and 0.5GH9:1 with calcium and 0.5GH9:1 without calcium was significantly higher as compared to 0.5G without calcium. This can be attributed to the reduction in the charged carboxyl groups due to crosslinking with calcium. The contact angle with PBS was significantly higher only in 0.5GH 8:2 with calcium. The contact angle with serum was significantly lower in 0.5GH 8:2 without calcium, while significantly higher in all others tested, as compared to 0.5G without calcium. The hydrophilicity of the gels is an asset when cells are combined in the presence of hydrogels to be administered as scaffolds at tissue sites. The hydrophilicity allows cellular contact and adhesion for support. This also facilitates passage of metabolites across surfaces and into cells, resulting in growth and proliferation of cells. Although the contact angle increases in the hydrogel scaffolds as compared to those that are uncrosslinked, it is not >90°. Also the hydrogels form stiffer matrices as explained in the rheology after crosslinking and are suited for entrapment of cells *in vivo* and *in vitro*, while uncrosslinked gels flow.

4.2.5 Scanning electron microscopy

The use of the scanning electron microscope to map the cross section of the lyophylised gel shows us the internal porosity of the hyrdogel matrix as seen in Fig 5. The porosity of the gel is considerable considering the gel was lyophylised and this facilitated ingrowth of entrapped cells, and at the same time, allowed 3 dimensionally relevant spaces for the cells to grow and proliferate.

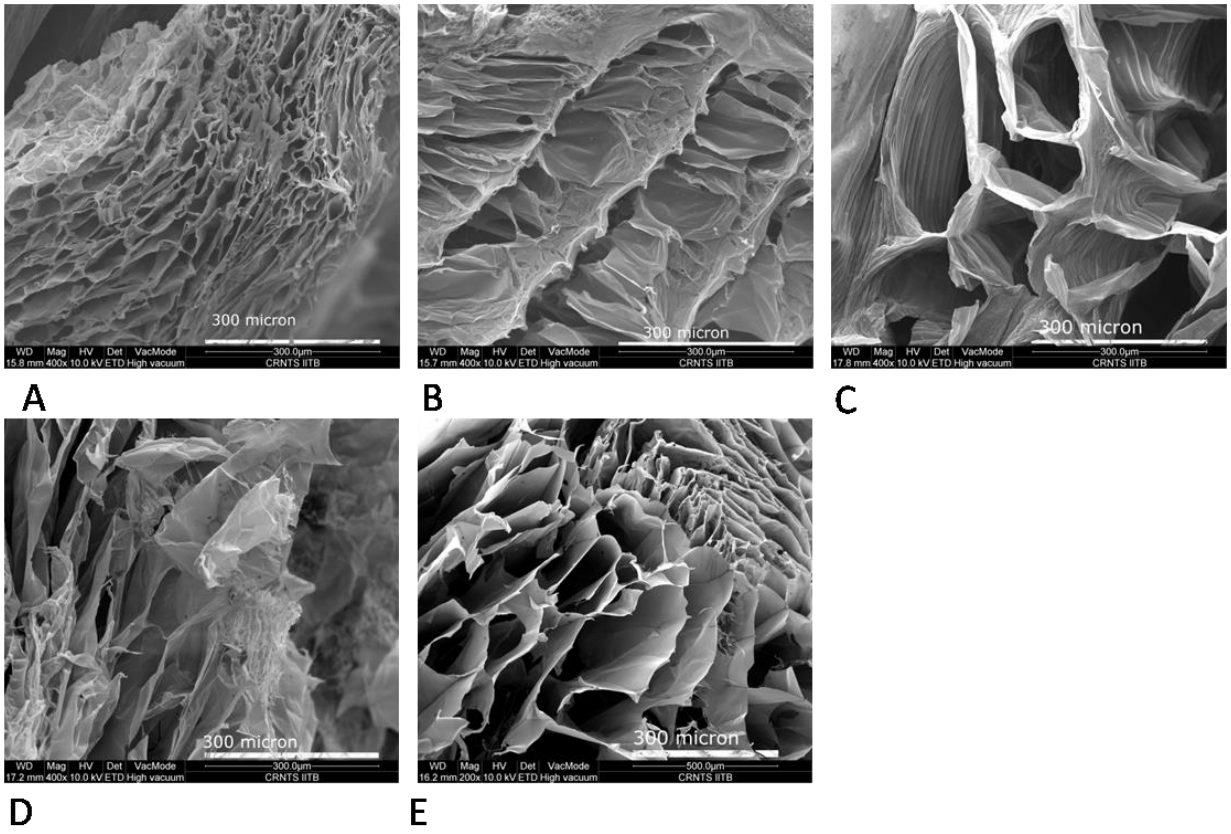

Figure 12 Scanning electron micrographs of the a. gellan crosslinked with 1.5mM calcium, b. 3mM calcium, c. 6mM calcium, gellan HPMC d. gellan HPMC 8:2 with 3mM calcium, e. gellan HPMC 9:1 with 3mM calcium

Pore diameter

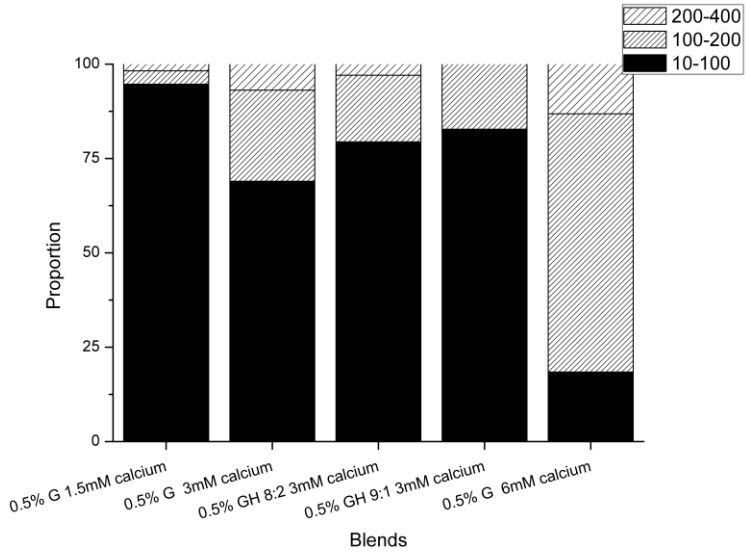

Figure 13*: Pore Size proportion for gellan and gellan HPMC blends*

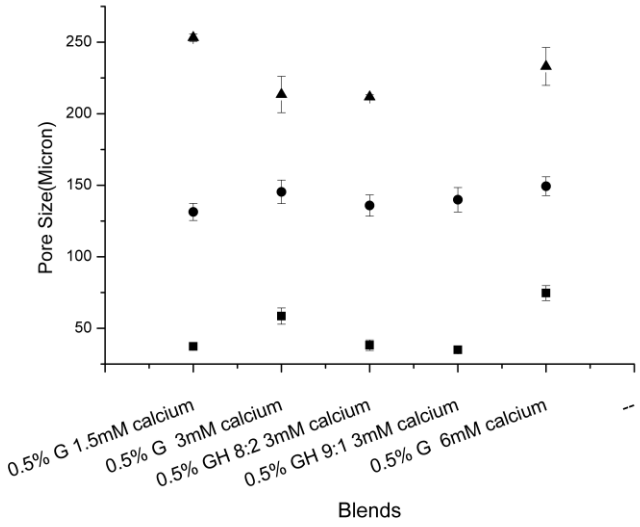

Figure 14*: Pore Size distribution for gellan and gellan HPMC blends*

0.5G6 has a higher proportion of pores within the range of 100-200microns, as opposed to the other hydrogel scaffolds, while 0.5G1.5 had a higher proportion of pores within the range of 10-100 micron as suggested in figure 14. This suggests a shift to a higher diameter of pores in scaffolds crosslinked with a higher concentration of calcium as

seen in figure 15. This further indicates that the scaffold inherently forming sheeted structures before coming together with other sheeted networks to form channels.

4.2.7 Pore Volume

The volume of pores present in all of the blends were in the range of 80 to 90 % suggesting that the porous volume of the scaffolds was occupied completely with water once hydrated as seen in figure 16.

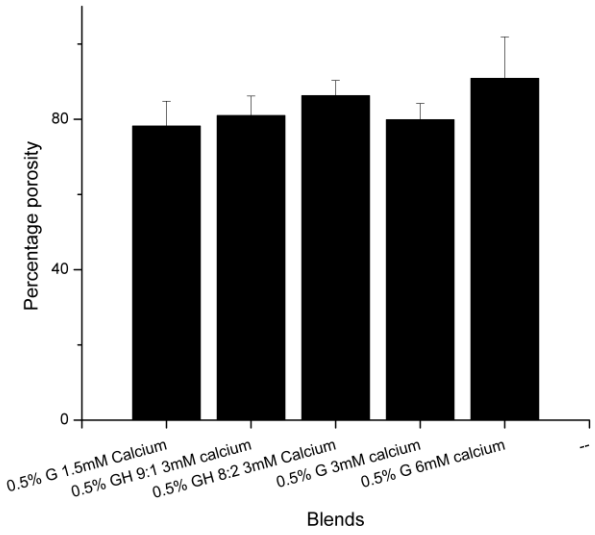

Figure 15 ***Pore volume of various hydrogels crosslinked with calcium with and without HPMC***

This also suggests that the hydrogels scaffolds have space for the cells to expand within its matrix structure and form vital three dimensional systems for cellular nutrient diffusion and support. No significant difference was found between any of the two hydrogel scaffolds.

4.2.8 Enzymatic biodegradation

Enzymatic degradation has been documented to cause the deposition of ECM in the form of vascular tissue in the cardiac space [251]. The process of degradation is also important for cellular incorporation to surrounding tissue, resulting in the loss and final elimination of scaffold and consequential integration of cells to tissue. The added deposition of vascular tissue at the site as reported will allow blood flow to the cellular components delivered through the scaffolds. The exposure to levels of amylase similar to blood levels demonstrated the mechanism *in vitro* degradation.

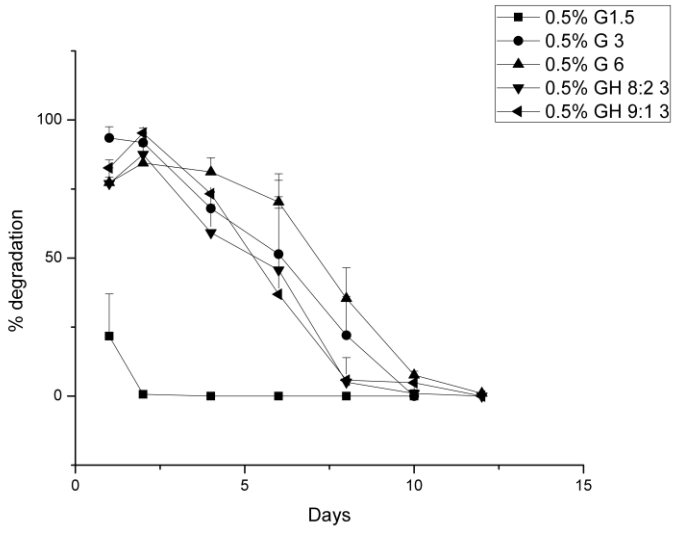

Figure 16 ***Effect of crosslinker concentration on the in vitro degradation of gellan and gellan HPMC blends***

As can be observed in figure 17 the scaffold incubated in the presence of amylase resulted in degradation over a period of 12 days. Crosslinking created a resistance to the rate of degradation with a lower concentration of calcium resulted in a faster rate of degradation compared to a higher concentration i.e. 3 and 6mM calcium. HPMC addition resulted in a degradation rate faster than 3mM calcium. In comparison to commercially available scaffolds all scaffolds fared better, while scaffolds crosslinked with 3mM calcium and 6mM calcium fared relatively better than those with 1.5mM calcium [252].

4.2.9 Cell cytocompatibility

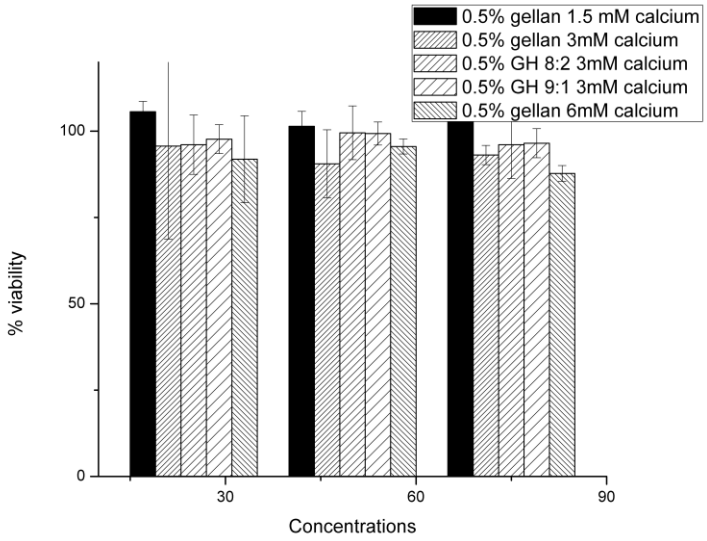

Figure 17 ***Cell viability with mouse oct4 GFP Embryonic stem cell line with gellan and various blends of gellan HPMC.***

Cytocompatibility was performed with mouse oct4 GFP Embryonic stem cell line. This was to demonstrate that normal cells as well as pluripotent stem cells are unaffected by the gel products that leach out into the surrounding medium. The viability was found to be in the range of 90-100 % when compared to the control. This property of the gels can further be used in cellular differentiation in combination with pluripotent and multipotent stem cells.

4.3 CONCLUSIONS and DISCUSSION

The average gelation time of the gellan:HPMC blends 9:1 and 8:2 was 12 min and 16 min respectively and that for 0.5% gellan was 26 min which was within the range of ASTM standards for in situ gelation [245]. Crosslinking with 1.5 and 6 mM calcium chloride formed gels which had gelling times unsuitable for in-situ gelation. This was further confirmed by rheology data which suggested that the gellan HPMC had a tan $\delta<1$ as compared to gellan without the addition of calcium. The 0.5GH8:2-3 blend showed promise and indicated that an increase in the concentration coupled with the addition of calcium improves the overall properties of the hydrogel so formed. Temperature dependent rheology suggested that 0.5GH8:2- with3mM calcium shared properties similar to 0.5%G-

with3mM calcium. The gels were stable as compared to 0.5G. The calcium crosslinked gels were porous and non-toxic indicating that the gels suitably network and ensure a viable environment. The extended viability of the cells in vitro within the gels makes 0.5G8:2 more similar to0.5G-3. The materials that can be administered under minimally invasive conditions in vivo are those that form the basis of delivery systems. As suggested these require a mechanism by which they can be administered in the sol form and must gel at site in order to enhance their capabilities as localized self-sustaining g entities. These entities must further support the infiltration and growth of cells by mimicking the environment at site. The blend of ion responsive gellan and thermoresponsive HPMC [248], whose gelation properties can be modulated by the concentration of HPMC and calcium is ideal for this application. The tunable rheological properties of the gellan can further be used for the differentiation of stem cells *in vitro*.

Chapter 5

Analysis of differentiation of embryonic stem cells within scaffolds

Stem cell differentiation has been studied extensively with the use of molecular as well as environmental triggers. In this regard Engler *et al*., proved categorically that the differentiation to specific lineages can be directed using the property of stiffness of the extracellular matrix [250]. Polymer materials have been studies in therapeutics for their properties of gelation and subsequent modulation of physical properties under the influence of triggers. Mechanisms based on pH induction such as in case of cellulose acetate phthalate are most suitably applied intra vaginally. Polycarbophil and poloxamer are temperature sensitive polymers while Alginate [253] and Gelrite ™ [254] are ion sensitive polymers, properties that are used to form hydrogels. Therapeutic use of the hydrogels has been studied based on the site of delivery to induce in situ gelation. Mechanisms based on pH induction such as in case of cellulose acetate phthalate are most suitably applied intra vaginally. Polycarbophil and poloxamer are temperature sensitive polymers while Alginate [253] and Gelrite ™ [254] are ion sensitive polymers, Furthermore triggers can be added externally to induce stiffening of the matrix in situ. Matrices to deliver stem cells can be used to effect differentiation via their properties of stiffness.

Gellan was chosen since random coils form double helices and subsequently aggregate to form three dimensional networks in an appropriate aqueous environment. Both monovalent and divalent cations stabilize the networks through cross-linking gellan double helices via carboxylate groups of gellan molecules. However, monovalent and divalent cations follow different mechanisms on gellan gelation. Divalent cations (M++) cross-link double helices directly (double helix-M++-double helix), while monovalent cations (M+) cross-link double helices indirectly (double helix-M+-water-M+-double helix)

[255]. As a result of different gelation mechanisms, divalent cations are more effective on gel formation than monovalent cations [256]. It has been studied for drug delivery and tissue engineering applications. Gelrite has been extensively has mostly been used for drug delivery [254, 257]. Some of the materials that have been evaluated include, Gellan HA [225]. Gellan HA based gels have been designed as substitutes for the vitreous humor.

ES cell differentiation to the cardiac lineage has been documented with defined protocols [106, 107]. Reports have also suggested improvements to existing methods in order to enhance the number of cardiac like cells that are produced during differentiation of ES cells *in vitro[258, 259]*.Three dimensional encapsulation of ES cells, or partially differentiated ES cells has been observed and studied recently[121]. But these approaches utilize ECM matrices isolated for xeno transplantation. Injectable matrices have also been evaluated but in the absence of a cellular payload, for support, and are being clinically tested [182, 260-262]. The need of the hour is a cellular transplantation along with the scaffold which can provide temporary support until the matrix scaffold degrades biologically *in vivo* and allows the cells to integrate within the host tissue.

In this chapter the approach of preparing gellan based scaffolds and encapsulating partially differentiated embryonic stem cells within the matrix was evaluated. This was done to evaluate whether the stiffness of matrices would three dimensionally affect the cardiac differentiation of partially differentiated ES cells and whether the cells would beat rhythmically. The effect of encapsulation on the cardiac gene expression of the cells was also evaluated.

5.1 EXPERIMENTAL

5.1.1 Material and methods

Gellan, in its deacetylated form, (food grade, KELCOGEL) was kindly provided by CP Kelco U.S. (Chicago, IL), Calcium chloride , D-Glucose, disodium hydrogen phosphate, potassium chloride, potassium dihydrogen phosphate, glacial acetic acid and hydrochloric acid were purchased from Qualigen Fine Chemicals (Mumbai, India). Calcein Am, Propidium Iodide (PI), Sulphorhodamine B (SRB) was procured from Sigma Aldrich (St

Louis, USA). Dulbecco's minimum essential media (DMEM), Penicillin streptomycin, Fetal Bovine serum (FBS) was procured from Invitrogen private limited (Carlsbad, CA, USA).

Mouse Embryonic stem cell media: DMEM(Invitrogen-11995-073) was supplemented with 15 % Fetal Bovine serum (Invitrogen- 10099-141), 1% GlutaMAX™ (Invitrogen-35050-061),1% penicillin streptomycin (Invitrogen 15140-122), 1X10^{3}units/ml mouse Leukemia Inhibitory factor (mLIF) of (Millipore ESGRO® (LIF)-ESG-1107), 0.1mM 2-β-Mercaptoethanol, 1%non-essential amino acids (NEAA). This was filtered through a 0.22 μ filter and stored at 4°C.

Mouse Embryonic stem cell media (ES media without LIF)

DMEM(Invitrogen-11995-073) was supplemented 15 % Fetal Bovine serum (JRH-ILO-403), 1% GlutaMAX™ (Invitrogen-35050-061),1% penicillin streptomycin (Invitrogen 15140-122), 0.1mM 2-β-Mercaptoethanol, 1% non-essential amino acids(NEAA). This was filtered through a 0.22 μ filter and stored at 4°C. Mouse Embryonic Fibroblast media (MEF media)

DMEM (Invitrogen-11995-073) was supplemented 10 % Fetal Bovine serum (JRH-ILO-403), 1% GlutaMAX™ (Invitrogen-35050-061), 1% penicillin streptomycin (Invitrogen 15140-122), 1%non-essential amino acids (NEAA). This was filtered through a 0.22 μ filter and stored at 4°C for further use. Each time the media brought to 37°C before use.

5.1.2 Hydrogel formation and gelation time

Gellan (G0.5) and was weighed to the final concentration of 0.5% and heated to 90°C until a clear solution was obtained. After which it was placed at 37°C until temperature is attained, calcium chloride was also maintained at the same temperature. When both attained the temperature the $CaCl_2$ was added into the gellan solution such that the final concentrations of 1.5mM, 3mM and 6mM were maintained.

5.1.3 Gel encapsulation and differentiation

Mouse Oct4 GFP cell line maintained in embryonic stem cell medium was trypsinised and counted. A final cell number of 600 cells in 15μl was placed on the lids of

10cm Petri dishes filled with potassium phosphate buffer (pH 7.8) in cultivation medium containing 15% FBS without LIF. EBs formed as part of the protocol shown in figure 4 were encapsulated on day 3 and day 5 within gellan scaffolds crosslinked with different final concentrations of calcium i.e. 1.5mM, 3mM and 6mM. 50 mg gellan was weighed and dispersed in MilliQ water; this was heated until a clear solution was obtained. For encapsulation gellan solution and calcium was maintained at 37°C and mixed along with embryoid bodies to a final concentration of 1.5mM, 3mM and 6mM calcium. These were incubated at 37°C for 10 min until gelling occurred. For differentiation the encapsulated EBs were maintained in ES media without LIF, until day 7 after which the media was changed to MEF media till day 19. Media change was performed after every 2-3 days. On day 19 cells were trypsinised and stored for further analysis. Gel was further processed for rt-PCR and Q-PCR analysis.

5.1.4 Scanning electron microscopy

Scanning electron microscopy (SEM) was performed (Hitachi 3400N, USA) on lyophilized hydrogels containing encapsulated EBs. The imaging was performed at 100x and 200x magnification at 5kV.

5.1.5 Beating efficiency

Encapsulated embryoid bodies were visually observed for beating cells/beating bodies. Beating bodies were counted along with the beat frequency for all embryoid bodies. Time points of day 7, day 9, day 13 and day 19 were used for these observations.

5.1.6 Semi quantitative and quantitative RT PCR

For RT-PCR, RNA was isolated from cells using the RNeasy kit (Qiagen) following the manufacturer's instructions. RNA quality and concentrations were measured using the NanoDrop ND-1000 (NanoDrop Technologies, Australia). The isolated RNA was subjected to RQ1 DNase (Promega, Australia) treatment to remove any contaminating genomic DNA. cDNA was generated using the Superscript III enzyme following the manufacturer's instructions. Oligonucleotide primers have been described in APPENDIX table 1. The PCR amplification included a total 30 cycles of denaturation at 94°C for 45 s followed by the appropriate annealing temperature for 45 s and extension at 72°C for 45 s with first

denaturation step at 94°C for 5 min and a final extension step at 74°C for 5 min. PCR products were run on a 2% agarose gel at 120 V for 30 min. The primer sequences and the annealing temperatures are as given in appendix 1.

Quantitative PCR was performed with Power SYBR®Green PCR master mix in a 96 well format according to the manufacturer's instructions. This comprised a final volume of 25 µl, with 12.5 µl being the master mix, cDNA at a final concentration of 20ng, ultra-pure water and primers. Amplifications were performed starting with 10 min AmpliTaq Gold Enzyme Activation step at 95 °C, followed by 45 cycles of denaturation at 95 °C for 15 s and combined primer annealing/extension as given in appendix 1 for mlc2v, flk1 and cTnT 1 min. Fluorescence increase of SYBR green was automatically measured during PCR. Cycle thresholds cT) for the individual reactions were determined using iCycler iQ Real Time Detection System Software data processing software (Biorad, USA). All cDNA samples were amplified in duplicates and normalized against a β actin in the same plate.

5.2 Results

5.2.1 Gel encapsulation and differentiation

As seen in figure 19 uniform sized embryoid bodies were formed. These embryoid bodies in culture were encapsulated in 1.5mM, 3mM and 6mM calcium chloride crosslinked gellan.

A B

Figure 18*Mouse ES cell derived Embryoid bodies formed by hanging drop culture on a. day 3 of differentiation and b. day 5 of differentiation*

A B C

Figure 19 ***Spreading of day 5 encapsulated and differentiated mouse ES Embryoid bodies within crosslinked gellan matrix on day 19 of differentiation A. 1.5mM calcium; B. 3mM calcium; C. 6mM calcium. Images were taken at the same focal length and the images are a compilation of an overlay of multiple images taken at 10x magnification with the Olympus X51***.

Further when the embryoid bodies were observed on day 19 there was obvious spreading of the cells within the matrix of the gel indicating that the porosity of gellan was sufficient for the cells to migrate within the matrix of the gel. This in turn indicates that the cells when encapsulated and administered *in vivo* will permeate through the gel and spread to surrounding tissue in order to make contact.

5.2.2 Scanning electron microscopy

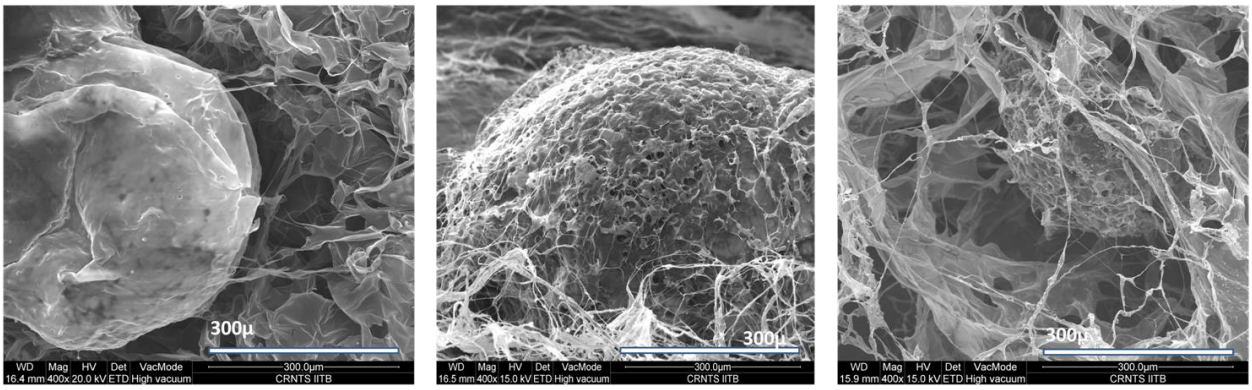

A B C

Figure 20 ***EB within gel encapsulated on day 5 of differentiation A EB encapsulated within 1.5mM crosslinked gellan as seen on day 19 B. EB encapsulated within 3mM crosslinked gellan as seen on day 19, C. EB encapsulated within 6mM crosslinked gellan as seen on day 19***

The scanning electron micrographs in figure 22 of EBs visualized on day 19 of encapsulated differentiation indicates the gel and cells from the EBs intermesh resulting in association of the gel matrix with the exterior cellular surface of the embryoid body. It was observed that the embryoid bodies are visibally embedded within the scaffold while the gellan fibres are intertwined within and around the embryoid bodies. It is clear from the figure 20 and 21 that the embryoid bodies were able to be encapsulaed within the scafffold matrix and could spread within the matrix architecture. This indicates that the gel matrix facilitates movement and growth of cells within its matrix through cellular association with matrix fibers for support. Spreading within matrix was not observed in day 3 encapsulated EBs as against day 5 encapsulated EBs.

5.2.3 Beating efficiency

A primary observation of the beating efficiency of EBs within crosslinked gels as against those plated were that on day 19 plated EBs ceased to beat And can be observed in figure 22A inset image there is an increasing beating efficiency on day 19 from 1.5 to 3 and 6 mM.

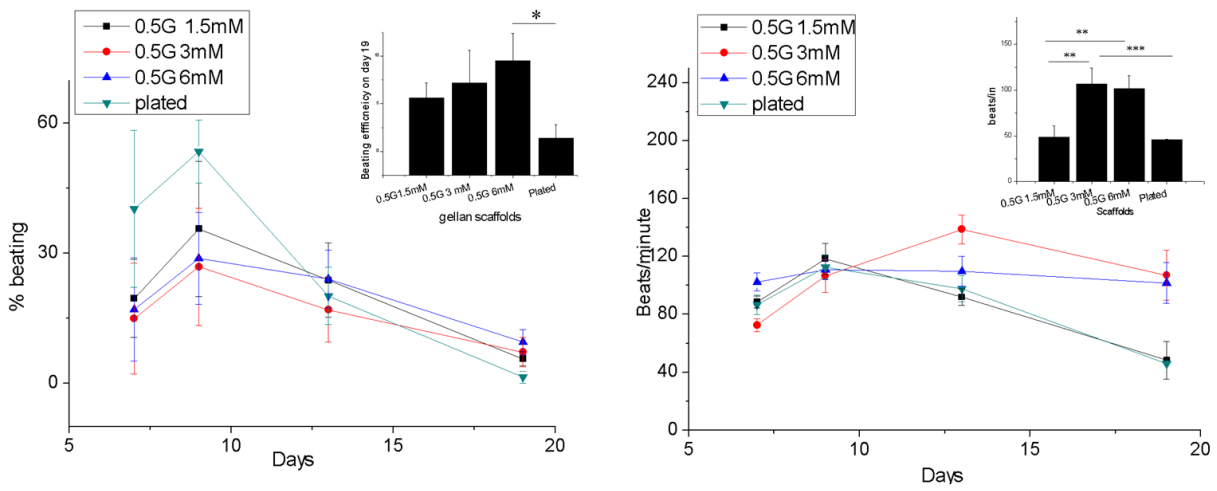

Figure 21 ***Percentage beating bodies on different days of differentiation when encapsulated as compared to EBs plated on day 5; A. total beating bodies at different time points; B. Average beating rate for different crosslink densities of gellan with calcium. * indicates p<0.1 with n=3, indicating biological replicates. **indicates p<0.05 and *** indicates p<0.005.***

Furthermore there is a significant difference at p<0.1 between 6mM crosslinked scaffold and the plated controls. The total percent beating EBs for the plated were much higher than the encapsulated EBs for day 3 and day 5, while on day 19 the number falls below 25% for plated EBs and further drops on day 19 of differentiation [106]. As seen in figure 21B inset, there is a significant difference in the beating rate of EBs encapsulated in 0.5G 1.5mM compared to 0.5G 3mM and 0.5G 6mM at p<0.05. Furthermore a significant difference in beating rates was observed between 0.5G 3mM when compared to the plated EBs p<0.005. The reduced number of beating bodies in encapsulated as against plated could be due to a lack of observation within the matrix. Encapsulation may restrict the beating rate and the enumeration of EBS. This can further be assessed by RT PCR analysis wherein gene expression levels can be assessed to elucidate whether the EBs do express cardiac markers and furthermore the quantification of these to assess whether the expression is greater than the plated EBs markers through Q-PCR.

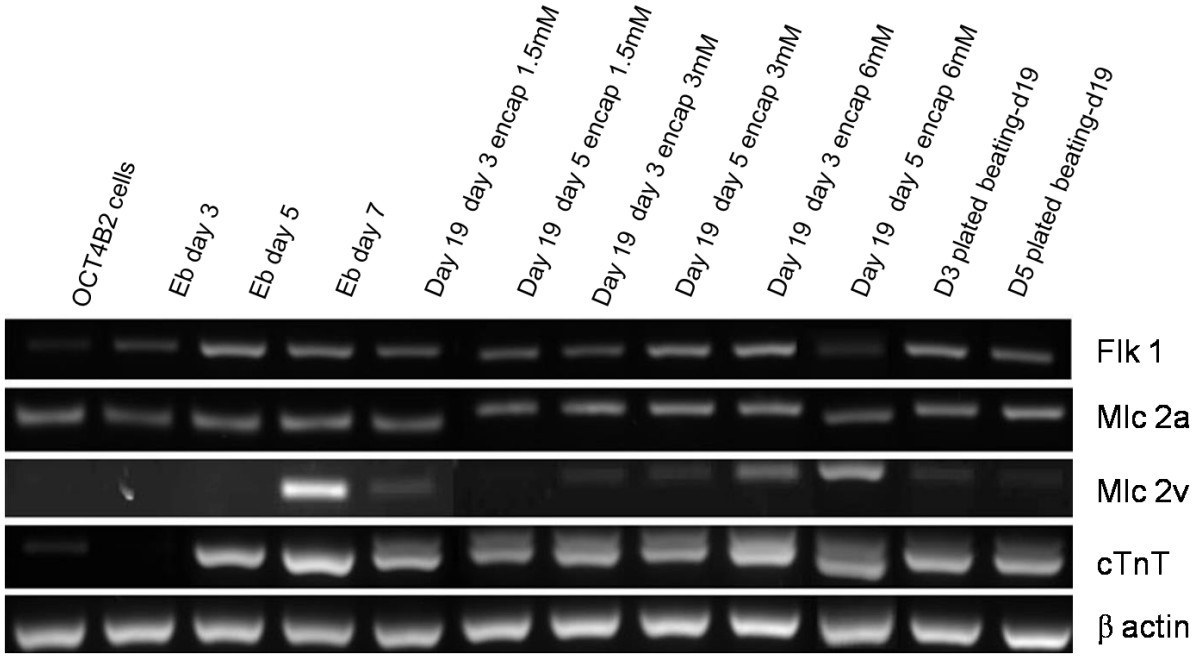

Figure 22 ***RT PCR for EBs encapsulated and plated at days 3, day 5.***

5.2.4 RT PCR

Early cardiac marker Flk 1was present in all samples although its expression was limited in undifferentiated cells which are expected. Late cardiac markers like Mlc 2a cardiac TnT showed expression uniformly after day 3 of differentiation. It can be observed that there was a difference in the expression of cardiac ventricular marker Mlc2v. While it was absent in 1.5mM crosslinked gel on day 19 its expression was faintly present in 3mM calcium encapsulated EBs on both day3 and day 5. Its expression was prominent in 6mM calcium encapsulated gellan and absent in day 3 and day 5 plated EBs. The atrial marker MLC 2a was expressed uniformly in all of the treatment sets while cardiac TnT too was expressed from day 5 onwards of differentiation. The MLC 2v, flk1 and cTnt were further assessed for quantitative PCR to assess whether there was any difference in the relative gene expression through quantitative PCR.

5.2.5 Q-PCR

To analyse relative expression of cardiac genes Q PCR analysis was performed for quantification of the gene expression of cardiac markers cTnT, MLC 2v and early cardiac

marker Flk 1. Data indicated in Appendix plot A1 shows linear increase in genes cTnT and Mlc2v from 3mM crosslinked gellan to 6mM crosslinked gellan. As seen in figure 24 the plot of fold change indicates that as against day 5 plated samples the day 5 encapsulated EBs in 6mM calcium crosslinked gellan had a 10 fold higher concentration of Mlc 2v while Flk 1 was 4 fold higher and cardiac TnT was close to 3 fold higher.

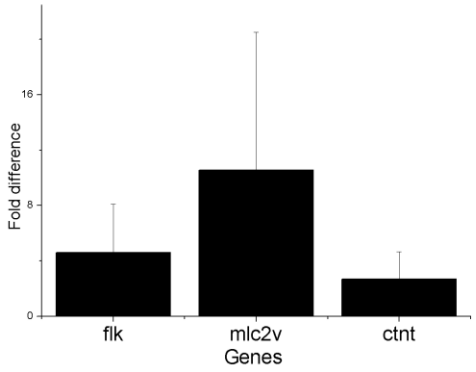

Figure 23 ***Relative gene expression of early gene Flk 1 , late genes MLC2v and cardiac cTnT of 0.5% gellan crosslinked with 6mM Calcium chloride encapsulated EBs as on day 5 as normalised to EBs plated on day 5 n=3,mean± SEM .***

Since normalized to the total beta actin within the cellular population it also suggests that the total cells expressing the copies of MLC 2v RNA were much higher than in the plated samples. Thus the results suggest that a higher stiffness resulted in a higher expression of MLC2v Vis a Vis a probable high number of cells. There is a linear increase in the expression of all three markers as the crosslink density increases as indicated in figure 3 in appendix. Crosslinking with 6mM calcium clearly proved to be beneficial in promoting a fold change increase in the expression of early and late cardiac markers. While it was evident that the expression of the ventricular marker MLC2v was is 9 fold higher, there was a 3 fold change in the expression of cardiac TnT and a 5 fold change in the expression of Flk 1 when normalized to the plated embryoid bodies on day 5.

5.3 CONCLUSION and DISCUSSION

Taken together, the beating efficiency and the number of beating bodies indicated that a stiffer matrix facilitated better beating efficiency as well as cardiac gene expression. 6mM calcium crosslinked gellan in this case makes the case for that stiff matrix. There is also evidence for consistently greater ventricular gene expression within a stiffer matrix during encapsulated differentiation of embryoid bodies encapsulated within the gellan gel. Although the matrix was stiff and was beneficial for differentiation to a cardiac lineage, it may not be a useful tool for the delivery of cells and scaffold material through an injectable system. For a minimally invasive injectable system a dual system which facilitates mixing of crosslinker and matrix polymer at the site of application to form a gel *in situ* will be preferable and will make it possible to deliver the scaffold along with cells. Furthermore it could be envisaged that a molecular mediated differentiation along with a relatively less stiff matrix can also form the solution for this. In this regard molecules like retinoic acid [106, 263-265], ascorbic acid [258, 266], may be injected along with pluripotent stem cells for enhanced differentiation.

Chapter 6

Analysis of differentiation of ES cells via delivery of retinoic through lipid nanocarriers

Differentiation of cells towards a cardiac lineage is accompanied by the patio-temporal expression of controlled expression of cardiac specific genes, i.e. a and b cardiac MHC, atrial natriuretic factor (ANF), ventricle-specific MLC-2 , of proteins (A -cardiac MHC, troponin-T) and of ion channels (Ca 2 +, Na +, K +) [267]. The process of cardiac specialization during ES cell-derived cardiogenic differentiation is accompanied by an up regulation of MLC-2v gene expression [268]. MLC-2v ventricle-specific activity has been demonstrated in embryonic, fetal and adult myocardium of transgenic mice [269]. Further evidence of the exclusive ventricular origin of the MLC2v gene was through the analysis of murine embryos showing expression in the ventricular region of the heart tube, with negligible expression in the atrial primordium [270]. Therefore, the MLC-2v gene may be useful as a marker to demonstrate ventricular specification during in vitro cardiogenesis. Furthermore the role of retinoic acid in cardiac differentiation in ES cells was elucidated by disrupting nearly all the retinoic acid receptor (RAR and RXR) subunits through homologous recombination and transgenic experiments with mice. Whereas targeted disruption of the RAR a [271], RAR b [272] and RAR c[273] genes mouse did not result in mutant phenotypes (except a decreased viability of RAR deficient mice), in- activation of the RXR a gene resulted in embryonal death as a consequence of cardiac hypoplasia be-cause of ventricular chamber defects [274]. Ventricular hypoplasia was also observed after vitamin A deficiency [275, 276]. In vitro studies with ES cells Wobus *et al*., and earlier studies with embryonic carcinoma (EC) cells demonstrated that all- Trans RA in a time- and concentration-dependent manner influenced the efficiency of cardiogenic differentiation[277, 278]. Treatment with high concentrations of RA (10^{-7} and 10^{-8} M RA) during the first 2 days or between day 2 and 5 of ES cell-derived embryoid body formation

significantly inhibited cardiogenesis, whereas treatment between day 5 and 7 resulted in an increased cardiomyocyte differentiation[267]. To deliver retinoic acid in a controlled manner to ES cells it is essential to have carriers which can be used to transport a measured quantity of retinoic acid to the cells. Phosphatidylethanolamine (PE) is a major membrane phospholipid in the heart comprising approximately 23–32% of the entire phospholipid mass of that organ [279]. The PE levels during cellular differentiation had been examined in a number of model systems and elevation in PE content during differentiation has been observed in several cell types [280, 281].Studies have shown that differentiation of p19 carcinoma cells to the cardiac lineage results in the elevation of phosphatidylethanolamine[282].

It is hypothesized that a carrier based on the lipid composition of the heart which is nontoxic and mimics the cellular characteristics may be beneficial in delivering retinoic acid for cardiac differentiation of ES cells. The targeted delivery through liposomes would also require a lower quantity of retinoic to mediate differentiation. To study the effect of all trans retinoic on the differentiation of ES cells through a controlled release of retinoic acid through liposomes retinoic acid loaded liposomes were prepared. Predominant composition of cardiac lipids are phosphatidylcholine and phsophatidylethoanolamine[283], and hence these were chosen to prepare lipid vesicles. Further retinoic acid being hydrophobic was encapsulated within the shell of the nanoparticles thus prepared.

6.1 EXPERIMENTAL METHODS

6.1.1 Material and methods

Sulforhodamine-B was purchased from Sigma Aldrich, Mumbai (India). Rhodamine-6G was purchased from Anaspec Inc. (San Jose, CA, USA), Soya lecithin or soya phosphatidylcholine (SPC) was purchased from Himedia Laboratories Pvt. Ltd., Mumbai (India). 1-palmitoyl-2-oleoyl-*sn*-glycero-3-phosphoethanolamine (POPE) was purchased from Avanti Pvt Ltd USA. Dulbecco's minimum essential media (DMEM), Penicillin streptomycin and fetal bovine serum (FBS) were procured from Invitrogen private limited (Carlsbad, CA, and USA). Antibiotic antimycotic solution was procured from Sigma aldrich

(USA). Sodium dodecyl sulfate (SDS), ethylene diamine tetra acetate (EDTA), phosphate buffered saline (PBS) and trypsin-EDTA solution were purchased from Himedia Laboratories Pvt. Ltd., Mumbai (India). High pressure liquid chromatography (HPLC) grade methanol and chloroform were purchased from Merck, Mumbai (India). High purity water purified by a Milli Q Plus water purifier system (Milli pore, USA), with a resistivity of 18.2 MΩ cm, was used in all experiments. All the tissue culture plates and tissue culture flasks were purchased from Corning (USA).

6.1.2 Preparation and characterization of lipid nanovesicles

Lipid nanovesicles containing retinoic acid were prepared by modified thin film hydration method [284]. Briefly, SPC and retinoic acid were dissolved in 2:1 (v/v) chloroform:methanol. SPC POPE liposomes were prepared by dissolving Soya PC and POPE in a 1:1 by weight ratio were dissolved in 2:1 (v/v) chloroform:methanol along with retinoic acid. The formulation was prepared with initial phospholipid:retinoic acid molar ratio of 5:1. Lipid film was prepared by slowly evaporating the solvent in a rotary vacuum evaporator and was further hydrated with phosphate buffered saline (PBS) pH 7.4 at 45 °C for 1 h at 120 rpm. The suspension was again centrifuged at 25,000*g*, 4 °C for 10 min and the pellet was reconstituted in PBS, pH 7.4. Blank nanovesicles were prepared by a similar method without the addition of retinoic acid. Lipid nanovesicles were further used at 10^{-9} M (0.3ng/ml), and 10^{-11} M(0.003ng/ml) for differentiation finally.

Size distribution of the nanovesicles was analyzed by dynamic light scattering (DLS) using laser particle analyzer (BI 200SM, Brookhaven Instruments Corporation, USA). In order to further confirm the size and morphology of the nanovesicles, transmission electron microscopy (TEM) was done as per the negative staining protocol [285]and images were analyzed by a transmission electron microscope, model:CM200 (Philips) operating at 120 kV, Cryo FEG-SEM JEOL (JSM-7600F), HR TEM JEOL JEM-2100. Surface charge on the nanovesicles was determined in terms of zeta potential using zeta potential analyzer (ZetaPALS, Brookhaven Instruments Corporation, USA). Encapsulation efficiency of retinoic acid was determined by breaking open the nanovesicles using 0.1% triton x100

and quantifying the drug using reverse phase HPLC (Agilent 1100 Binary LC pump liquid chromatograph, Agilent Technologies, USA)[286].

6.1.3 In vitro retinoic acid release

In vitro release study of retinoic acid from SPC-RA and SPCPE-RA was performed and analyzed for the determination of the free drug content by RP-HPLC pH 7.4 and 37 °C with proper sink conditions using a C18 column eluted with acetonitrile and 0.5% acetic acid at a ratio of 85:15 and UV–VIS detector at 353 nm. Sink conditions maintained were similar to those maintained during differentiation.

6.1.4 Cellular uptake and its mechanism

Cellular uptake and internalization studies were done for PC and PCPE by loading rhodamine-6G (Rh-6G) dye in these nanovesicles and then studying their uptake and internalization by differentiated ES cells on day 5 of differentiation after incubation with cells for 4 hours. These were further washed with buffered saline and fixed for observation under using confocal laser scanning microscope (CLSM) (Olympus Fluoview, FV500, Tokyo, Japan) with an excitation wavelength of 570 nm and emission wavelength of 590 nm for Rh-6G. Images were acquired and analyzed with 100X oil immersion objective using the Fluoview software (Olympus, Tokyo, Japan). Cells incubated with equivalent amount of free Rh-6G were used as control.

Cellular uptake and internalization studies were done for SPC and SPC:POPE by loading rhodamine-6G (Rh-6G) dye in place of retinoic acid in these nano- vesicles and then studying their uptake and internalization by differentiated ES cells at day 3 of differentiation Cells incubated with equivalent amount of free Rh-6G were used as control. In order to understand the mechanism of cellular uptake and interaction of the nanovesicles, differentiated EBS were plated on day 3 of differentiation and on day 5, cells were incubated in the presence of Rh-6G loaded SPC and SPC POPE suspension in normal and ATP depleted conditions. Cells ere incubated in the presence of 0.1% sodium azide , a known metabolic inhibitor by way depletion of ATP, by pre-incubating cells for 30 min in its presence [287] . To further understand the mechanism of cellular endocytosis, cells

were incubated in the presence of various endocytic inhibitors viz. 2 µg/ml nystatin, 10 µg/ml phenothiazine and 4 µg/ml colchicine [288-291].

6.1.5 Proliferation and Cellular viability

EBs differentiated to day 5 were plated with 1 EB per well and allowed to grow till day 13 and finally till day 19 before being analyzed for proliferation, in the presence of differentiation conditions. Medium was refreshed every 3 days. On days 13 and 19 3-(4, 5-methyl-thiazol-2-yl)-5-(3-carboxymethoxyphenyl)-2-(4-sulfophenyl)-2H-tetrazolium (MTT) assay was performed. Briefly cells were incubated with MTT at 5mg/ml in PBS for 4 hours at 37°C. Following which media was discarded and 100µl DMSO was added for solubalisation of dye. The absorbance of the supernatant was measured using a plate reader (Thermo Electron Corp., Vantaa, Finland) at 560 nm.

6.1.5 Differentiation of ES cells in the presence nanovesicle loaded retinoic acid

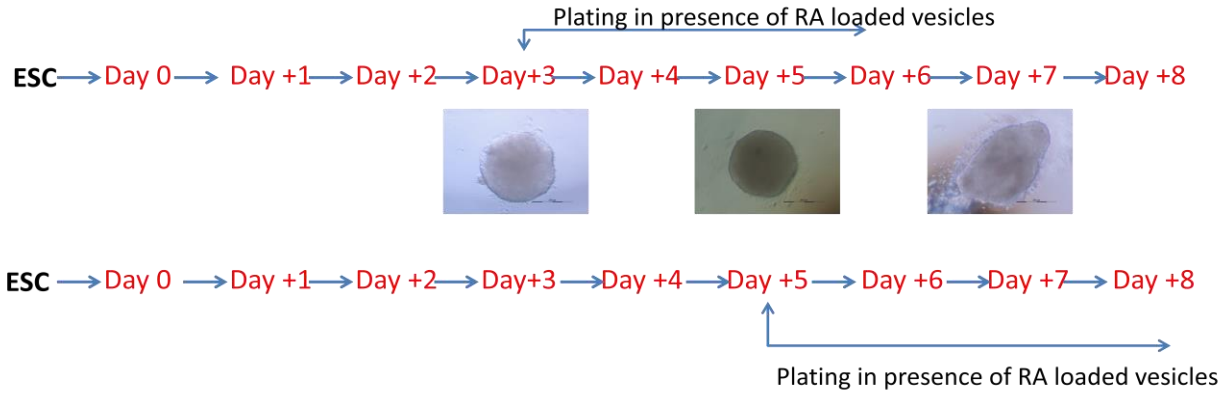

Figure 24 ***Schematic for differentiation of cells in the presence of RA loaded nanovesicles.***

Mouse Oct4 GFP cell line maintained in embryonic stem cell medium was trypsinised and counted. A final cell number of 600 cells in 15µl was placed on the lids of 10cm Petri dishes filled with potassium phosphate buffer (pH 7.8) in cultivation medium containing 15% FBS without LIF.[107, 267]. EBs formed, were on day 3 and day 5 were plated onto 0.1% gelatin

coated plates in the presence and absence of retinoic acid loaded vesicles. Beating rate for the embryoid bodies that beat as a result of cardiac differentiation was assessed on days 7,9,13 and 19 of differentiation.

6.1.6 Semi quantitative and quantitative RT PCR

For RT-PCR, RNA was isolated from cells using the RNeasy kit (Qiagen) following the manufacturer's instructions. RNA quality and concentrations were measured using the NanoDrop ND-1000 (NanoDrop Technologies, Australia). The isolated RNA was subjected to RQ1 DNase (Promega, Australia) treatment to remove any contaminating genomic DNA. cDNA was generated using the Superscript III enzyme following the manufacturer's instructions. Oligonucleotide primers have been described in appendix table 1. The PCR amplification included a total 30 cycles of denaturation at 94°C for 45 s followed by the appropriate annealing temperature for 45 s and extension at 72°C for 45 s with first denaturation step at 94°C for 5 min and a final extension step at 74°C for 5 min. PCR products were run on a 2% agarose gel at 120 V for 30 min. The primer sequences and the annealing temperatures are as given in appendix 1.

Quantitative PCR was performed with Power SYBR®Green PCR Master Mix in a 96 well format according to the manufacturer's instructions. This comprised a final volume of 25 µl, with 12.5 µl being the master mix, cDNA at a final concentration of 20ng, ultra-pure water and primers. Amplifications were performed starting with 10 min AmpliTaq Gold Enzyme Activation step at 95 °C, followed by 45 cycles of denaturation at 95 °C for 15 s and combined primer annealing/extension as given in appendix 1 for mlc2v, and cTnt 1 min. Fluorescence increase of SYBR green was automatically measured during PCR. Cycle thresholds C T) for the individual reactions were determined using iCycler iQ Real Time Detection System Software data processing software (Biorad, USA). All cDNA samples were amplified in duplicates and normalized against a triplicate of β actin in the same plate.

6.2. Results

6.2.1 Particle sizing and zeta potential

As observed in figure 26A, on and average SPC liposomes were found to be of 178 nm ±13nm. On encapsulating retinoic acid, the average size was 153nm ± 15nm. This was similar to that of the bare liposomes. Similarly SPC POPE liposomes were found to be of 210nm ± 7nm on an average. There was an increase in size to 255nm ±20nm with the addition of retinoic acid within the shell of the liposome matrix.β

A B

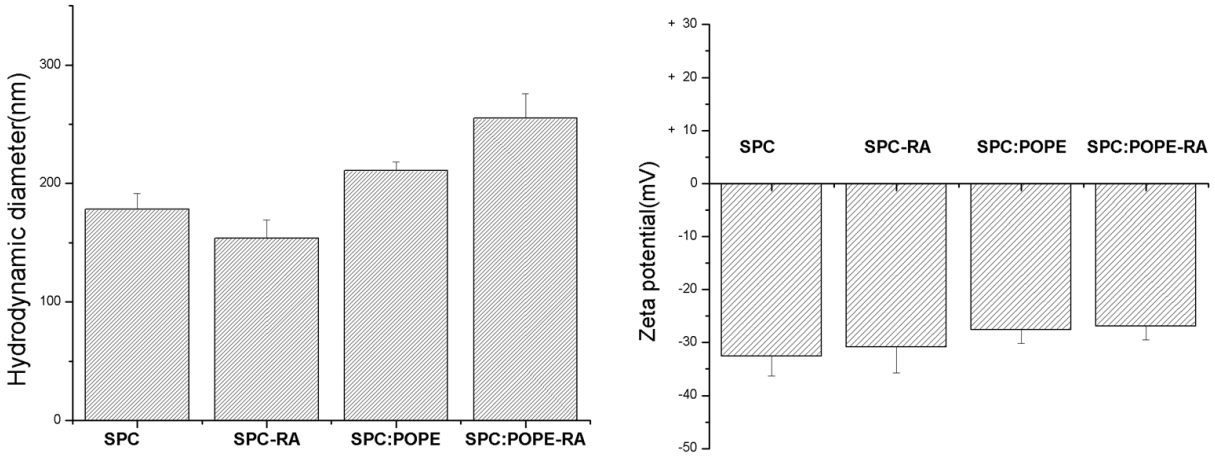

Figure 25 ***Plot of A hydrodynamic diameter of various formulations with and without retinoic acid B plot of zeta potential of various formulations with and without retinoic acid***

The surface charge as indicated in figure 26B for SPC and SPC-RA was - 32 ±3 mV and - 30 ± 4 mV respectively, while that of SPC:POPE and SPC:POPE-RA were - 26 ± 2.5 mV and - 27± 2.6 mV respectively. SPC POPE liposomes were larger in size than SPC liposomes. POPE addition increases size of liposomes and reduces zeta potential due to the positive charge that the ethanolamine imparts on the overall charge of the liposome. The encapsulation efficiency for the SPC-RA liposomes was 57.2% ± 0.9 and while that for PCPE-RA liposomes was 54.8% ± 0.5.

6.2.2 Imaging

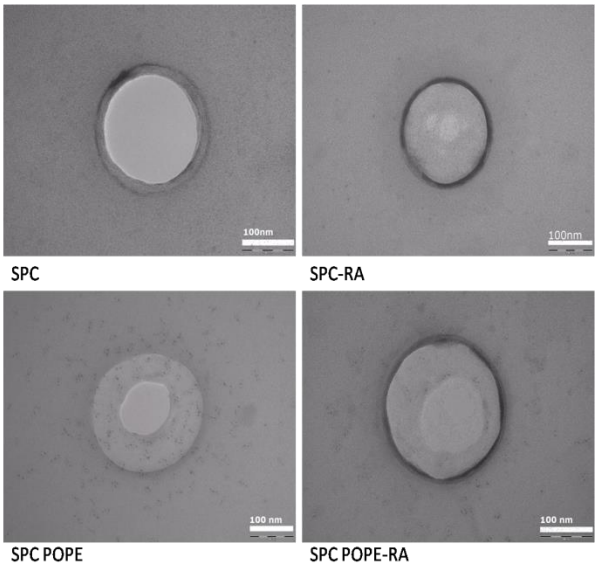

A

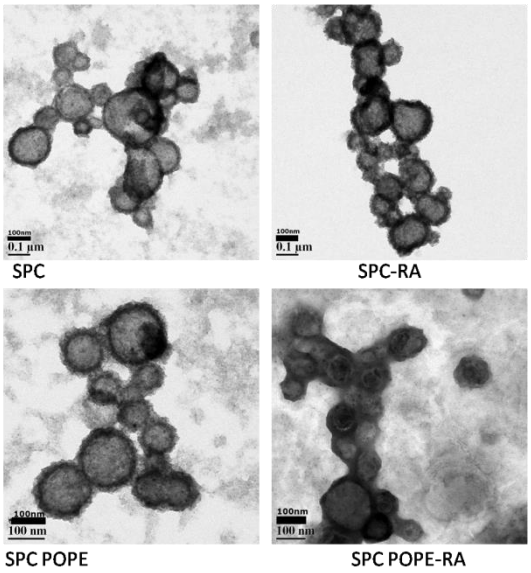

B

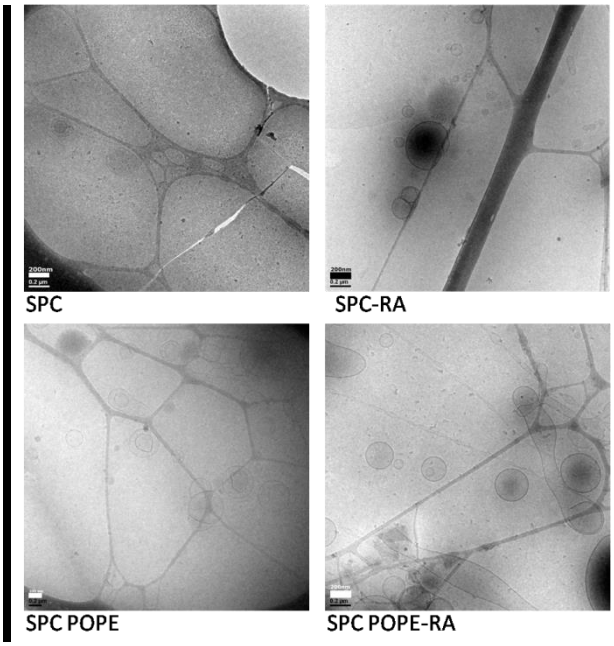

C

Figure 26 ***TEM images of A. TEM images of liposomes with and without retinoic acid B. FEG TEM images of liposomes with and without retinoic acid c. High Resolution TEM images of liposomes with and without retinoic acid.***

The lipid bilayer was visible in transmission electron microscopy. The various methods if imaging in figure 27 a, b, c also indicated population of uniformly sized particles as indicated in figure 27B.All methods of imaging point to the fact that the liposomes prepared were of uniform size and spherical.

6.2.3 Rhodamine 6G dye uptake

The cells which were differentiated on day 3 were plated onto gelatin coated coverslips and further when attached on day 5 were treated with R6G loaded SPC and SPC:PE liposomes for a duration of 4 hours. After which they were washed and fixed. These fixed cells were then imaged. It was found that rhodamine R6G fluorescence was presence throughout the cells as indicated in figure 28.

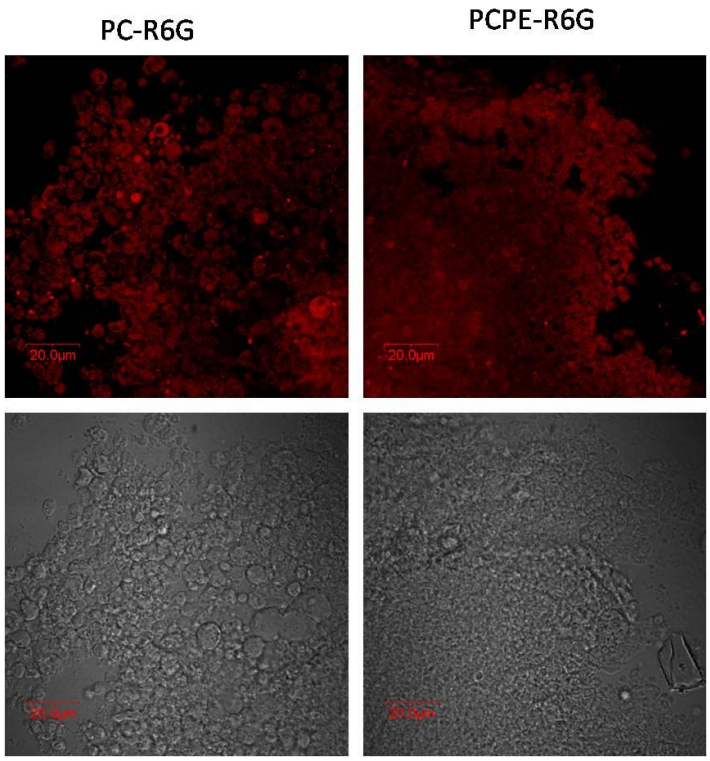

Figure 27 ***Day 3 differentiated EBs when plated and treated with rhodamine 6g loaded liposomes on day 5.***

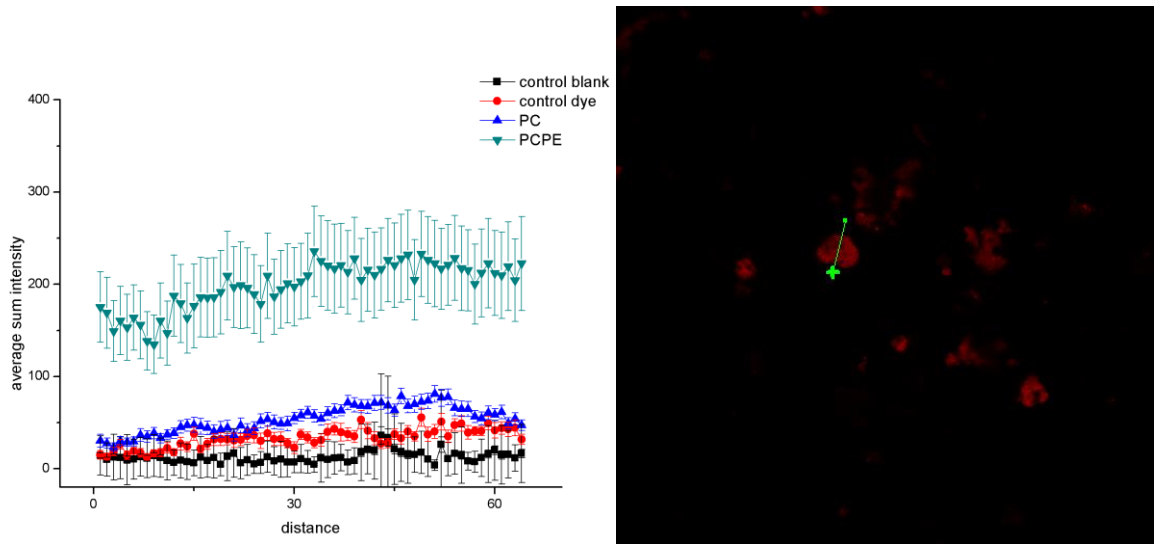

A B

Figure28*. Rhodamine 6g dye intensity in a xz depth scan of cells when treated with R6G SPC, R6G SPC POPE, free R6G and control without any R6G A. intensity graph summed from a depth scan of a total of 15 micron. B. Orientation of line to indicate the depth scans of orientation and position before scan*

Quantitative analysis was performed to obtain a depth XZ scan to measure the dye intensity within the cells. It can be seen that the depth scan made out across the length as in Figure 29 B of the cell for 50 cells suggests that R6G loaded PCPE liposomes had a higher intensity of dye within the cell as compared to R6G loaded SPC liposomes. The graph also indicated that the dye was uniformly distributed within the cells as indicated by the distribution of the dye in the xz scan suggesting that rhodamine R6G which represents retinoic acid entered the cells efficiently if delivered through liposomes and was uniformly distributed.

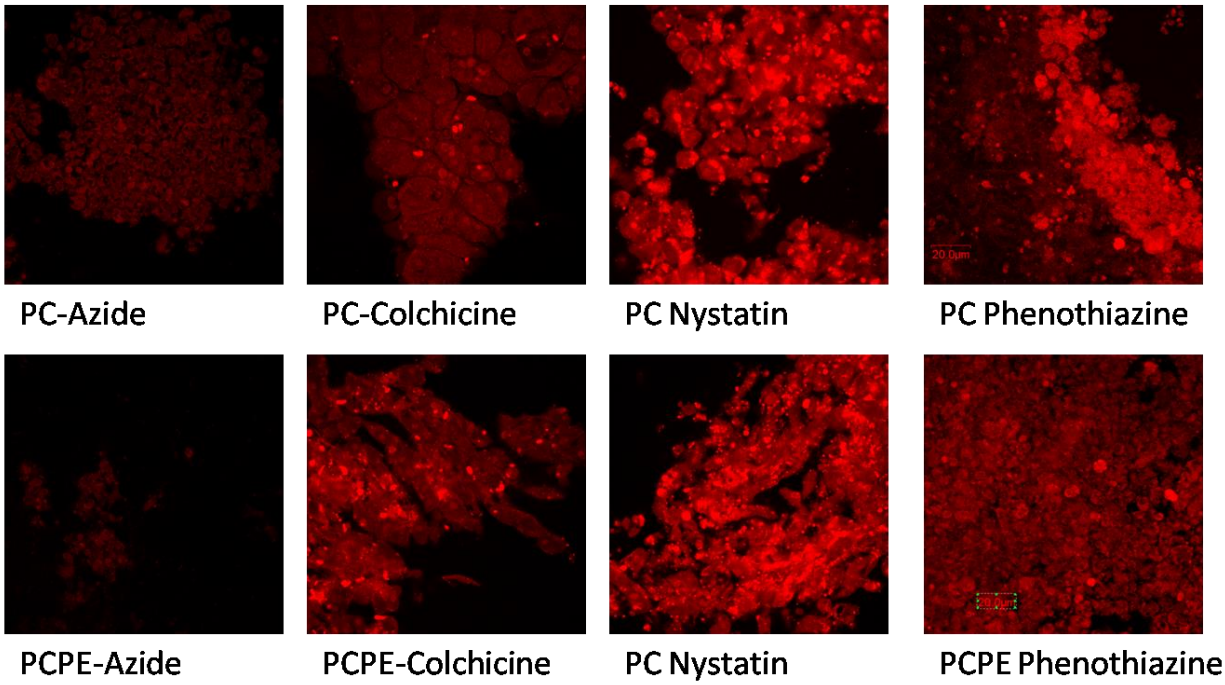

Figure 29*Mechanism involved in the internalization of liposomes, after treatment with inhibitors Azide, Colchicine, Nystatin,* Phenothiazine.

The cellular uptake mechanism as indicated in figure 30 suggested that ATP depleted conditions as a result of treatment with sodium azide, resulted in reduced uptake of the R6G encapsulated liposome. This indicated that the mechanism of uptake of liposomes is an ATP dependent active process of endocytosis. Furthermore since there was no effect of inhibitors colchicine, nystatin and phenothiazine on the uptake of dye loaded liposome. Internalisation was not affected in after the inhibition of calveolae mediated endocytosis inhibited by nystatin which depletes cholesterol from caveolae, and clathrin dependent endocytosis inhibited by colchicine and phenothiazine [292]. This suggests that the mechanism of internalization is an active ATP dependent process independent of clathrin or calveole dependent endocytosis.

6.2.4 *In vitro* retinoic acid release

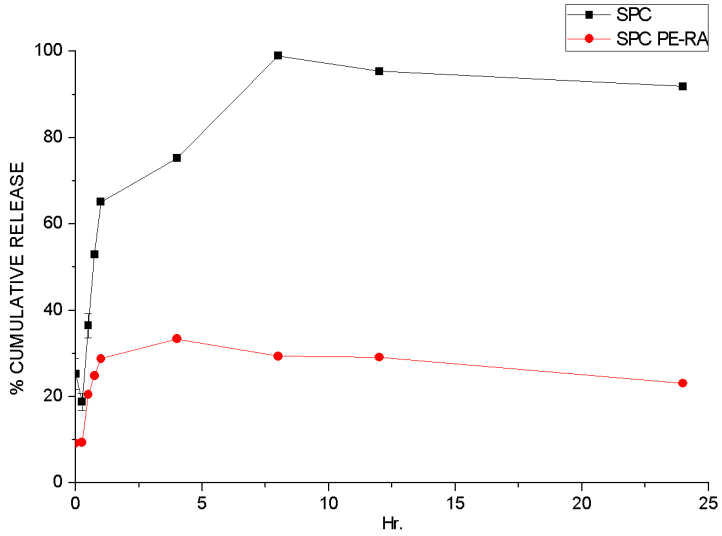

Figure 30 ***In vitro drug release from SPC and SPC:POPE liposomes loaded with Retinoic acid, n=3, mean± SEM.***

Retinoic released from both liposomal formulations indicated that SPC:POPE liposomes results in a lower Retinoic acid release over 24 hours as compared to SPC loaded retinoic acid, as shown in figure 31. The percentage cumulative release followed an initial burst release until the first few hours with a sustained pattern of release after that. Although the SPC:POPE liposomes shared similar entrapment efficiencies with SPC-liposomes the percent released over time indicated an initial burst release for 2 hours with a sustained release at an average of 30% thereon until 24 hours. The peak release rate was about 7.5 hours of SPC liposomes while that for SPC POPE liposomes was 4 hours.

6.2.5 Proliferation and viability

The embryoid bodies were not found to be affected by treatment with retinoic acid in the form of liposome encapsulated retinoic acid as well as free retinoic acid in their proliferative potential.

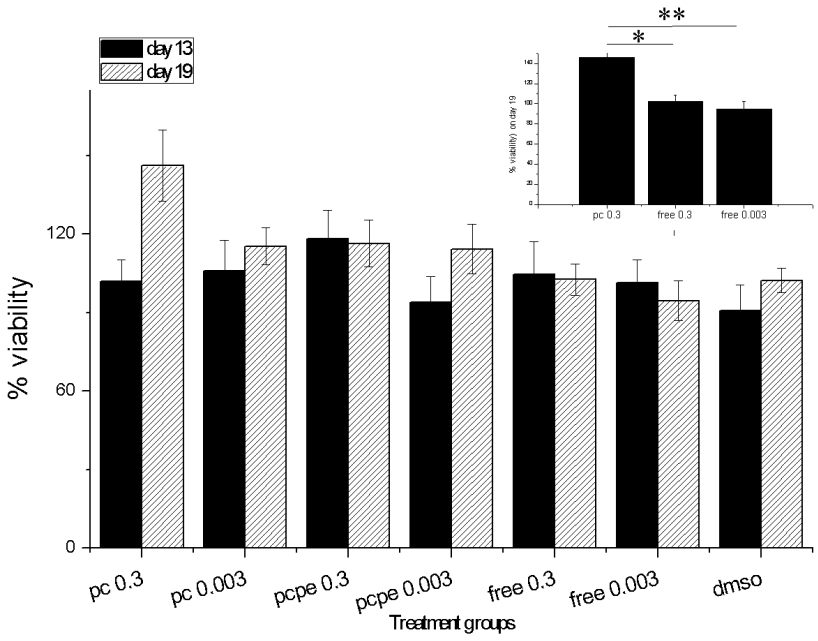

Figure 31 ***Effect of treatment groups on the proliferation of EBs plated in the presence of liposomal formulations of retinoic acid as well as free retinoic acid. * indicates the level of significance at p<0.05, and ** indicates the level of significance at p<0.01***

100 % viability was found to be present in embryoid bodies tested over 19 days of differentiation. There was a significant difference between PC-RA at 10^{-9} M treated embryoid bodies and those treated with free retinoic acid at a concentration of 10^{-9} as well as 10^{-11} Moles at $p<0.05$ and $p<0.01$ respectively as indicated in figure 32 inset.

6.2.6 Differentiation

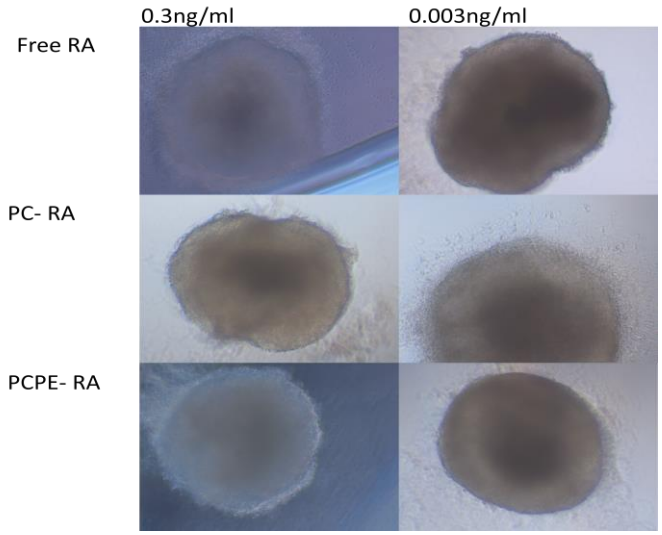

Figure 32*Ebs plated on day7*

Beating Efficiency i.e. number of EBs with beating centers were observed, as shown in figure 3 A. Beating rate i.e. the beats/minute as observed for EBs with beating centers were observed on respective days of incubation as shown in figure 34B.

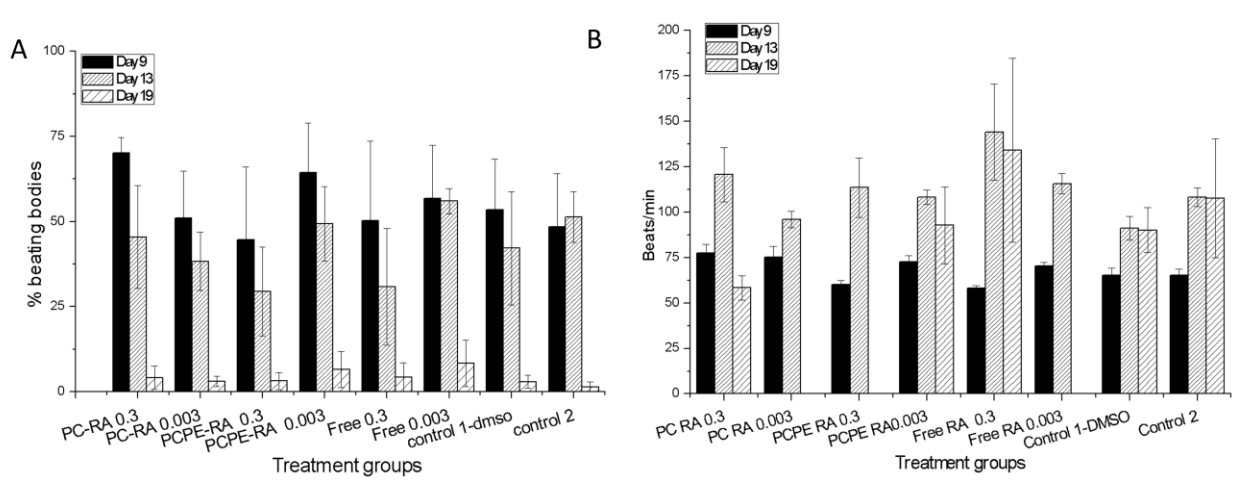

Figure 34 ***A. Average beating efficiency i.e. number of beating bodies on each of the time points Day 9, day 13 and day 19 n=3. B. Average beating rate of EBS plated in the presence of various conditions where n>48 bodies plated individually.***

It can be observed that the beating rate increased on day 13 of free 10^{-9} M and 10^{-11} M and EBs in the presence of 1% DMSO substituted media. While with liposomes loaded

retinoic acid the beating rate decreased indicating less stress within the cells. % beatings EBs were found to be higher with PC loaded with retinoic acid at a concentration of 0.3ng/ml. The number of beating EBs also remained constant form day 9 to day 13. The numbers of beating bodies were low in the free 10^{-9} M retinoic acid and the PCPE 10^{-9} M loaded liposomes; this did not change from day 9 to day 13. There was a greater change in the percentage beating bodies with the untreated EBs, DMSO controls, free 10^{-11} M, SPC 10^{-11} M and SPC POPE 10^{-11} M from day 9 to day 13, although this change was not as great as SPC RA at 10^{-9} M. Plots for beating rates above 200 beats/min were not plotted. A set pattern was observed with all the treatment groups where in beating follows a level at day 9 which increases at day 13 and then falls at day 19, similarly with the beating efficiency which similarly occurs as the days of differentiation advances from day 9-19.

6.2.7 Gene Expression

Semi quantitative gene expression with and without treatment were studied as observed in figure 35 a-d. Figure 34 a indicates that Flk 1 expression diminishes after day 7, and on day 19 the expression in all of the retinoic acid treated samples as well as the control was diminished. There was no expression in DMSO control. Mlc2a, i.e. atrial myocin, expression was only observed on day 7 embryoid bodiesMlc2v was expressed on day 7 EB and at very low levels in day 5 plated EBs treated with retinoic acid and controls on day 19. Comparatively SPC-RA at 10^{-11} M showed higher expression of Mlc2v as compared to SPC-RA at 10^{-9} M.

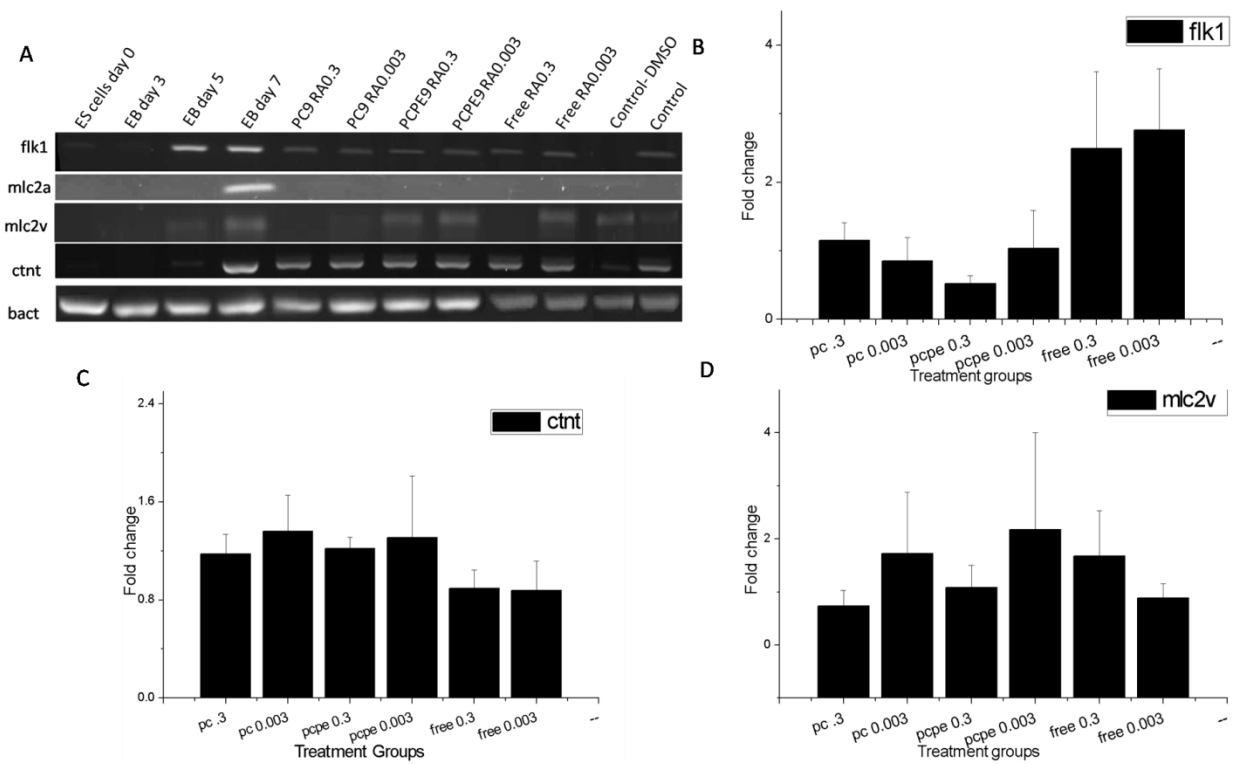

Figure 35 ***Effect of various retinoic acid treatments on the gene expression of embryoid bodies. A. Levels of early Flk1 and late cardiac gene expression in treated and untreated cells analysed by semi-quantitative RT-PCR. Fold change of expression levels of gene b. Flk1 c. cTnT d. Mlc2v for treated samples normalised to control analysed by quantitative RT-PCR. n=3, mean+ SEM.***

Early gene Flk1 showed lowest expression with SPC at 10^{-9} Mat. Quantitatively, expression of Mlc2v was found in SPC POPE-RA at 10^{-11} M was 2 fold and SPC POPE-RA at 10^{-9} was 1 fold as indicated in figure 35 C . While that for SPC -RA at 10^{-11} M was 1.7 fold and SPC-RA at 10^{-9} was 0.7 fold. This indicated a higher expression at a lower concentration of RA. Free 10^{-11} M was 0.6 fold while Free at 10^{-9} was 1.6 fold. Similar relative cTnT expression was observed for treated samples as indicated in figure 35C.

6.3 CONCLUSIONS AND DISCUSSION

The liposomal formulation mimicked the cardiac lipid composition with phosphotidyl choline and phosphatidyl ethanolamine. Treatment resulted in liposomes which encapsulated retinoic acid with an efficiency of 57.2% $\pm$ 0.9 for_SPC-RA and_while that for 54.8% $\pm$ 0.5 for SPC POPE-RA. Particle characterization also indicated suitably

sized liposomes with uniform sizes. These liposomes were internalized within differentiating cells on day 5 of differentiation, affecting a free transfer of payload to the inside of the cell to effect differentiation and maintain lower than studied concentrations. An active ATP mediated mechanism of internalization was elucidated. Furthermore the liposomal entrapment facilitated a sustained release of retinoic after an initial burst release to effect differentiation by its presence within the vicinity of the differentiating cells. While SPC provided a near 100 % release SPC :POPE formulation provided a sustained release at 30%, increasing the complimentarity with which both liposomes could be used to act upon differentiating cells to provide a spatio-temporal as well an intracellular depot of retinoic acid for signaling. The liposomal formulation did not affect the cells negatively and made for 100% viability within differentiating cells even to the extent of promoting proliferation in SPC 10^{-9} M liposomes. Mlc2v was chosen as a ventricular marker to indicate the effect of expression after treatment with retinoic acid. Furthermore cardiac TnT expression was expression via protein and mRNA was confirmed as indicated in appendix figure A2. Retinoic was chosen as a molecule solely to demonstrate that a molecular mediator is required in conjunction to facilitate the delivery and differentiation of stem cells within matrices once injected as *in situ* gels.

Chapter 7

Conclusions and future work

7.1 In situ scaffolds

The characterization of gellan and gellan-HPMC scaffolds revealed that there was a linear increase in the storage moduli when the concentration of calcium from 1.5mM to 6mM subsequently increasing its stiffness. All scaffolds were found to be porous with a porosity of <80% and were nontoxic. These scaffolds were wettable and provided suitable matrices for the passage of nutrients through the pores. All scaffolds that were studied were degradable over a 12 day period in which complete degradation was observed. Addition of HPMC was intended to improve the properties of the in situ gelling system but was not found to improve the overall rheological properties as indicated by the tan δ values of the scaffold.

7.2 Nanoparticle mediated differentiation

SPC and SPC POPE liposomes were prepared to encapsulate and delivery retinoic acid. The hydrodynamic diameter and the surface charge of the nanoparticles established their preparation. The liposomes were internalized through an ATP dependent, clathrin and calveolae independent process. The drug release with from the liposomes indicated that SPC liposomes showed an initial burst release while SPC POPE liposomes showed an initial burst release with a sustained release after 2 hours. Both liposome formulations were able to effect a fold difference in cardiac MLC2v gene expression indicating a ventricular lineage, over untreated controls. This places liposomes prepared from SPC and SPC POPE as suitable delivery systems for differentiation of ES cells. The release kinetics also proves that they are able to provide an extracellular localized source of retinoic acid if present in the vicinity of ES cells for differentiation.

7.3 Nanoparticles and scaffolds

This work demonstrates that the scaffolds and nanoparticle delivery vehicles individually are instrumental in directing cardiac differentiation of ES cells. Stiffness is a key criteria and a storage moduli of 15kPa of 6mM crosslinked gellan was found to be suitable for a higher expression of cardiac ventricular gene Mlc2v and cardiac TnT over 3mM crosslinked gellan at a storage moduli of 3kPa. Nanoparticles were also found to be suitable in delivering retinoic acid and promoting the expression of cardiac ventricular gene Mlc2v. Retinoic acid at a pico molar concentration enabled a greater effect over nanomoler concentration when delivered through nanoparticles, while the opposite effect was observed with free retinoic at the same concentration. This indicated that the nanoparticle mediated delivery facilitates differentiation at a lower concentration. It can be envisaged that 3mM crosslinked gellan which forms gels at suitable gelling times can be used in conjunction with liposomes to deliver retinoic acid to mediate effective cardiac differentiation in vitro. This can further be used in vivo to facilitate support as well as differentiation.

7.4 Future work

Implantations of patches, cardiac assist devices, and injectable non contractile supports have been studied. Injectable hydrogels accompanied with cells can be administered at the border zone to prevent remodeling due to scarring. ECM derived injectable scaffolds as well as biopolymer scaffolds are undergoing clinical trials for their use as cardiac support devices. Their usefulness hinges on the premise that they can utilize their properties of stiffness and their property to act as anchors for blood derived adult stem cells from circulation to ameliorate the loss of cells brought about by scarring due to myocardial infarction. This work proposes to have a new approach of delivering cells along with *in situ* gelling scaffolds and furthermore demonstrate the use of nanoparticles to drive differentiation. The in-situ gelling nature of the scaffold can be used to administer it via a trans-catheter system, or during normal cardiomyoplasty, epicardially or endocardially. The scaffolds will degrade over time and also elicit differentiation of the stem cells towards the cardiac lineage. This population of differentiated cells can further integrate into the

host tissue to form viable electro-mechanical connections, hence improving the condition of the heart. The work has demonstrated that differentiation could be carried out with pluripotent stem cells to further making a case for patient specific pluripotent stem cell like sources of induced pluripotent stem cell populations. Pluripotent stem cells accompanying the implant could address the problem of remodeling. The administration of hydrogel material serves as a two pronged approach; first, acting as a support matrix to the heart and prevent any remodeling due to the infarct; and, second, to allow retention of cells administered within it, further improving LV ejection fractions. Further work is required to assess whether the nanoparticulate systems and scaffolds can be used in conjunction to synergistically effect differentiation *in situ*. There is also scope to take this combined approach to the clinic using patient specific iPSCs.

References

1. Olivetti G, Abbi R, Quaini F *et al*. Apoptosis in the failing human heart. *N Engl J Med* 336(16), 1131-1141 (1997).
2. Siwik DA, Tzortzis JD, Pimental DR *et al*. Inhibition of copper-zinc superoxide dismutase induces cell growth, hypertrophic phenotype, and apoptosis in neonatal rat cardiac myocytes in vitro. *Circ Res* 85(2), 147-153 (1999).
3. Pinsky DJ, Cai B, Yang X, Rodriguez C, Sciacca RR, Cannon PJ. The lethal effects of cytokine-induced nitric oxide on cardiac myocytes are blocked by nitric oxide synthase antagonism or transforming growth factor beta. *J Clin Invest* 95(2), 677-685 (1995).
4. Fukuo K, Hata S, Suhara T *et al*. Nitric oxide induces upregulation of fas and apoptosis in vascular smooth muscle. *Hypertension* 27(3 Pt 2), 823-826 (1996).
5. Wu CF, Bishopric NH, Pratt RE. Atrial natriuretic peptide induces apoptosis in neonatal rat cardiac myocytes. *J Biol Chem* 272(9169455), 14860-14866 (1997).
6. Sam F, Sawyer DB, Xie Z *et al*. Mice lacking inducible nitric oxide synthase have improved left ventricular contractile function and reduced apoptotic cell death late after myocardial infarction. *Circ Res* 89(4), 351-356 (2001).
7. Balligand JL, Ungureanu D, Kelly RA *et al*. Abnormal contractile function due to induction of nitric oxide synthesis in rat cardiac myocytes follows exposure to activated macrophage-conditioned medium. *J Clin Invest* 91(5), 2314-2319 (1993).
8. Brady AJ, Poole-Wilson PA, Harding SE, Warren JB. Nitric oxide production within cardiac myocytes reduces their contractility in endotoxemia. *Am J Physiol* 263(6 Pt 2), H1963-1966 (1992).
9. Pfeffer MA, Braunwald E. Ventricular remodeling after myocardial infarction. Experimental observations and clinical implications. *Circulation* 81(2138525), 1161-1172 (1990).
10. Silverman KJ, Bulkley BH, Hutchins GM. Anomalous left circumflex coronary artery: "Normal" variant of uncertain clinical and pathologic significance. *Am J Cardiol* 41(7), 1311-1314 (1978).
11. Takahashi N, Calderone A, Izzo NJ, Maki TM, Marsh JD, Colucci WS. Hypertrophic stimuli induce transforming growth factor-beta 1 expression in rat ventricular myocytes. *J Clin Invest* 94(7929822), 1470-1476 (1994).
12. Sadoshima J, Xu Y, Slayter HS, Izumo S. Autocrine release of angiotensin ii mediates stretch-induced hypertrophy of cardiac myocytes in vitro. *Cell* 75(8252633), 977-984 (1993).

13. Yamazaki T, Komuro I, Kudoh S *et al*. Endothelin-1 is involved in mechanical stress-induced cardiomyocyte hypertrophy. *J Biol Chem* 271(6), 3221-3228 (1996).
14. Cheng W, Li B, Kajstura J *et al*. Stretch-induced programmed myocyte cell death. *J Clin Invest* 96(5), 2247-2259 (1995).
15. Von Harsdorf R. "Fas-ten" your seat belt: Anti-apoptotic treatment in heart failure takes off. *Circ Res* 95(6), 554-556 (2004).
16. Abraham MR, Henrikson CA, Tung L *et al*. Antiarrhythmic engineering of skeletal myoblasts for cardiac transplantation. *Circ Res* 97(2), 159-167 (2005).
17. Colucci WS. Molecular and cellular mechanisms of myocardial failure. *Am J Cardiol* 80(9412539), 25 (1997).
18. Seale P, Rudnicki MA. A new look at the origin, function, and "stem-cell" status of muscle satellite cells. *Dev Biol* 218(10656756), 115-124 (2000).
19. Winitsky SO, Gopal TV, Hassanzadeh S *et al*. Adult murine skeletal muscle contains cells that can differentiate into beating cardiomyocytes in vitro. *PLoS Biol* 3(4), e87 (2005).
20. Menasché P, Alfieri O, Janssens S *et al*. The myoblast autologous grafting in ischemic cardiomyopathy (magic) trial. *Circulation* 117(9), 1189-1200 (2008).
21. Wang QD, Sjoquist PO. Myocardial regeneration with stem cells: Pharmacological possibilities for efficacy enhancement. *Pharmacol Res* 53(4), 331-340 (2006).
22. Menasche P. Skeletal myoblasts and cardiac repair. *J Mol Cell Cardiol* 45(4), 545-553 (2008).
23. Smits PC, Van Geuns R-JM, Poldermans D *et al*. Catheter-based intramyocardial injection of autologous skeletal myoblasts as a primary treatment of ischemic heart failure: Clinical experience with six-month follow-up. *J Am Coll Cardiol* 42(14680727), 2063-2069 (2003).
24. Siminiak T, Kalawski R, Fiszer D *et al*. Autologous skeletal myoblast transplantation for the treatment of postinfarction myocardial injury: Phase i clinical study with 12 months of follow-up. *Am Heart J* 148(3), 531-537 (2004).
25. Siminiak T, Fiszer D, Jerzykowska O *et al*. Percutaneous trans-coronary-venous transplantation of autologous skeletal myoblasts in the treatment of post-infarction myocardial contractility impairment: The poznan trial. *Eur Heart J* 26(15764613), 1188-1195 (2005).
26. Reinecke H, Poppa V, Murry CE. Skeletal muscle stem cells do not transdifferentiate into cardiomyocytes after cardiac grafting. *J Mol Cell Cardiol* 34(11851363), 241-249 (2002).
27. Tedesco FS, Dellavalle A, Diaz-Manera J, Messina G, Cossu G. Repairing skeletal muscle: Regenerative potential of skeletal muscle stem cells. *J Clin Invest* 120(1), 11-19 (2010).
28. Dib N, Dinsmore J, Lababidi Z *et al*. One-year follow-up of feasibility and safety of the first u.S., randomized, controlled study using 3-dimensional guided catheter-based delivery of autologous skeletal myoblasts for ischemic cardiomyopathy (causmic study). *JACC: Cardiovascular Interventions* 2(1), 9-16 (2009).
29. Bioheart I, Nct00526253. To assess safety and efficacy of myoblast implantation into myocardium post myocardial infarction (marvel). *Available at http://clinicaltrials.gov/ct2/show/NCT00526253*, (accessed on 3rd April 2015).

30. Bioheart I, Nct00054678. Myoheart™ (myogenesis heart efficiency and regeneration trial). *Available at http://clinicaltrials.gov/ct2/show/NCT00054678* (accessed on 3rd April 2015).
31. Ferrari G, Cusella-De Angelis G, Coletta M *et al*. Muscle regeneration by bone marrow-derived myogenic progenitors. *Science* 279(9488650), 1528-1530 (1998).
32. Gussoni E, Soneoka Y, Strickland CD *et al*. Dystrophin expression in the mdx mouse restored by stem cell transplantation. *Nature* 401(10517639), 390-394 (1999).
33. Lagasse E, Connors H, Al-Dhalimy M *et al*. Purified hematopoietic stem cells can differentiate into hepatocytes in vivo. *Nat Med* 6(11062533), 1229-1234 (2000).
34. Krause DS, Theise ND, Collector MI *et al*. Multi-organ, multi-lineage engraftment by a single bone marrow-derived stem cell. *Cell* 105(11348593), 369-377 (2001).
35. Mezey E, Chandross KJ, Harta G, Maki RA, Mckercher SR. Turning blood into brain: Cells bearing neuronal antigens generated in vivo from bone marrow. *Science* 290(11099419), 1779-1782 (2000).
36. Brazelton TR, Rossi FM, Keshet GI, Blau HM. From marrow to brain: Expression of neuronal phenotypes in adult mice. *Science* 290(11099418), 1775-1779 (2000).
37. Jackson KA, Majka SM, Wang H *et al*. Regeneration of ischemic cardiac muscle and vascular endothelium by adult stem cells. *J Clin Invest* 107(11390421), 1395-1402 (2001).
38. Orlic D, Kajstura J, Chimenti S *et al*. Bone marrow cells regenerate infarcted myocardium. *Nature* 410(6829), 701-705 (2001).
39. Manginas A, Goussetis E, Koutelou M *et al*. Pilot study to evaluate the safety and feasibility of intracoronary cd133(+) and cd133(-) cd34(+) cell therapy in patients with nonviable anterior myocardial infarction. *Catheter Cardiovasc Interv* 69(6), 773-781 (2007).
40. Xu M, Wani M, Dai Y-S *et al*. Differentiation of bone marrow stromal cells into the cardiac phenotype requires intercellular communication with myocytes. *Circulation* 110(15492307), 2658-2665 (2004).
41. Koninckx R, Hensen K, Daniels A *et al*. Human bone marrow stem cells co-cultured with neonatal rat cardiomyocytes display limited cardiomyogenic plasticity. *Cytotherapy* 11(19878064), 778-792 (2009).
42. Valarmathi MT, Goodwin RL, Fuseler JW, Davis JM, Yost MJ, Potts JD. A 3-d cardiac muscle construct for exploring adult marrow stem cell based myocardial regeneration. *Biomaterials* 31(12), 3185-3200 (2010).
43. Duran JM, Makarewich CA, Sharp TE *et al*. Bone-derived stem cells repair the heart after myocardial infarction through transdifferentiation and paracrine signaling mechanisms. *Circ Res* 113(5), 539-552 (2013).
44. Kajstura J, Rota M, Whang B *et al*. Bone marrow cells differentiate in cardiac cell lineages after infarction independently of cell fusion. *Circ Res* 96(1), 127-137 (2005).
45. Mitchell AJ, Sabondjian E, Sykes J *et al*. Comparison of initial cell retention and clearance kinetics after subendocardial or subepicardial injections of endothelial progenitor cells in a canine myocardial infarction model. *J Nucl Med* 51(3), 413-417 (2010).

46. Ma N, Ladilov Y, Moebius JM *et al*. Intramyocardial delivery of human cd133+ cells in a scid mouse cryoinjury model: Bone marrow vs. Cord blood-derived cells. *Cardiovasc Res* 71(1), 158-169 (2006).
47. Leor J, Guetta E, Feinberg MS *et al*. Human umbilical cord blood-derived cd133+ cells enhance function and repair of the infarcted myocardium. *STEM CELLS* 24(16195418), 772-780 (2006).
48. Ott I, Keller U, Knoedler M *et al*. Endothelial-like cells expanded from cd34+ blood cells improve left ventricular function after experimental myocardial infarction. *FASEB J* 19(8), 992-994 (2005).
49. Strauer BE, Brehm M, Zeus T *et al*. Repair of infarcted myocardium by autologous intracoronary mononuclear bone marrow cell transplantation in humans. *Circulation* 106(12370212), 1913-1918 (2002).
50. Assmus B, Schachinger V, Teupe C *et al*. Transplantation of progenitor cells and regeneration enhancement in acute myocardial infarction (topcare-ami). *Circulation* 106(12473544), 3009-3017 (2002).
51. Uemura R, Xu M, Ahmad N, Ashraf M. Bone marrow stem cells prevent left ventricular remodeling of ischemic heart through paracrine signaling. *Circ Res* 98(11), 1414-1421 (2006).
52. Kearns-Jonker M, Dai W, Kloner RA. Stem cells for the treatment of heart failure. *Curr Opin Mol Ther* 12(4), 432-441 (2010).
53. Sun L, Zhang T, Lan X, Du G. Effects of stem cell therapy on left ventricular remodeling after acute myocardial infarction: A meta-analysis. *Clin Cardiol* 33(5), 296-302 (2010).
54. Rangappa S, Makkar R, Forrester J. Review article: Current status of myocardial regeneration: New cell sources and new strategies. *J Cardiovasc Pharmacol Ther* 15(21098418), 338-343 (2010).
55. Trounson A, Thakar R, Lomax G, Gibbons D. Clinical trials for stem cell therapies. *BMC Medicine* 9(1), 52 (2011).
56. Klein HM, Ghodsizad A, Marktanner R *et al*. Intramyocardial implantation of cd133+ stem cells improved cardiac function without bypass surgery. *Heart Surg Forum* 10(1), E66-69 (2007).
57. Koninckx R, Daniels A, Windmolders S *et al*. Mesenchymal stem cells or cardiac progenitors for cardiac repair? A comparative study. *Cell Mol Life Sci* 68(20972814), 2141-2156 (2011).
58. Murry CE, Soonpaa MH, Reinecke H *et al*. Haematopoietic stem cells do not transdifferentiate into cardiac myocytes in myocardial infarcts. *Nature* 428(15034593), 664-668 (2004).
59. Breitbach M, Bostani T, Roell W *et al*. Potential risks of bone marrow cell transplantation into infarcted hearts. *Blood* 110(17483296), 1362-1369 (2007).
60. Ljubljana UMC, Nct01350310. Safety and efficacy study of intramyocardial stem cell therapy in patients with dilated cardiomyopathy (noga-dcm). *Available at https://clinicaltrials.gov/ct2/show/NCT01350310*, (Accessed on 3rd April 2015).
61. Group T, Nct00984178. Trial of hematopoietic stem cells in acute myocardial infarction (tecam2). *Available at http://clinicaltrials.gov/ct2/show/NCT00984178*, (Accessed on 3rd April 2015).

62. All India Institute of Medical Sciences ND, Nct01625949. Stem cell therapy in patients with myocardial infarction and persistent total occlusion of infarct related artery (coat). *Available at http://clinicaltrials.gov/ct2/show/NCT01625949*, (Accessed on 3rd April 2015).
63. Roberto Corti M, Thomas F Luescher M, Nct00355186. Swiss multicenter intracoronary stem cells study in acute myocardial infarction (swiss-ami). *Available at https://clinicaltrials.gov/ct2/show/NCT00355186*, (Accessed on 24th August 2014).
64. Dominici M, Le Blanc K, Mueller I *et al*. Minimal criteria for defining multipotent mesenchymal stromal cells. The international society for cellular therapy position statement. *Cytotherapy* 8(4), 315-317 (2006).
65. Lien CL, Wu C, Mercer B, Webb R, Richardson JA, Olson EN. Control of early cardiac-specific transcription of nkx2-5 by a gata-dependent enhancer. *Development (Cambridge, England)* 126(1), 75-84 (1999).
66. Makino S, Fukuda K, Miyoshi S *et al*. Cardiomyocytes can be generated from marrow stromal cells in vitro. *J Clin Invest* 103(10074487), 697-705 (1999).
67. Yoon J, Min BG, Kim YH, Shim WJ, Ro YM, Lim DS. Differentiation, engraftment and functional effects of pre-treated mesenchymal stem cells in a rat myocardial infarct model. *Acta Cardiol* 60(3), 277-284 (2005).
68. Lei Y, Gojgini S, Lam J, Segura T. The spreading, migration and proliferation of mouse mesenchymal stem cells cultured inside hyaluronic acid hydrogels. *Biomaterials* 32(1), 39-47 (2011).
69. Ho W, Tawil B, Dunn JC, Wu BM. The behavior of human mesenchymal stem cells in 3d fibrin clots: Dependence on fibrinogen concentration and clot structure. *Tissue Eng* 12(6), 1587-1595 (2006).
70. Zhou Y, Wang S, Yu Z *et al*. Direct injection of autologous mesenchymal stromal cells improves myocardial function. *Biochem Biophys Res Commun* 390(19852944), 902-907 (2009).
71. Nascimento DS, Mosqueira D, Sousa LM *et al*. Human umbilical cord tissue-derived mesenchymal stromal cells attenuate remodeling after myocardial infarction by proangiogenic, antiapoptotic, and endogenous cell-activation mechanisms. *Stem Cell Res Ther* 5(1), 5 (2014).
72. Hattan N, Kawaguchi H, Ando K *et al*. Purified cardiomyocytes from bone marrow mesenchymal stem cells produce stable intracardiac grafts in mice. *Cardiovasc Res* 65(15639472), 334-344 (2005).
73. Wang JS, Shum-Tim D, Chedrawy E, Chiu RC. The coronary delivery of marrow stromal cells for myocardial regeneration: Pathophysiologic and therapeutic implications. *J Thorac Cardiovasc Surg* 122(4), 699-705 (2001).
74. Miyahara Y, Nagaya N, Kataoka M *et al*. Monolayered mesenchymal stem cells repair scarred myocardium after myocardial infarction. *Nat Med* 12(16582917), 459-465 (2006).
75. Zhang H, Song P, Tang Y *et al*. Injection of bone marrow mesenchymal stem cells in the borderline area of infarcted myocardium: Heart status and cell distribution. *J Thorac Cardiovasc Surg* 134(17976455), 1234-1240 (2007).
76. Zeng L, Hu Q, Wang X *et al*. Bioenergetic and functional consequences of bone marrow-derived multipotent progenitor cell transplantation in hearts with

postinfarction left ventricular remodeling. *Circulation* 115(17389266), 1866-1875 (2007).
77. Toma C, Pittenger MF, Cahill KS, Byrne BJ, Kessler PD. Human mesenchymal stem cells differentiate to a cardiomyocyte phenotype in the adult murine heart. *Circulation* 105(1), 93-98 (2002).
78. Tan J, Weil BR, Abarbanell AM *et al*. Ablation of tnf-alpha receptors influences mesenchymal stem cell-mediated cardiac protection against ischemia. *Shock* 34(3), 236-242 (2010).
79. Hare JM, Traverse JH, Henry TD *et al*. A randomized, double-blind, placebo-controlled, dose-escalation study of intravenous adult human mesenchymal stem cells (prochymal) after acute myocardial infarction. *Journal of the American College of Cardiology* 54(24), 2277-2286 (2009).
80. Yokokawa M, Ohnishi S, Ishibashi-Ueda H *et al*. Transplantation of mesenchymal stem cells improves atrioventricular conduction in a rat model of complete atrioventricular block. *Cell Transplant* 17(19181209), 1145-1155 (2008).
81. Noiseux N, Gnecchi M, Lopez-Ilasaca M *et al*. Mesenchymal stem cells overexpressing akt dramatically repair infarcted myocardium and improve cardiac function despite infrequent cellular fusion or differentiation. *Molecular therapy : the journal of the American Society of Gene Therapy* 14(16965940), 840-850 (2006).
82. Miami UO, Nct00768066. The transendocardial autologous cells (hmsc or hbmc) in ischemic heart failure trial (tac-hft). *Available at https://clinicaltrials.gov/ct2/show/NCT00768066*, (Accessed on 3rd April 2015).
83. Linke A, Muller P, Nurzynska D *et al*. Stem cells in the dog heart are self-renewing, clonogenic, and multipotent and regenerate infarcted myocardium, improving cardiac function. *Proc Natl Acad Sci U S A* 102(25), 8966-8971 (2005).
84. Oh H, Bradfute SB, Gallardo TD *et al*. Cardiac progenitor cells from adult myocardium: Homing, differentiation, and fusion after infarction. *Proc Natl Acad Sci U S A* 100(14530411), 12313-12318 (2003).
85. Bergmann O, Bhardwaj RD, Bernard S *et al*. Evidence for cardiomyocyte renewal in humans. *Science* 324(5923), 98-102 (2009).
86. Bearzi C, Rota M, Hosoda T *et al*. Human cardiac stem cells. *Proc Natl Acad Sci U S A* 104(17709737), 14068-14073 (2007).
87. Wu SM, Chien KR, Mummery C. Origins and fates of cardiovascular progenitor cells. *Cell* 132(18295570), 537-543 (2008).
88. Matsuura K, Nagai T, Nishigaki N *et al*. Adult cardiac sca-1-positive cells differentiate into beating cardiomyocytes. *J Biol Chem* 279(12), 11384-11391 (2004).
89. Messina E, De Angelis L, Frati G *et al*. Isolation and expansion of adult cardiac stem cells from human and murine heart. *Circ Res* 95(15472116), 911-921 (2004).
90. Barile L, Messina E, Giacomello A, Marban E. Endogenous cardiac stem cells. *Prog Cardiovasc Dis* 50(17631436), 31-48 (2007).
91. Rosenblatt-Velin N, Lepore MG, Cartoni C, Beermann F, Pedrazzini T. Fgf-2 controls the differentiation of resident cardiac precursors into functional cardiomyocytes. *J Clin Invest* 115(15951838), 1724-1733 (2005).
92. Ellison GM, Vicinanza C, Smith AJ *et al*. Adult c-kit(pos) cardiac stem cells are necessary and sufficient for functional cardiac regeneration and repair. *Cell* 154(4), 827-842 (2013).

93. Tateishi K, Ashihara E, Takehara N *et al*. Clonally amplified cardiac stem cells are regulated by sca-1 signaling for efficient cardiovascular regeneration. *J Cell Sci* 120(17502484), 1791-1800 (2007).
94. Liang SX, Tan TYL, Gaudry L, Chong B. Differentiation and migration of sca1+/cd31- cardiac side population cells in a murine myocardial ischemic model. *Int J Cardiol* 138(19254813), 40-49 (2010).
95. Tillmanns J, Rota M, Hosoda T *et al*. Formation of large coronary arteries by cardiac progenitor cells. *Proc Natl Acad Sci U S A* 105(18216245), 1668-1673 (2008).
96. Takehara N, Tsutsumi Y, Tateishi K *et al*. Controlled delivery of basic fibroblast growth factor promotes human cardiosphere-derived cell engraftment to enhance cardiac repair for chronic myocardial infarction. *J Am Coll Cardiol* 52(19038683), 1858-1865 (2008).
97. Smith RR, Barile L, Cho HC *et al*. Regenerative potential of cardiosphere-derived cells expanded from percutaneous endomyocardial biopsy specimens. *Circulation* 115(17283259), 896-908 (2007).
98. Bolli R, Chugh AR, D'amario D *et al*. Cardiac stem cells in patients with ischaemic cardiomyopathy (scipio): Initial results of a randomised phase 1 trial. *The Lancet* 378(9806), 1847-1857 (2011).
99. Stamm C, Nasseri B, Hetzer R. Cardiac stem cells in patients with ischaemic cardiomyopathy. *Lancet* 379(9819), 891; author reply 891-892 (2012).
100. Makkar RR, Smith RR, Cheng K *et al*. Intracoronary cardiosphere-derived cells for heart regeneration after myocardial infarction (caduceus): A prospective, randomised phase 1 trial. *Lancet* 379(9819), 895-904 (2012).
101. Takahashi K, Yamanaka S. Induction of pluripotent stem cells from mouse embryonic and adult fibroblast cultures by defined factors. *Cell* 126(16904174), 663-676 (2006).
102. Robinton DA, Daley GQ. The promise of induced pluripotent stem cells in research and therapy. *Nature* 481(7381), 295-305 (2012).
103. Kehat I, Kenyagin-Karsenti D, Snir M *et al*. Human embryonic stem cells can differentiate into myocytes with structural and functional properties of cardiomyocytes. *J Clin Invest* 108(11489934), 407-414 (2001).
104. Xu C, Police S, Rao N, Carpenter MK. Characterization and enrichment of cardiomyocytes derived from human embryonic stem cells. *Circ Res* 91(6), 501-508 (2002).
105. Mummery C, Ward D, Van Den Brink CE *et al*. Cardiomyocyte differentiation of mouse and human embryonic stem cells. *J Anat* 200(12033727), 233-242 (2002).
106. Wobus AM, Kaomei G, Shan J *et al*. Retinoic acid accelerates embryonic stem cell-derived cardiac differentiation and enhances development of ventricular cardiomyocytes. *J Mol Cell Cardiol* 29(6), 1525-1539 (1997).
107. Wobus AM, Wallukat G, Hescheler J. Pluripotent mouse embryonic stem cells are able to differentiate into cardiomyocytes expressing chronotropic responses to adrenergic and cholinergic agents and ca2+ channel blockers. *Differentiation* 48(3), 173-182 (1991).
108. Kehat I, Khimovich L, Caspi O *et al*. Electromechanical integration of cardiomyocytes derived from human embryonic stem cells. *Nat Biotechnol* 22(15448703), 1282-1289 (2004).

109. Xue T, Cho HC, Akar FG *et al*. Functional integration of electrically active cardiac derivatives from genetically engineered human embryonic stem cells with quiescent recipient ventricular cardiomyocytes: Insights into the development of cell-based pacemakers. *Circulation* 111(15611367), 11-20 (2005).
110. Fijnvandraat AC, Van Ginneken ACG, Schumacher CA *et al*. Cardiomyocytes purified from differentiated embryonic stem cells exhibit characteristics of early chamber myocardium. *J Mol Cell Cardiol* 35(14654372), 1461-1472 (2003).
111. Snir M, Kehat I, Gepstein A *et al*. Assessment of the ultrastructural and proliferative properties of human embryonic stem cell-derived cardiomyocytes. *Am J Physiol Heart Circ Physiol* 285(14613910), 2355-2363 (2003).
112. Narazaki G, Uosaki H, Teranishi M *et al*. Directed and systematic differentiation of cardiovascular cells from mouse induced pluripotent stem cells. *Circulation* 118(5), 498-506 (2008).
113. Mauritz C, Schwanke K, Reppel M *et al*. Generation of functional murine cardiac myocytes from induced pluripotent stem cells. *Circulation* 118(5), 507-517 (2008).
114. Schenke-Layland K, Rhodes KE, Angelis E *et al*. Reprogrammed mouse fibroblasts differentiate into cells of the cardiovascular and hematopoietic lineages. *STEM CELLS* 26(18450826), 1537-1546 (2008).
115. Zhang J, Wilson GF, Soerens AG *et al*. Functional cardiomyocytes derived from human induced pluripotent stem cells. *Circ Res* 104(4), e30-41 (2009).
116. Sarvi F, Jain K, Arbatan T *et al*. Cardiogenesis of embryonic stem cells with liquid marble micro-bioreactor. *Adv Healthc Mater*, n/a-n/a (2014).
117. Burridge PW, Anderson D, Priddle H *et al*. Improved human embryonic stem cell embryoid body homogeneity and cardiomyocyte differentiation from a novel v-96 plate aggregation system highlights interline variability. *STEM CELLS* 25(4), 929-938 (2007).
118. Bratt-Leal AM, Carpenedo RL, Ungrin MD, Zandstra PW, Mcdevitt TC. Incorporation of biomaterials in multicellular aggregates modulates pluripotent stem cell differentiation. *Biomaterials* 32(1), 48-56 (2011).
119. Laflamme MA, Chen KY, Naumova AV *et al*. Cardiomyocytes derived from human embryonic stem cells in pro-survival factors enhance function of infarcted rat hearts. *Nat Biotechnol* 25(9), 1015-1024 (2007).
120. Mummery C, Ward-Van Oostwaard D, Doevendans P *et al*. Differentiation of human embryonic stem cells to cardiomyocytes: Role of coculture with visceral endoderm-like cells. *Circulation* 107(12742992), 2733-2740 (2003).
121. Duan Y, Liu Z, O'neill J, Wan LQ, Freytes DO, Vunjak-Novakovic G. Hybrid gel composed of native heart matrix and collagen induces cardiac differentiation of human embryonic stem cells without supplemental growth factors. *Journal of cardiovascular translational research* 4(5), 605-615 (2011).
122. Li Z, Guo X, Matsushita S, Guan J. Differentiation of cardiosphere-derived cells into a mature cardiac lineage using biodegradable poly(n-isopropylacrylamide) hydrogels. *Biomaterials* 32(12), 3220-3232 (2011).
123. Young JL, Engler AJ. Hydrogels with time-dependent material properties enhance cardiomyocyte differentiation in vitro. *Biomaterials* 32(4), 1002-1009 (2011).

124. Heng BC, Haider HK, Sim EK-W, Cao T, Ng SC. Strategies for directing the differentiation of stem cells into the cardiomyogenic lineage in vitro. *Cardiovasc Res* 62(1), 34-42 (2004).
125. Herzenberg LA, Parks D, Sahaf B, Perez O, Roederer M. The history and future of the fluorescence activated cell sorter and flow cytometry: A view from stanford. *Clin Chem* 48(10), 1819-1827 (2002).
126. Zhao T, Zhang ZN, Rong Z, Xu Y. Immunogenicity of induced pluripotent stem cells. *Nature* 474(7350), 212-215 (2011).
127. Araki R, Uda M, Hoki Y *et al*. Negligible immunogenicity of terminally differentiated cells derived from induced pluripotent or embryonic stem cells. *Nature* 494(7435), 100-104 (2013).
128. Ménard C, Hagège AA, Agbulut O *et al*. Transplantation of cardiac-committed mouse embryonic stem cells to infarcted sheep myocardium: A preclinical study. *The Lancet* 366(9490), 1005-1012 (2005).
129. Laflamme MA, Gold J, Xu C *et al*. Formation of human myocardium in the rat heart from human embryonic stem cells. *Am J Pathol* 167(16127147), 663-671 (2005).
130. Jezierska-Wozniak K, Mystkowska D, Tutas A, Jurkowski MK. Stem cells as therapy for cardiac disease - a review. *Folia Histochemica Et Cytobiologica* 49(1), 13-25 (2011).
131. Cyranoski D. Stem cells cruise to clinic. *Nature* 494(7438), 413 (2013).
132. Au K-W, Liao S-Y, Lee Y-K *et al*. Effects of iron oxide nanoparticles on cardiac differentiation of embryonic stem cells. *Biochem Biophys Res Commun* 379(4), 898-903 (2009).
133. Huang Z, Shen Y, Sun A *et al*. Magnetic targeting enhances retrograde cell retention in a rat model of myocardial infarction. *Stem Cell Res Ther* 4(6), 149 (2013).
134. Sengstock C, Diendorf J, Epple M, Schildhauer TA, Koller M. Effect of silver nanoparticles on human mesenchymal stem cell differentiation. *Beilstein J Nanotechnol* 5, 2058-2069 (2014).
135. Yi C, Liu D, Fong CC, Zhang J, Yang M. Gold nanoparticles promote osteogenic differentiation of mesenchymal stem cells through p38 mapk pathway. *ACS Nano* 4(11), 6439-6448 (2010).
136. Niu J, Azfer A, Rogers LM, Wang X, Kolattukudy PE. Cardioprotective effects of cerium oxide nanoparticles in a transgenic murine model of cardiomyopathy. *Cardiovasc Res* 73(3), 549-559 (2007).
137. Pagliari F, Mandoli C, Forte G *et al*. Cerium oxide nanoparticles protect cardiac progenitor cells from oxidative stress. *ACS Nano* 6(5), 3767-3775 (2012).
138. Fleischer S, Shevach M, Feiner R, Dvir T. Coiled fiber scaffolds embedded with gold nanoparticles improve the performance of engineered cardiac tissues. *Nanoscale* 6(16), 9410-9414 (2014).
139. Shevach M, Fleischer S, Shapira A, Dvir T. Gold nanoparticle-decellularized matrix hybrids for cardiac tissue engineering. *Nano Letters* 14(10), 5792-5796 (2014).
140. Jawad H, Boccaccini AR, Ali NN, Harding SE. Assessment of cellular toxicity of tio2 nanoparticles for cardiac tissue engineering applications. *Nanotoxicology* 5(3), 372-380 (2011).

141. Mallik A, Bryan S, Puukila S, Chen A, Khaper N. Efficacy of pt-modified tio(2) nanoparticles in cardiac cells. *Experimental and clinical cardiology* 16(1), 6-10 (2011).
142. Galagudza M, Korolev D, Postnov V *et al*. Passive targeting of ischemic-reperfused myocardium with adenosine-loaded silica nanoparticles. *Int J Nanomedicine* 7, 1671-1678 (2012).
143. Zhang Y, Li W, Ou L *et al*. Targeted delivery of human vegf gene via complexes of magnetic nanoparticle-adenoviral vectors enhanced cardiac regeneration. *PLoS ONE* 7(7), e39490 (2012).
144. Rezzani R, Rodella LF, Fraschini F *et al*. Melatonin delivery in solid lipid nanoparticles: Prevention of cyclosporine a induced cardiac damage. *Journal of pineal research* 46(3), 255-261 (2009).
145. Jee JP, Lim SJ, Park JS, Kim CK. Stabilization of all-trans retinol by loading lipophilic antioxidants in solid lipid nanoparticles. *Eur J Pharm Biopharm*63(2), 134-139 (2006).
146. Lim SJ, Kim CK. Formulation parameters determining the physicochemical characteristics of solid lipid nanoparticles loaded with all-trans retinoic acid. *Int J Pharm* 243(1-2), 135-146 (2002).
147. Lim SJ, Lee MK, Kim CK. Altered chemical and biological activities of all-trans retinoic acid incorporated in solid lipid nanoparticle powders. *J Control Release*100(1), 53-61 (2004).
148. Kawakami S, Opanasopit P, Yokoyama M *et al*. Biodistribution characteristics of all-trans retinoic acid incorporated in liposomes and polymeric micelles following intravenous administration. *Journal of pharmaceutical sciences* 94(12), 2606-2615 (2005).
149. Kirby CJ, Whittle CJ, Rigby N, Coxon DT, Law BA. Stabilization of ascorbic-acid by microencapsulation in liposomes. *Int J Food Sci Tech* 26(5), 437-449 (1991).
150. Rajam M, Pulavendran S, Rose C, Mandal AB. Chitosan nanoparticles as a dual growth factor delivery system for tissue engineering applications. *International Journal of Pharmaceutics* 410(1-2), 145-152 (2011).
151. Zhou W, Zhao M, Zhao Y, Mou Y. A fibrin gel loaded with chitosan nanoparticles for local delivery of rhegf: Preparation and in vitro release studies. *J Mater Sci Mater Med* 22(5), 1221-1230 (2011).
152. Scott RC, Rosano JM, Ivanov Z *et al*. Targeting vegf-encapsulated immunoliposomes to mi heart improves vascularity and cardiac function. *FASEB J* 23(10), 3361-3367 (2009).
153. Tiwari MD, Mehra S, Jadhav S, Bellare JR. All-trans retinoic acid loaded block copolymer nanoparticles efficiently induce cellular differentiation in hl-60 cells. *Eur J Pharm Sci* 44(5), 643-652 (2011).
154. Ku B, Kim J-E, Chung BH, Chung BG. Retinoic acid-polyethyleneimine complex nanoparticles for embryonic stem cell-derived neuronal differentiation. *Langmuir* 29(31), 9857-9862 (2013).
155. Moribe K, Limwikrant W, Higashi K, Yamamoto K. Drug nanoparticle formulation using ascorbic acid derivatives. *J Drug Deliv* 2011, 138929 (2011).

156. Ye L, Zhang W, Su LP *et al*. Nanoparticle based delivery of hypoxia-regulated vegf transgene system combined with myoblast engraftment for myocardial repair. *Biomaterials* 32(9), 2424-2431 (2011).
157. Lu Z-X, Mao L-L, Lian F *et al*. Cardioprotective activity of placental growth factor in a rat model of acute myocardial infarction: Nanoparticle-based delivery versus direct myocardial injection. *BMC Cardiovascular Disorders* 14(1), 53 (2014).
158. Gray WD, Che P, Brown M, Ning X, Murthy N, Davis ME. N-acetylglucosamine conjugated to nanoparticles enhances myocyte uptake and improves delivery of a small molecule p38 inhibitor for post-infarct healing. *Journal of cardiovascular translational research* 4(5), 631-643 (2011).
159. Barbash IM, Chouraqui P, Baron J *et al*. Systemic delivery of bone marrow-derived mesenchymal stem cells to the infarcted myocardium: Feasibility, cell migration, and body distribution. *Circulation* 108(12900340), 863-868 (2003).
160. Janssens S, Dubois C, Bogaert J *et al*. Autologous bone marrow-derived stem-cell transfer in patients with st-segment elevation myocardial infarction: Double-blind, randomised controlled trial. *Lancet* 367(16413875), 113-121 (2006).
161. Perin EC, Lopez J. Methods of stem cell delivery in cardiac diseases. *Nat Clin Pract Cardiovasc Med* 3 Suppl 1, S110-113 (2006).
162. Gyongyosi M, Lang I, Dettke M *et al*. Combined delivery approach of bone marrow mononuclear stem cells early and late after myocardial infarction: The mystar prospective, randomized study. *Nat Clin Pract Cardiovasc Med* 6(1), 70-81 (2009).
163. Sherman W, Martens TP, Viles-Gonzalez JF, Siminiak T. Catheter-based delivery of cells to the heart. *Nat Clin Pract Cardiovasc Med* 3 Suppl 1(16501633), 57-64 (2006).
164. Pozzobon M, Bollini S, Iop L *et al*. Human bone marrow-derived cd133(+) cells delivered to a collagen patch on cryoinjured rat heart promote angiogenesis and arteriogenesis. *Cell Transplant* 19(10), 1247-1260 (2010).
165. Alperin C, Zandstra PW, Woodhouse KA. Polyurethane films seeded with embryonic stem cell-derived cardiomyocytes for use in cardiac tissue engineering applications. *Biomaterials* 26(35), 7377-7386 (2005).
166. Mcdevitt TC, Woodhouse KA, Hauschka SD, Murry CE, Stayton PS. Spatially organized layers of cardiomyocytes on biodegradable polyurethane films for myocardial repair. *J Biomed Mater Res A* 66(12918042), 586-595 (2003).
167. Fujimoto KL, Tobita K, Merryman WD *et al*. An elastic, biodegradable cardiac patch induces contractile smooth muscle and improves cardiac remodeling and function in subacute myocardial infarction. *J Am Coll Cardiol* 49(23), 2292-2300 (2007).
168. Ravichandran R, Seitz V, Reddy Venugopal J *et al*. Mimicking native extracellular matrix with phytic acid-crosslinked protein nanofibers for cardiac tissue engineering. *Macromol Biosci* 13(3), 366-375 (2013).
169. Miki K, Uenaka H, Saito A *et al*. Bioengineered myocardium derived from induced pluripotent stem cells improves cardiac function and attenuates cardiac remodeling following chronic myocardial infarction in rats. *Stem Cells Transl Med*1(5), 430-437 (2012).
170. Chen Q-Z, Bismarck A, Hansen U *et al*. Characterisation of a soft elastomer poly(glycerol sebacate) designed to match the mechanical properties of myocardial tissue. *Biomaterials* 29(17915309), 47-57 (2008).

171. Krupnick AS, Kreisel D, Engels FH *et al*. A novel small animal model of left ventricular tissue engineering. *J Heart Lung Transplant* 21(2), 233-243 (2002).
172. Vallée J-P, Hauwel M, Lepetit-Coiffé M *et al*. Embryonic stem cell-based cardiopatches improve cardiac function in infarcted rats. *Stem Cells Transl Med* 1(3), 248-260 (2012).
173. Dai W, Wold LE, Dow JS, Kloner RA. Thickening of the infarcted wall by collagen injection improves left ventricular function in rats: A novel approach to preserve cardiac function after myocardial infarction. *J Am Coll Cardiol* 46(16098441), 714-719 (2005).
174. Eschenhagen T, Fink C, Remmers U *et al*. Three-dimensional reconstitution of embryonic cardiomyocytes in a collagen matrix: A new heart muscle model system. *FASEB J* 11(9240969), 683-694 (1997).
175. Zimmermann WH, Fink C, Kralisch D, Remmers U, Weil J, Eschenhagen T. Three-dimensional engineered heart tissue from neonatal rat cardiac myocytes. *Biotechnol Bioeng* 68(10699878), 106-114 (2000).
176. Li Z, Guo X, Guan J. A thermosensitive hydrogel capable of releasing bfgf for enhanced differentiation of mesenchymal stem cell into cardiomyocyte-like cells under ischemic conditions. *Biomacromolecules* 13(6), 1956-1964 (2012).
177. Iwakura A, Fujita M, Kataoka K *et al*. Intramyocardial sustained delivery of basic fibroblast growth factor improves angiogenesis and ventricular function in a rat infarct model. *Heart Vessels* 18(12756606), 93-99 (2003).
178. Leor J, Aboulafia-Etzion S, Dar A *et al*. Bioengineered cardiac grafts : A new approach to repair the infarcted myocardium? *Circulation* 102(suppl 3), III-56-III-61 (2000).
179. Zimmermann WH, Didie M, Wasmeier GH *et al*. Cardiac grafting of engineered heart tissue in syngenic rats. *Circulation* 106(12 Suppl 1), I151-157 (2002).
180. Naito H, Melnychenko I, Didié M *et al*. Optimizing engineered heart tissue for therapeutic applications as surrogate heart muscle. *Circulation* 114(1 suppl), I-72-I-78 (2006).
181. Christman KL, Fok HH, Sievers RE, Fang Q, Lee RJ. Fibrin glue alone and skeletal myoblasts in a fibrin scaffold preserve cardiac function after myocardial infarction. *Tissue Eng* 10(15165457), 403-409 (2004).
182. Christman KL, Vardanian AJ, Fang Q, Sievers RE, Fok HH, Lee RJ. Injectable fibrin scaffold improves cell transplant survival, reduces infarct expansion, and induces neovasculature formation in ischemic myocardium. *J Am Coll Cardiol* 44(15358036), 654-660 (2004).
183. Ou L, Li W, Zhang Y *et al*. Intracardiac injection of matrigel induces stem cell recruitment and improves cardiac functions in a rat myocardial infarction model. *J Cell Mol Med* 15(6), 1310-1318 (2011).
184. Ifkovits JL, Tous E, Minakawa M *et al*. Injectable hydrogel properties influence infarct expansion and extent of postinfarction left ventricular remodeling in an ovine model. *Proc Natl Acad Sci U S A* 107(25), 11507-11512 (2010).
185. Shen D, Wang X, Zhang L *et al*. The amelioration of cardiac dysfunction after myocardial infarction by the injection of keratin biomaterials derived from human hair. *Biomaterials* 32(35), 9290-9299 (2011).

186. Singelyn JM, Dequach JA, Seif-Naraghi SB, Littlefield RB, Schup-Magoffin PJ, Christman KL. Naturally derived myocardial matrix as an injectable scaffold for cardiac tissue engineering. *Biomaterials* 30(29), 5409-5416 (2009).
187. Singelyn JM, Sundaramurthy P, Johnson TD *et al*. Catheter-deliverable hydrogel derived from decellularized ventricular extracellular matrix increases endogenous cardiomyocytes and preserves cardiac function post-myocardial infarction. *J Am Coll Cardiol* 59(8), 751-763 (2012).
188. Dar A, Shachar M, Leor J, Cohen S. Optimization of cardiac cell seeding and distribution in 3d porous alginate scaffolds. *Biotechnol Bioeng* 80(12226863), 305-312 (2002).
189. Landa N, Miller L, Feinberg MS *et al*. Effect of injectable alginate implant on cardiac remodeling and function after recent and old infarcts in rat. *Circulation* 117(11), 1388-1396 (2008).
190. Balakrishnan B, Joshi N, Banerjee R. Borate aided schiff's base formation yields in situ gelling hydrogels for cartilage regeneration. *Journal of Materials Chemistry B* 1(41), 5564-5577 (2013).
191. Balakrishnan B, Joshi N, Jayakrishnan A, Banerjee R. Self-crosslinked oxidized alginate/gelatin hydrogel as injectable, adhesive biomimetic scaffolds for cartilage regeneration. *Acta Biomater* 10(8), 3650-3663 (2014).
192. Dyondi D, Chandra V, Bhonde RR, Banerjee R. Development and characterization of dual growth factor loaded in situ gelling biopolymeric system for tissue engineering applications. *J Biomater Tiss Eng* 2(1), 67-75 (2012).
193. Dyondi D, Webster TJ, Banerjee R. A nanoparticulate injectable hydrogel as a tissue engineering scaffold for multiple growth factor delivery for bone regeneration. *Int J Nanomedicine* 8, 47-59 (2013).
194. Davis ME, Motion JPM, Narmoneva DA *et al*. Injectable self-assembling peptide nanofibers create intramyocardial microenvironments for endothelial cells. *Circulation* 111(4), 442-450 (2005).
195. Yu J, Christman KL, Chin E, Sievers RE, Saeed M, Lee RJ. Restoration of left ventricular geometry and improvement of left ventricular function in a rodent model of chronic ischemic cardiomyopathy. *J Thorac Cardiovasc Surg* 137(1), 180-187 (2009).
196. Ryu JH, Kim IK, Cho SW *et al*. Implantation of bone marrow mononuclear cells using injectable fibrin matrix enhances neovascularization in infarcted myocardium. *Biomaterials* 26(3), 319-326 (2005).
197. Huang NF, Yu J, Sievers R, Li S, Lee RJ. Injectable biopolymers enhance angiogenesis after myocardial infarction. *Tissue Eng* 11(16411832), 1860-1866 (2005).
198. Thompson CA, Nasseri BA, Makower J *et al*. Percutaneous transvenous cellular cardiomyoplasty. A novel nonsurgical approach for myocardial cell transplantation. *J Am Coll Cardiol* 41(12798567), 1964-1971 (2003).
199. Kofidis T, De Bruin JL, Hoyt G *et al*. Injectable bioartificial myocardial tissue for large-scale intramural cell transfer and functional recovery of injured heart muscle. *The Journal of thoracic and cardiovascular surgery* 128(4), 571-578 (2004).
200. Kofidis T, Lebl DR, Martinez EC, Hoyt G, Tanaka M, Robbins RC. Novel injectable bioartificial tissue facilitates targeted, less invasive, large-scale tissue restoration on

the beating heart after myocardial injury. *Circulation* 112(9 Suppl), I173-177 (2005).
201. Wall ST, Walker JC, Healy KE, Ratcliffe MB, Guccione JM. Theoretical impact of the injection of material into the myocardium: A finite element model simulation. *Circulation* 114(17130342), 2627-2635 (2006).
202. Davis ME, Hsieh PCH, Takahashi T *et al*. Local myocardial insulin-like growth factor 1 (igf-1) delivery with biotinylated peptide nanofibers improves cell therapy for myocardial infarction. *Proc Natl Acad Sci U S A* 103(16698918), 8155-8160 (2006).
203. Ungerleider JL, Christman KL. Concise review: Injectable biomaterials for the treatment of myocardial infarction and peripheral artery disease: Translational challenges and progress. *Stem Cells Transl Med*3(9), 1090-1099 (2014).
204. Bellerophon Bcm Llc, Nct01226563. Ik-5001 for the prevention of remodeling of the ventricle and congestive heart failure after acute myocardial infarction (preservation 1). *Available at http://clinicaltrials.gov/ct2/show/NCT01226563*, (Accessed 3rd April 29th 2015).
205. Lonestar Heart I, Nct01311791. A randomized, controlled study to evaluate algisyl-lvr™ as a method of left ventricular augmentation for heart failure (augment-hf). *Available at http://clinicaltrials.gov/show/NCT01311791*, (Accessed on 3rd April 2015).
206. Lonestar Heart I, Nct00847964. Safety and feasibility of algisyl-lvr™ as a method of left ventricular restoration in patients with dcm undergoing open-heart surgery. *Available at http://clinicaltrials.gov/show/NCT00847964*, (Accessed on 3rd April 2015).
207. Radhakrishnan J, Krishnan UM, Sethuraman S. Hydrogel based injectable scaffolds for cardiac tissue regeneration. *Biotechnology advances* 32(2), 449-461 (2014).
208. Sabbah HN. Effects of cardiac support device on reverse remodeling: Molecular, biochemical, and structural mechanisms. *J Card Fail* 10(6), S207-S214 (2004).
209. Rastogi S, Gupta RC, Mishra S, Morita H, Tanhehco EJ, Sabbah HN. Long-term therapy with the acorn cardiac support device normalizes gene expression of growth factors and gelatinases in dogs with heart failure. *J Heart Lung Transplant* 24(10), 1619-1625 (2005).
210. Pilla JJ, Blom AS, Brockman DJ *et al*. Ventricular constraint using the acorn cardiac support device reduces myocardial akinetic area in an ovine model of acute infarction. *Circulation* 106(12 suppl 1), I-207-I-211 (2002).
211. Mann DL, Kubo SH, Sabbah HN *et al*. Beneficial effects of the corcap cardiac support device: Five-year results from the acorn trial. *Journal of Thoracic and Cardiovascular Surgery* 143(5), 1036-1042 (2012).
212. Mann DL, Acker MA, Jessup M, Sabbah HN, Starling RC, Kubo SH. Rationale, design, and methods for a pivotal randomized clinical trial for the assessment of a cardiac support device in patients with new york health association class iii-iv heart failure. *J Card Fail* 10(3), 185-192 (2004).
213. Maher TR, Butler KC, Poirier VL, Gernes DB. Heartmate left ventricular assist devices: A multigeneration of implanted blood pumps. *Artif Organs* 25(5), 422-426 (2001).
214. Copeland JG, Copeland H, Gustafson M *et al*. Experience with more than 100 total artificial heart implants. *J Thorac Cardiovasc Surg* 143(3), 727-734 (2012).

215. Patel-Raman SM, Chen EA. Past, present, and future regulatory aspects of ventricular assist devices. *J Cardiovasc Transl Res* 3(6), 600-603 (2010).
216. Yildirimer L, Seifalian AM. Three-dimensional biomaterial degradation - material choice, design and extrinsic factor considerations. *Biotechnology advances* 32(5), 984-999 (2014).
217. Vidarsson H, Hyllner J, Sartipy P. Differentiation of human embryonic stem cells to cardiomyocytes for in vitro and in vivo applications. *Stem cell reviews* 6(1), 108-120 (2010).
218. Rajala K, Pekkanen-Mattila M, Aalto-Setala K. Cardiac differentiation of pluripotent stem cells. *Stem Cells Int* 2011, 383709 (2011).
219. Yakubov E, Rechavi G, Rozenblatt S, Givol D. Reprogramming of human fibroblasts to pluripotent stem cells using mrna of four transcription factors. *Biochem Biophys Res Commun* 394(1), 189-193 (2010).
220. Subramanyam D, Lamouille S, Judson RL *et al*. Multiple targets of mir-302 and mir-372 promote reprogramming of human fibroblasts to induced pluripotent stem cells. *Nat Biotechnol* 29(21490602), 443-448 (2011).
221. Shi Y, Desponts C, Do JT, Hahm HS, Schöler HR, Ding S. Induction of pluripotent stem cells from mouse embryonic fibroblasts by oct4 and klf4 with small-molecule compounds. *Cell stem cell* 3(5), 568-574 (2008).
222. Nelson TJ, Martinez-Fernandez A, Yamada S, Perez-Terzic C, Ikeda Y, Terzic A. Repair of acute myocardial infarction by human stemness factors induced pluripotent stem cells. *Circulation* 120(19620500), 408-416 (2009).
223. Shake JG, Gruber PJ, Baumgartner WA *et al*. Mesenchymal stem cell implantation in a swine myocardial infarct model: Engraftment and functional effects. *Ann Thorac Surg* 73(6), 1919-1925; discussion 1926 (2002).
224. Engler AJ, Carag-Krieger C, Johnson CP *et al*. Embryonic cardiomyocytes beat best on a matrix with heart-like elasticity: Scar-like rigidity inhibits beating. *J Cell Sci* 121(18957515), 3794-3802 (2008).
225. Suri S, Banerjee R. In vitro evaluation of in situ gels as short term vitreous substitutes. *J Biomed Mater Res A* 79(16826595), 650-664 (2006).
226. Topp MDC, Dijkstra PJ, Talsma H, Feijen J. Thermosensitive micelle-forming block copolymers of poly(ethylene glycol) and poly(n-isopropylacrylamide). *Macromolecules* 30(26), 8518-8520 (1997).
227. Tanaka Y, Kagami Y, Matsuda A, Osada Y. Thermoreversible transition of tensile modulus of hydrogel with ordered aggregates. *Macromolecules* 28(7), 2574-2576 (1995).
228. Lowman AM, Peppas NA. Solute transport analysis in ph-responsive, complexing hydrogels of poly(methacrylic acid-g-ethylene glycol). *J Biomater Sci Polym Ed* 10(9), 999-1009 (1999).
229. Kubota N, Tatsumoto N, Sano T, Matsukawa Y. Temperature-responsive properties of poly(acrylic acid-co-acrylamide)-graft-oligo(ethylene glycol) hydrogels. *Journal of Applied Polymer Science* 80(5), 798-805 (2001).
230. Huffman AS, Afrassiabi A, Dong LC. Thermally reversible hydrogels: Ii. Delivery and selective removal of substances from aqueous solutions. *J Control Release*4(3), 213-222 (1986).

231. Ebara M, Aoyagi T, Sakai K, Okano T. Introducing reactive carboxyl side chains retains phase transition temperature sensitivity in n-isopropylacrylamide copolymer gels. *Macromolecules* 33(22), 8312-8316 (2000).
232. Haque A, Morris ER. Thermogelation of methylcellulose. Part i: Molecular structures and processes. *Carbohydrate Polymers* 22(3), 161-173 (1993).
233. Colombo P. Swelling-controlled release in hydrogel matrices for oral route. *Advanced Drug Delivery Reviews* 11(1–2), 37-57 (1993).
234. Pham AT, Lee PI. Probing the mechanisms of drug release from hydroxypropylmethyl cellulose matrices. *Pharm Res* 11(7855038), 1379-1384 (1994).
235. Maderuelo C, Zarzuelo A, Lanao JM. Critical factors in the release of drugs from sustained release hydrophilic matrices. *J Control Release*154(21497624), 2-19 (2011).
236. Zhang J, Peppas NA. Synthesis and characterization of ph- and temperature-sensitive poly(methacrylic acid)/poly(n-isopropylacrylamide) interpenetrating polymeric networks. *Macromolecules* 33(1), 102-107 (1999).
237. Lee H, Fisher S, Kallos MS, Hunter CJ. Optimizing gelling parameters of gellan gum for fibrocartilage tissue engineering. *Journal of Biomedical Materials Research Part B: Applied Biomaterials* 98B(2), 238-245 (2011).
238. De Las Heras Alarcon C, Pennadam S, Alexander C. Stimuli responsive polymers for biomedical applications. *Chemical Society reviews* 34(3), 276-285 (2005).
239. Ciardelli G, Chiono V, Vozzi G *et al*. Blends of poly-(epsilon-caprolactone) and polysaccharides in tissue engineering applications. *Biomacromolecules* 6(4), 1961-1976 (2005).
240. Jeong B, Bae YH, Kim SW. Thermoreversible gelation of peg−plga−peg triblock copolymer aqueous solutions. *Macromolecules* 32(21), 7064-7069 (1999).
241. Liu SQ, Joshi SC, Lam YC, Tam KC. Thermoreversible gelation of hydroxypropylmethylcellulose in simulated body fluids. *Carbohydrate Polymers* 72(1), 133-143 (2008).
242. Zhang M, Li XH, Gong YD, Zhao NM, Zhang XF. Properties and biocompatibility of chitosan films modified by blending with peg. *Biomaterials* 23(12059013), 2641-2648 (2002).
243. Zreiqat H, Ramaswamy Y, Wu CT *et al*. The incorporation of strontium and zinc into a calcium-silicon ceramic for bone tissue engineering. *Biomaterials* 31(12), 3175-3184 (2010).
244. Skehan P, Storeng R, Scudiero D *et al*. New colorimetric cytotoxicity assay for anticancer-drug screening. *J Natl Cancer Inst* 82(13), 1107-1112 (1990).
245. Moritaka H, Fukuba H, Kumeno K, Nakahama N, Nishinari K. Effect of monovalent and divalent cations on the rheological properties of gellan gels. *Food Hydrocolloids* 4(6), 495-507 (1991).
246. Nilsson M, Carlson J, Fernandez E, Planell JA. Monitoring the setting of calcium-based bone cements using pulse-echo ultrasound. *J Mater Sci Mater Med* 13(12), 1135-1141 (2002).
247. Cement, lime, gypsum (philadelphia). *ASTM C266-89, in Annual Book of ASTM Standards, Vol. 04.01:* 04, 198-191 (1993).

248. Joshi SC, Lam YC, Tan BK, Liu SQ. Modeling of thermal gelation and degelation of mc and hpmc hydrogels. Presented at: *Biomedical and Pharmaceutical Engineering, 2006. ICBPE 2006. International Conference on*. 2006.
249. Carvalho E, Verma P, Hourigan K, Banerjee R. Development of dual-triggered in situ gelling scaffolds for tissue engineering. *Polymer International* 63(9), 1593-1599 (2014).
250. Engler AJ, Sen S, Sweeney HL, Discher DE. Matrix elasticity directs stem cell lineage specification. *Cell* 126(16923388), 677-689 (2006).
251. Van Amerongen MJ, Harmsen MC, Petersen AH, Kors G, Van Luyn MJA. The enzymatic degradation of scaffolds and their replacement by vascularized extracellular matrix in the murine myocardium. *Biomaterials* 27(10), 2247-2257 (2006).
252. Annor AH, Tang ME, Pui CL *et al*. Effect of enzymatic degradation on the mechanical properties of biological scaffold materials. *Surg Endosc* 26(10), 2767-2778 (2012).
253. Sriamornsak PS, Srisagul. Modification of theophylline release with alginate gel formed in hard capsules. *AAPS PharmSciTech* 8(3), E1-E8 (2007).
254. Jagdish Balasubramaniam SK, Jayanta Kumar Pandit. In vitro and in vivo evaluation of the gelrite® gellan gum-based ocular delivery system for indomethacin. *Acta Pharmaceutica* 53(4), 251-261 (2003).
255. G. R. Sanderson PH. "Gellan gum," in food gels. *Elsevier Applied Science, New York, Chapter 6*,
256. Chandrasekaran R, Radha A, Thailambal VG. Roles of potassium ions, acetyl and l-glyceryl groups in native gellan double helix: An x-ray study. *Carbohydrate research* 224, 1-17 (1992).
257. Gutowska A, Jeong B, Jasionowski M. Injectable gels for tissue engineering. *The Anatomical Record* 263(4), 342-349 (2001).
258. Cao N, Liu Z, Chen Z *et al*. Ascorbic acid enhances the cardiac differentiation of induced pluripotent stem cells through promoting the proliferation of cardiac progenitor cells. *Cell Res* 22(1), 219-236 (2012).
259. Choi SC, Yoon J, Shim WJ, Ro YM, Lim DS. 5-azacytidine induces cardiac differentiation of p19 embryonic stem cells. *Exp Mol Med* 36(6), 515-523 (2004).
260. Christman KL, Fok HH, Sievers RE, Fang Q, Lee RJ. Fibrin glue alone and skeletal myoblasts in a fibrin scaffold preserve cardiac function after myocardial infarction. *Tissue Eng* 10(3-4), 403-409 (2004).
261. Johnson TD, Christman KL. Injectable hydrogel therapies and their delivery strategies for treating myocardial infarction. *Expert Opin Drug Deliv* 10(1), 59-72 (2013).
262. Rane AA, Christman KL. Biomaterials for the treatment of myocardial infarction: A 5-year update. *J Am Coll Cardiol* 58(25), 2615-2629 (2011).
263. Bilbija D, Haugen F, Sagave J *et al*. Retinoic acid signalling is activated in the postischemic heart and may influence remodelling. *PLoS One* 7(9), e44740 (2012).
264. Chen T, Chang TC, Kang JO *et al*. Epicardial induction of fetal cardiomyocyte proliferation via a retinoic acid-inducible trophic factor. *Dev Biol* 250(1), 198-207 (2002).
265. Drysdale TA, Patterson KD, Saha M, Krieg PA. Retinoic acid can block differentiation of the myocardium after heart specification. *Dev Biol* 188(2), 205-215 (1997).

266. Takahashi T, Lord B, Schulze PC *et al*. Ascorbic acid enhances differentiation of embryonic stem cells into cardiac myocytes. *Circulation* 107(14), 1912-1916 (2003).
267. Maltsev VA, Wobus AM, Rohwedel J, Bader M, Hescheler J. Cardiomyocytes differentiated in vitro from embryonic stem cells developmentally express cardiac-specific genes and ionic currents. *Circ Res* 75(2), 233-244 (1994).
268. Fassler R, Rohwedel J, Maltsev V *et al*. Differentiation and integrity of cardiac muscle cells are impaired in the absence of beta 1 integrin. *J Cell Sci* 109 (Pt 13), 2989-2999 (1996).
269. Franz WM, Breves D, Klingel K, Brem G, Hofschneider PH, Kandolf R. Heart-specific targeting of firefly luciferase by the myosin light chain-2 promoter and developmental regulation in transgenic mice. *Circ Res* 73(4), 629-638 (1993).
270. O'brien TX, Lee KJ, Chien KR. Positional specification of ventricular myosin light chain 2 expression in the primitive murine heart tube. *Proc Natl Acad Sci U S A* 90(11), 5157-5161 (1993).
271. Lufkin T, Lohnes D, Mark M *et al*. High postnatal lethality and testis degeneration in retinoic acid receptor alpha mutant mice. *Proc Natl Acad Sci U S A* 90(15), 7225-7229 (1993).
272. Rhinn M, Dolle P. Retinoic acid signalling during development. *Development (Cambridge, England)* 139(5), 843-858 (2012).
273. Lohnes D, Mark M, Mendelsohn C *et al*. Function of the retinoic acid receptors (rars) during development (i). Craniofacial and skeletal abnormalities in rar double mutants. *Development (Cambridge, England)* 120(10), 2723-2748 (1994).
274. Mascrez B, Ghyselinck NB, Chambon P, Mark M. A transcriptionally silent rxralpha supports early embryonic morphogenesis and heart development. *Proc Natl Acad Sci U S A* 106(11), 4272-4277 (2009).
275. Wilson JG, Roth CB, Warkany J. An analysis of the syndrome of malformations induced by maternal vitamin a deficiency. Effects of restoration of vitamin a at various times during gestation. *Am J Anat* 92(2), 189-217 (1953).
276. Wilson JG, Warkany J. Aortic-arch and cardiac anomalies in the offspring of vitamin a deficient rats. *Am J Anat* 85(1), 113-155 (1949).
277. Van Der Heyden MaG, Defize LHK. Twenty one years of p19 cells: What an embryonal carcinoma cell line taught us about cardiomyocyte differentiation. *Cardiovasc Res* 58(2), 292-302 (2003).
278. Blank RS, Swartz EA, Thompson MM, Olson EN, Owens GK. A retinoic acid-induced clonal cell line derived from multipotential p19 embryonal carcinoma cells expresses smooth muscle characteristics. *Circ Res* 76(5), 742-749 (1995).
279. D.A. White IGBA, J.N. Hawthorne, R.M.C. Dawson (Eds.),. Form and function of phospholipids. *Biochem Soc Trans* 441–482. (1973).
280. Murakami M, Kudo I, Inoue K. Change in phospholipid composition of mouse bone marrow-derived mast cells during cultivation with fibroblasts. *Biochimica et biophysica acta* 1124(1), 17-22 (1992).
281. Murphy EJ, Horrocks LA. Effects of differentiation on the phospholipid and phospholipid fatty acid composition of n1e-115 neuroblastoma cells. *Biochimica et Biophysica Acta (BBA) - Lipids and Lipid Metabolism* 1167(2), 131-136 (1993).

282. Fotheringham J, Xu FY, Nemer M, Kardami E, Choy PC, Hatch GM. Lysophosphatidylethanolamine acyltransferase activity is elevated during cardiac cell differentiation. *Bba-Mol Cell Biol L* 1485(1), 1-10 (2000).
283. Wheeldon LW, Schumert Z, Turner DA. Lipid composition of heart muscle homogenate. *J Lipid Res* 6(4), 481-489 (1965).
284. Bangham AD, Standish MM, Watkins JC. Diffusion of univalent ions across the lamellae of swollen phospholipids. *J Mol Biol* 13(1), 238-252 (1965).
285. Egerdie B, Singer M. Morphology of gel state phosphatidylethanolamine and phosphatidylcholine liposomes: A negative stain electron microscopic study. *Chem Phys Lipids* 31(1), 75-85 (1982).
286. Joshi N, Shanmugam T, Kaviratna A, Banerjee R. Proapoptotic lipid nanovesicles: Synergism with paclitaxel in human lung adenocarcinoma a549 cells. *J Control Release*156(3), 413-420 (2011).
287. Cryan SA, Devocelle M, Moran PJ, Hickey AJ, Kelly JG. Increased intracellular targeting to airway cells using octaarginine-coated liposomes: In vitro assessment of their suitability for inhalation. *Mol Pharm* 3(2), 104-112 (2006).
288. Ramoino P, Gallus L, Beltrame F *et al*. Endocytosis of gabab receptors modulates membrane excitability in the single-celled organism paramecium. *J Cell Sci* 119(Pt 10), 2056-2064 (2006).
289. Li RJ, Ying X, Zhang Y *et al*. All-trans retinoic acid stealth liposomes prevent the relapse of breast cancer arising from the cancer stem cells. *J Control Release*149(3), 281-291 (2011).
290. Kuromi H, Yoshihara M, Kidokoro Y. An inhibitory role of calcineurin in endocytosis of synaptic vesicles at nerve terminals of drosophila larvae. *Neuroscience research* 27(2), 101-113 (1997).
291. Kitchens KM, Kolhatkar RB, Swaan PW, Ghandehari H. Endocytosis inhibitors prevent poly(amidoamine) dendrimer internalization and permeability across caco-2 cells. *Mol Pharm* 5(2), 364-369 (2008).
292. Dutta D, Donaldson JG. Search for inhibitors of endocytosis: Intended specificity and unintended consequences. *Cell Logist* 2(4), 203-208 (2012).

APPENDIX

Q-PCR

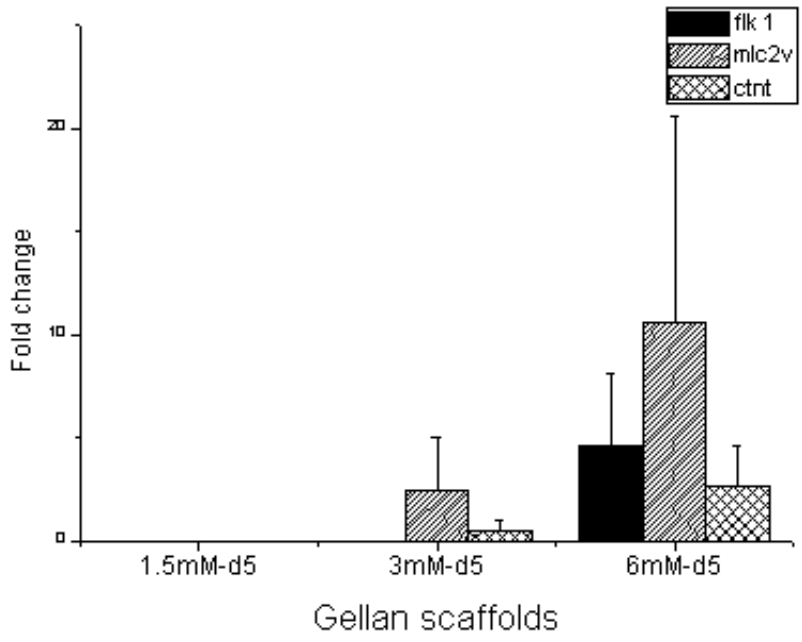

Figure A1: Effect of crosslink density on the early Flk1 and late gene MLC2V and cTnT expression.

Table A1: Primer sequence

Genes	Sequence	Amplicon base pairs(bp)	Tm
Flk1	Forward: 5'-GGCGGTGGTGACAGTATCTT-3'	**203**	**50°C**
	Reverse: 5'-CTCGGTGATGTACACGATGC-3'		
Mlc2v	Forward: 5'-AAAGAGGCTCCAGGTCCAAT-3'	**177**	**51°C**
	Reverse: 5'-CCTCTCTGCTTGTGTGGTCA-3'		
Mlc2a	Forward: 5'-TCAGCTGCATTGACCAGAAC-3'	**148**	**50°C**
	Reverse: 5'-AAGACGGTGAAGTTGATGGG-3'		
cTnt	Forward: 5'-GAAGGAAGGCAGAACCG-3'	**292**	**50°C**
	Reverse: 5'-AGCCTCCAGGTTGTGAAT-3'		
βActin	Forward: 5'-CACCACACCTTCTACAATGAGC-3'	**242**	**58°C**
	Reverse: 5'-TCGTAGATGGGCACAGTGTGGG -3'		

Western blot

Method

` For immunoblots, cells from various stages of differentiation were harvested and lysed in cell lysis buffer (Cell signalling). Samples were mixed (1:1) on ice with non-reducing tris-glycine SDS sample buffer and heated in a boiling water bath for 5 mins. When reducing conditions were required, β-mercaptoethanol (5% v/v) was added to the sample buffer. Denatured samples (20 µL) were loaded onto 12% Laemmli tris-glycine SDS polyacrylamide gels and subjected to electrophoresis in tris-glycine running buffer (SDS-PAGE machine, Biorad, USA). Protein concentration was measured with Nanodrop spectrophotometer (ThermoScientific) and concentration of all proteins in all samples was made up to a final concentration of 2.5 mg/ml, uniformly. Proteins were transferred to nitrocellulose (Life Technologies, 0.45 µm pore size) overnight at 40 mA. Western blots were probed for MEF2C, POUF1, CD-15, cTnT as follows, all steps being carried out at room temperature, with gentle shaking. After 4hrs in blocking buffer (5% skimmed milk in PBS), membranes were incubated for 6 hrs with the following optimal dilutions of primary antibodies in PBS: MEF2C (1:1000, Abcam), POUF1 (1:1000, Sigma Aldrich), CD-15 (1:1000, Sigma Aldrich), cTnT (1:1000, Abcam). After thorough washing in PBS containing 1% Tween 20 (wash buffer), membranes were incubated for 6 hrs in 1:10000 dilution of the second antibody (both Goat pAb to mouse IgG and Goat pAb to Rabbit IgG horseradish peroxidase (HRP)-conjugated, Abcam, UK) in wash buffer. After thorough washing in PBS containing 1% Tween 20 (wash buffer), membranes were incubated for 15 mins with Amersham ECL Prime western blotting detection reagent (1:1 dilution) and imaged in gel doc.

Results

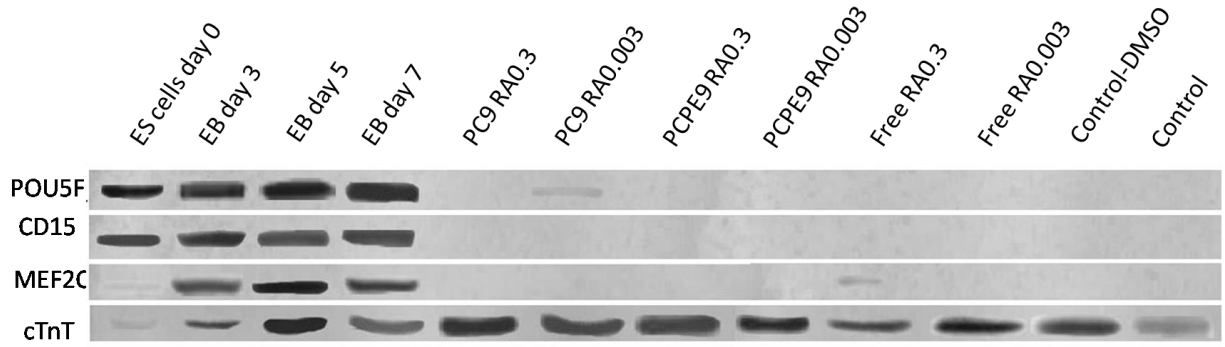

Figure A2: Western blot for cells expressing cardiac markers when treated in the presence of liposomal formulations of retinoic acid as well as free retinoic acid.

Western blot analysis of the differentiation indicates that within the first 7 days of differentiation indicated the expression of early pluripotency markers as well as cardiac markers, on day 19 after treatment with retinoic acid. Early marker MEF2c was observed only with partially differentiated maintained in the presence of free retinoic acid and none in other liposomal treatment containing retinoic acid cardiac TnT.

List of publications

Publications

- **Carvalho E**, Verma P, Hourigan K, Banerjee R. Development of dual-triggered in situ gelling scaffolds for tissue engineering. *Polymer International* 63(9), 1593-1599 (2014).
- **Edmund Carvalho** , Rinti Banerjee, Kerry Hourigan, Paul Verma. Myocardial infarction: Stem cell therapy from bench to clinic. (Manuscript under review- Regenerative medicine- Future medicine 2015).
- Edmund Carvalho , Rinti Banerjee, Kerry Hourigan, Paul Verma.
- Singh PK, Ghosh D, Tewari D, Mohite GM, **Carvalho E**, Jha NN, *et al*. Cytotoxic Helix-Rich Oligomer Formation by Melittin and Pancreatic Polypeptide. PLoS ONE. 2015;10:e0120346.
- Ghosh D, Sahay S, Ranjan P, Salot S, Mohite GM, Singh PK, *et al*. The newly Discovered Parkinson's Disease Associated Finnish Mutation (A53E) Attenuates α-Synuclein Aggregation and Membrane Binding. Biochemistry. 2014.

Book chapter

- Heffernan C, Liu J, Sumer H *et al*. Induction of pluripotency. *Adv Exp Med Biol* 786, 5-25 (2013).

Conferences

- Edmund CARVALHO RB, Paul VERMA, Kerry HOURIGAN. Development of Dual Triggered In-situ Gelling Scaffolds for Tissue Engineering. The International Conference on Materials for Advanced Technologies(ICMAT 2013). 2013.
- CARVALHO E, VERMA P, HOURIGAN K, BANERJEE R. Tunable hydrogels for differentiation of tissue progenitors using nanoparticles. 40th Annual Meeting & Exposition of the Controlled Release Society. 2013.

- Carvalho E, Banerjee R, Verma P. Development of scaffolds for cardiac differentiation of pluripotent stem cells World Congress on Reproductive Biology. Cairns, Australia2011. p. 135.